R. & M. No. 3069
(18,733)
A.R.C. Technical Report

MINISTRY OF SUPPLY

AERONAUTICAL RESEARCH COUNCIL
REPORTS AND MEMORANDA

The Optics of the Mach-Zehnder Interferometer

By
L. H. TANNER, B.A.,
of the Aerodynamics Division, N.P.L.

LONDON : HER MAJESTY'S STATIONERY OFFICE
1959
PRICE £1 2*s*. 6*d*. NET

The Optics of the Mach-Zehnder Interferometer

By

L. H. TANNER, B.A.,
of the Aerodynamics Division, N.P.L.

Reports and Memoranda No. 3069

October, 1956

Summary.—The paper is intended to give a complete optical theory of the Mach-Zehnder interferometer, without using difficult mathematical methods or complicated three-dimensional diagrams.

The topics covered include the effect of the spectral distribution of the source, with and without dispersion. The effect on the fringe contrast of the size and shape of the source are considered. These effects are related to the fringe pattern which is produced near the usual source position if a source is placed in what is normally the emergent beam. This fringe pattern is related to the displacement of the two images of a co-ordinate system in the emergent beam, as seen through the four-mirror system. The effects of all such displacements are discussed and illustrated. The effect of mirror movements on these displacements is analysed, to show the number of fine adjustments required, and the effect of each.

A section on the imperfections of the optical elements includes discussions of the effects of differences of thickness, incidence and refractive index, wedge angles, surface flatness and refractive index variation. Except for the permissible wedge angles, the limits found necessary are less strict than those usually given. Aberration of the collimating lens has practically no effect.

A review of methods of adjustment of the interferometer includes descriptions of some of the well-known methods and of two which do not appear to have been described previously. Of these, one is a method for obtaining a parallelogram arrangement, which was used by K. J. Habell, and the other is an accurate method for final adjustment based on the source-plane fringe pattern.

1. *Introduction.*—The problem of evolving a general treatment of the optics of the Mach-Zehnder interferometer, so as to show the effects on the spacing, position and contrast of the fringes of all possible adjustments of the four mirrors, of the size, shape and spectral distribution of the source, and of imperfections of the optical elements, seems *a priori* to be one of extreme complexity. The result has been that until comparatively recently no such treatment was attempted. Much has been written, mainly in German, on various aspects of the optics, but the results are unduly restricted and not always accurate, and not all of the papers on the subject can be interpreted, even in translation, by anyone not having considerable practical experience of the interferometer.

Hansen[1] and Schardin[2] show that the effect of using an extended source is to localize the fringes at a certain plane, and give expressions for the position of this plane in terms of mirror rotations, for simple cases. Hansen discusses the effect of difference of incidence of the two semi-reflecting plates, and rightly points out that the linear term may be compensated. Schardin shows qualitatively the effect of spectral band width of the source on the number of clear fringes.

Zobel[3] describes a method of adjustment which uses a pentaprism, and by which all the mirrors may be made parallel. When fringes are obtained they are focussed by rotating the mirrors and observing with a telescope; no account of the necessary rotations or their effects is given.

Lamla[4] goes more deeply into the optics of the 45-deg interferometer. He gives a condition for obtaining sharp fringes which is, however, rather difficult to visualize in practical terms. He investigates the fringe contrast obtained with a rectangular source, apparently for states of

Published with permission of the Director, National Physical Laboratory.

adjustment giving what is described in the present report as a linear source-plane path variation. He shows that with horizontal fringes there is a limit to the permissible source size even with the best adjustment. His paper, and that of Schardin, suggest wrongly that only the semi-reflecting plates should be used for adjustment while the plane mirrors should be kept fixed. This renders his conclusion that for each fringe spacing and location there is an optimum position of the mirrors incorrect, unless two are kept fixed. The conclusion that, at this position, the source size is immaterial, is also usually incorrect.

Hottenroth[5] points out that an exactly rectangular arrangement of the plates is not essential, and then describes the near and far cross-hair method of adjustment. He also points out that normally any two mirrors may be used for the adjustment. He appears to have noticed the distinction made in the present paper between ' emergent beam ' and ' source-plane ' fringes. He uses an extended source for accurate focussing, and notices that for ease of adjustment it is convenient to have mirror 3 and the model equidistant from mirror 4*. This appears, however, to have been noticed and patented earlier by Kinder.

Kinder[6] gives diagrams similar to Figs. 21 and 22 of the present report, showing the effect of mirror rotations on the focal position of the fringes, but for certain special conditions only. He uses a method similar to that of Hansen in discussing the effect of source size.

Winkler[7] attempted for the first time to give a fairly complete account of the subject, and discusses the effect of mirror positions and of most of the possible imperfections of the optics, on the fringe contrast. The paper is unfortunately difficult to interpret, and a few of the results appear incorrect. Thus he wrongly states that the linear terms of the source-plane path distribution for difference of incidence of the plates or windows cannot be compensated (despite Hansen[1] and Kinder's[6] correct statements on this point) and he thus gives a strict limit on this difference which, as experiment shows, is quite unnecessary.

For wedge angles Winkler gives curves of ' equal ω path difference ', which correspond to the source-plane fringe pattern of the present paper. These are calculated for the mid-point of the mirrors only, and Winkler wrongly states that they are the same for other points in a plane parallel to the mirrors. He thus fails to notice the important linear term, which in this case cannot be compensated.

Bennett[8], in a paper using vector notation, repeats Winkler's work on the ideal inferferometer and goes into more detail as regards the source-plane fringe patterns. In a further paper[9] he calculates the contrast-fringe number variation due to a Gaussian spectral intensity distribution, and also discusses the effect of source size for a rather unusual source-plane fringe pattern, namely a parabolic variation of equal amount in both directions, giving circular fringes.

Price[10] gives a useful alternative to the near and far cross-hair method of adjustment, and an account of his method is given in the present paper (section 6.3(b)).

Hannes[11] shows that for zero image displacements the necessary and sufficient condition is that the planes of the four mirrors should all intersect in the same line. Hence, for the special case of a parallelogram interferometer, with sides of ratio 2 : 1, he deduced the equations governing the possible angular and linear displacements of the mirrors which preserve the zero image displacements.

The present paper collects many of the results previously obtained, and presents these in a way which, it is hoped, may be easy to understand. It also shows which are generally applicable to all two-beam interferometers and which are restricted, for example, to the parallel-plate Mach-Zehnder instrument.

The first section on the general optics of two-beam interferometers shows how the contrast of fringes in the emergent beam is related to the fringe pattern in the source plane which is obtained when a source is placed at the point in question in the emergent beam. This fringe pattern in the source plane determines the size and shape of source which may be used.

---

* The condition is wrongly stated in the English translation.

Following this there is a discussion of the effects of the spectral distribution of the source, and of the effects of dispersion.

The next section is on the ideal four-mirror interferometer, that is, one whose mirrors are perfectly plane and whose semi-reflecting plates have no thickness. The discussion shows that the source-plane fringe distribution depends on the separation of the two images of the screen, as seen through the four-mirror system. This leads to a great simplification of the problem, since the two images of any co-ordinate system in the emergent beam may be treated as rigid bodies, and the effects of all possible displacements of one relative to the other may be investigated independently of any discussion of the effect of the mirror movements on these displacements.

Various other considerations which are independent of the exact mirror arrangement are discussed, including the effects of aberrations of the collimating lens and their relation to the use of the instrument as a wave-shearing interferometer, and the relation between the two emergent beams.

The effects of the mirror adjustments are then discussed, for the plane, but not parallelogram, interferometer. This shows the number of fine adjustments which are necessary and sufficient to determine the image displacements completely. When the interferometer is a parallelogram there are two of these which cannot be adjusted independently of each other, and so one less fine adjustment is required.

A section of the effects of imperfections of the optical elements follows. The source-plane fringe distributions due to differences in thickness, incidence and refractive index of the plates and windows are calculated. Since these are independent of the position of the point in the emergent beam, the linear terms may all be compensated by mirror translations, and the quadratic terms give rise only to very loose restrictions on the imperfections. For wedge angles, on the other hand, the linear terms are proportional to the change of thickness and thus vary linearly with the co-ordinates in the emergent beam, and cannot be compensated.

A discussion of the effect of the disturbance under investigation (a two-dimensional wind tunnel is taken as an example) leads to practical values for source size, and this is used to determine suitable limits for the imperfections of the optical elements.

Finally, a review and discussion of methods of adjustment is given, including a more complete discussion of the source-size and fringe-contrast method than has previously appeared, a method based on direct observation of the source-plane fringes, and a method for initial adjustment based on one which was used by K. J. Habell, but has not previously been described.

2. *General Optical Properties of Two-Beam Interferometers.*—2.1. *Conditions for the appearance of Interference Fringes.*—Interference fringes may be produced when monochromatic light originating at one point travels round two or more distinct paths and then arrives, in the same plane of polarisation if it is polarised, at a second point. The present paper will consider only two-beam interferometers, in which there are two light paths only.

The optical path length round each path is determined by Fermat's principle of stationary path. The length of one path may, however, differ from that of the other. If the path lengths differ by an integral number of wave-lengths the waves arrive in phase and reinforce, while if the difference is an odd number of half wavelengths they arrive out of phase and cancel. If the wavelength is λ and the path difference $N\lambda$, the phase difference is $2\pi N$. If the amplitude arriving *via* each path is a, the amplitude of the sum is $2a \cos \pi N$ and the intensity $4a^2 \cos^2 \pi N$ or $4I_0 \cos^2 \pi N$; where I_0 is the intensity which results when either beam is removed.

The phase difference $2\pi N$ between the two paths at the point in question usually varies with the wavelength of the light and with the position of the source. Arising from this there are certain limitations on the configuration of the source and its spectral intensity distribution which are necessary for the production of clear fringes.

2.2. *Relation between Fringe Pattern and Path-Difference Variation.*—Consider light from a source whose co-ordinates are x', y', z', travelling along two paths and arriving at a point whose co-ordinates are x, y, z. The two optical paths will differ by an amount l which will in general depend on all these co-ordinates. If the intensity arriving at x, y, z from a source of unit volume at x', y', z' via each path is i, and if the two beams are similarly polarised, then the total intensity is:

$$I(x, y, z) = \int 4i \cos^2 \frac{\pi l}{\lambda} \, dx' \, dy' \, dz' \, . \quad .. \quad .. \quad .. \quad .. \quad (2.1)$$

Now consider a small source; that is, one of dimensions $\delta x'$, $\delta y'$, $\delta z'$ such that $(\partial l/\partial x')\delta x' << \lambda$, etc. Then if its total intensity at x, y, z via each path separately is I_0, $I(x, y, z) = 4I_0 \cos^2 (\pi l/\lambda)$.

The contours of constant path difference are thus surfaces on which the intensity is a constant fraction of what it would be if one beam were removed. The intensity is a maximum on surfaces (the bright fringes) on which the path difference is an integral number of wavelengths, and a minimum on the dark fringes when the difference is an odd number of half waves. Between two consecutive fringes the path difference changes by one wavelength and the fringe number $N = l/\lambda$ changes by unity.

Since the fringes are surfaces of constant path difference, the gradient of l is normal to the fringes. If this gradient is approximately constant, the spacing b between two fringes is given by b grad $l = \lambda$.

2.3. *Relation between Fringe Pattern and Inclination of Rays or Wave Fronts.*—In general at any point x, y, z, one light ray arrives from x', y', z' via each of two paths. Suppose these meet at an angle α (Fig. 1), and take co-ordinates ζ along the bisector to the angle and ξ normal to this, in the plane of the two rays, and η normal to this plane. Then if the path lengths are l_1 and l_2,

$$\frac{\partial l_1}{\partial \eta} = \frac{\partial l_2}{\partial \eta} = 0 \, ,$$

$$\frac{\partial l_1}{\partial \zeta} = \frac{\partial l_2}{\partial \zeta} = \mu \cos \frac{\alpha}{2} \, ,$$

$$\frac{\partial l_1}{\partial \xi} = -\frac{\partial l_2}{\partial \xi} = \mu \sin \frac{\alpha}{2} \, .$$

Hence, since $l = l_1 - l_2$,

$$\frac{\partial l}{\partial \eta} = \frac{\partial l}{\partial \zeta} = 0 \, ; \quad .. \quad .. \quad .. \quad .. \quad .. \quad .. \quad (2.2)$$

$$\frac{\partial l}{\partial \xi} = \text{grad } l = 2\mu \sin \frac{\alpha}{2} \, . \quad .. \quad .. \quad .. \quad .. \quad (2.3)$$

Equation (2.2) shows that the fringe passing through x, y, z lies in a plane perpendicular to that of the two rays and that the rays are incident on the fringe at equal angles on opposite sides of it. Equation (2.3) shows that the fringe spacing is given approximately by $2\mu b \sin (\alpha/2) = \lambda$, or, since α is usually small, $b = \lambda/(\mu\alpha)$.

Fig. 2 is a diagram which shows this relation for plane wave-fronts, for $\mu = 1$. In practice we are usually concerned with the fringe spacing in air in the emergent beam, and so throughout the rest of the paper the usual expression $b = \lambda/\alpha$ will be used for the fringe spacing. Note that if the light is then incident approximately normally on a plane surface of another medium, the angle between the rays and the wavelength are both reduced by the factor $1/\mu$, and so the fringe spacing is unchanged.

2.4. *Fringes in Two Dimensions.*—The wavelength of visible light is from about $1{\cdot}6$ to $2{\cdot}8 \times 10^{-5}$ in., and the useful range of fringe spacing is from about 100λ upwards. The inclination α with which we are normally concerned is thus less than one degree. Thus the fringes lie roughly parallel to the light rays.

We normally observe the intensity on a screen, which may be a photographic plate or the retina of the eye, placed roughly perpendicular to the rays. On this screen the fringes are lines given by $I = 4I_0 \cos^2(\pi l/\lambda)$ for constant values of the path difference l.

2.5. *Reciprocal Relation between Source and Screen—Effects of Source Position and Size.*—Consider the two points A and B (Fig. 3) such that light from A arrives via the two paths at B with path difference l_{AB}. Now if AB is a possible light path, so is the reverse path BA, and the path difference is the same, $l_{AB} = l_{BA}$. Thus the fringe number at B due to source A is the same as that at A due to a source at B.

Now consider point C such that $l_{BC} = l_{AB} + N\lambda$. Then the difference in fringe numbers between C and A due to a source at B is N.

Consider the fringes produced near the point B by a source at C. The fringe number at B due to C differs by N from that due to A. The relative intensity of the fringes due to A and C will be the same, and its gradient will have the same sign, if N is an integer, so that the path differences differ by zero or by an integral number of wavelengths. If, on the other hand, $l_{CB} - l_{AB}$ is an odd number of half waves, the fringes due to A and C will cancel at B.

Thus the effect at B of adding a second source, or of moving the source, may be determined by considering the fringes produced by placing a source at B. For example if A lies on a bright fringe, C will reinforce A at B if C lies on the same, or any other, bright fringe. If A moves across N fringes, N fringes will move across B. If A moves along a fringe, the fringe at B will not move.

2.6. *Relation between Source Size and Ray Inclination at the Source Position.*—Usually it is not practicable to use two or more separate sources. If, therefore, a source placed at the point B (Fig. 3) produces a fringe spacing b' at A, then for good contrast the dimension of the source at A normal to these fringes must be limited to a fraction of b'. Appendix I gives the variation of fringe contrast with this fraction for a rectangular source, and shows that practical values are from $\frac{1}{4}$ to $\frac{3}{4}$, depending on the contrast required.

In practice the fringe spacing and direction at A due to B may depend both on the position of B and on the changes of path in the wind tunnel or optical system under observation. This may limit the size of the source in three dimensions, since its dimension in any direction must not exceed a fraction, from $\frac{1}{4}$ to $\frac{3}{4}$, of the least fringe spacing in this direction.

If the fringe spacing at A is b', then section 2.3 shows that the inclination of the rays producing the fringes is $\alpha = \lambda/(\mu b')$. This is therefore also the inclination of rays from A which meet at B and interfere there. Now the permissible source size d' is given by $d' = kb'$ where k is a constant. Thus d' and α are related by $d' = k\lambda/(\mu\alpha)$. This shows that, to allow the use of a large source, and hence to obtain bright fringes, the interferometer must be so designed that the rays which meet on the screen emerge from the source in very nearly the same direction.

2.7. *Effect of the Spectral Distribution of the Source.*—Section 2.2 showed that, with monochromatic light and a small source, the intensity ratio to that with one beam removed is $4\cos^2 \pi l/\lambda$. This ratio is the same at the same position on successive fringes, and so the fringe contrast is independent of the fringe number l/λ.

If the source is not monochromatic, equation (2.1) becomes

$$I(x, y, z) = \int 4i \cos^2 \frac{\pi l}{\lambda} dx'\, dy'\, dz'\, d\lambda ,$$

where both i and l will in general be functions of λ as well as of the six co-ordinates. For a small source

$$I(x, y, z) = \int 4I_0(\lambda) \cos^2 \frac{\pi l}{\lambda} d\lambda .$$

Fringes due to wavelengths near λ will reinforce if the fringe number l/λ has a stationary value. That is, the path difference l is given by

$$\frac{\partial}{\partial \lambda}\left(\frac{l}{\lambda}\right) = 0 ,$$

or

$$\frac{l}{\lambda} - \frac{\partial l}{\partial \lambda} = 0 .$$

When dispersion is present, $\partial l/\partial \lambda$ will usually vary with λ. If, therefore, the source spectrum covers a large range of wavelengths, the fringe number l/λ at which the condition $l/\lambda = \partial l/\partial \lambda$ is satisfied will itself depend on the wavelength.

2.8. *Effect of Source Spectrum with no Dispersion.*—If there is no dispersion, or an equal dispersion in the two beams, then $\partial l/\partial \lambda = 0$, and the fringes due to all wavelengths reinforce where the path difference l is zero. At other positions, fringes due to wavelengths λ_1 and λ_2 will reinforce if the fringe number difference $l/\lambda_1 - l/\lambda_2$ is an integer, and cancel if $2(l/\lambda_1 - l/\lambda_2)$ is an odd integer. They therefore alternately reinforce and cancel as l increases, and so, if $(\lambda_1 - \lambda_2)/\lambda_1$ is small, beats appear, the path difference interval between groups of clear fringes being $\lambda_1\lambda_2/(\lambda_1 - \lambda_2)$, and the number of fringes in each beat $\lambda_2/(\lambda_1 - \lambda_2)$ or $\lambda_1/(\lambda_1 - \lambda_2)$ according as the intensity at λ_1 is greater or less than that at λ_2. Fig. 4 shows beats obtained with the two blue mercury lines, $\lambda_1 = 4358$ A.U. and $\lambda_2 = 4046$ A.U. The number of fringes per beat is theoretically $4046/(4358 - 4046) = 12{\cdot}9$*.

If the spectral distribution covers a range of wavelengths, the fringe pattern obtained is a group of fringes, whose contrast decreases as l increases. For a given shape of spectral distribution, if the band width is small, the number of fringes of acceptable contrast is proportional to, and of the same order as, the ratio of the mean wavelength to the band width. Appendix II gives the relation between fringe number and contrast for a rectangular intensity distribution, and compares this with the result for a Gaussian distribution given by Bennett[9].

Figs. 4b to 4d show the fringe patterns obtained with unfiltered white light and with three filters of different band widths.

Fig. 4f shows the effect of superimposing a narrow band and a nearly continuous spectrum. If the two band widths are λ_1 and λ_2, and their maximum intensities i_1 and i_2, then, except near the zero fringe, the large band width λ_2 will contribute a uniform intensity which reduces the contrast of the fringes due to the peak of width λ_1. The ratio of minimum to maximum intensities will be approximately

$$\frac{\lambda_2 i_2}{\lambda_2 i_2 + 2\lambda_1 i_1} = \left(1 + 2\frac{\lambda_1}{\lambda_2}\frac{i_1}{i_2}\right)^{-1}$$

A reasonable minimum contrast is about 2, giving $\lambda_2 i_2 = 2\lambda_1 i_1$, $i_2 = 2(\lambda_1/\lambda_2) i_1$. This places a severe restriction on the intensity of continuous spectrum which is tolerable, since in a practical case λ_1/λ_2 may be of the order of 1/50.

2.9. *Effect of Band-Width on Accuracy of Measurement of Fringe Shift.*—A spectral band width λ_1 at wavelength λ gives a number of clear fringes of the order λ/λ_1. If the interferometer is used

* In fact there appear to be about 11·7 fringes per beat. The reason for the discrepancy is not clear, but it may be due to dispersion or to the finite width of the lines at high pressure.

to measure the effective wavelength, this may be done by measuring the fringe spacing. The accuracy with which the position of the centre of the fringe may be determined will be a fraction, say ε, of the fringe spacing. The accuracy of the measurement is thus limited to $\varepsilon(\lambda_1/\lambda)$.

In practice, however, this limit is of little importance. The fringe shift to be measured must be less than the number of available fringes λ/λ_1. The error of measurement of the fringe shift N is ε/N which is greater than $\varepsilon\lambda_1/\lambda$. The accuracy thus depends mainly on the fringe shift to be measured, while this fringe shift limits the permissible band width λ_1. The error ε/N is in any case usually negligible, since if $\varepsilon = 1/10$ the error exceeds 1 per cent only if the fringe shift is less than 10 fringes.

If the fringe shift to be measured involves dispersion, the question is more complicated. If clear fringes are obtained, however, the error will again not exceed ε/N, where ε may be increased by the dispersion but will remain less than unity.

2.10. *Effect of Dispersion.*—(*a*) *Refracting plate.*—Suppose that one beam passes at zero incidence through a plate of uniform thickness D and refractive index μ, while the other suffers no dispersion. Suppose the beams are then incident approximately normally on a plane screen, where they are inclined to each other at angle α. The path difference l is then $l = (\mu - 1)D + \alpha x$, and the relative intensity for wavelength λ is $\cos^2(\pi/\lambda)\{(\mu - 1)D + \alpha x\}$.

This has a stationary value for variations of λ when

$$\frac{(\mu - 1)D + \alpha x}{\lambda} - D\frac{d\mu}{d\lambda} = 0\,,$$

i.e., when

$$\alpha x = -D\left\{(\mu - 1) - \lambda\frac{d\mu}{d\lambda}\right\}.$$

The change in path difference due to the plate is $(\mu - 1)D$ and so the plate produces a fringe shift $(\mu - 1)D/\lambda$. Fringes due to wavelengths near λ, however, reinforce each other not at the zero fringe $l = (\mu - 1)D + \alpha x = 0$, but at the fringe number $l/\lambda = D(d\mu/d\lambda)$. The group index $(\mu - 1) - \lambda(d\mu/d\lambda)$ is a function of wavelength, and so the position x at which fringes reinforce changes with wavelength. Thus at any position x there will be one band of wavelengths producing clear fringes. The result with white light if D/λ is large is that many fringes appear, the contrast is everywhere rather low and varies only slowly, while the colour and spacing of the fringes also change gradually as x increases. Fig. 5 shows the result obtained with a glass plate 0·067 in. thick. The figure also shows that a gelatin filter produces no increase in the number of fringes (it may even reduce the number) but does increase the contrast of the group due to light of the waveband passed by the filter.

To determine the effect of a filter on the number of fringes, consider the variation with λ of the position for fringe reinforcement. We have $x = -(D/\alpha)\{(\mu - 1) - \lambda(d\mu/d\lambda)\}$ and hence $dx/d\lambda = (D/\alpha)\lambda(d^2\mu/d\lambda^2)$. If the band width is λ_1, the range of x is

$$\lambda_1\frac{dx}{d\lambda} = \lambda_1\frac{D}{\alpha}\lambda\frac{d^2\mu}{d\lambda^2}\,.$$

Since the fringe spacing is λ/α, the number of fringes due to dispersion is of the order $\lambda_1 D(d^2\mu/d\lambda^2)$. But from section 2.8 and Appendix II, the number of fringes obtained with no dispersion is of the order λ/λ_1. Thus the total number is $(\lambda/\lambda_1) + \lambda_1 D(d^2\mu/d\lambda^2)$, which has a minimum with respect to λ_1 when $\lambda/\lambda_1 = \lambda_1 D(d^2\mu/d\lambda^2)$.

The contrast of the central fringes begins to decrease when the number of fringes due to dispersion, $\lambda_1 D(d^2\mu/d\lambda^2)$, becomes comparable with the number which would be obtained in the absence of dispersion, λ/λ_1. There is thus a limit to the permissible dispersion, and a reasonable criterion for this is $(\lambda/\lambda_1) = \lambda_1 D(d^2\mu/d\lambda^2)$, or, denoting the number of fringes, λ/λ_1, obtained in the absence of dispersion by M, $D\lambda(d^2\mu/d\lambda^2) = M^2$.

For a typical glass at $\lambda = 4{,}500$ A.U., $(d^2\mu/d\lambda^2) = 1{\cdot}375 \times 10^8$ per cm^2.

Hence $\lambda(d^2\mu/d\lambda^2) = 6{,}200$ per cm, and the limit on difference of thickness is given by:

$$D = \frac{M^2}{6{,}200} \text{ cm}$$

or

$$D = \frac{M^2}{15{,}700} \text{ in.}$$

The limit is most critical when white light is used, for which the number of fringes is about 5 to 8. A small amount of dispersion then noticeably increases the number of fringes and makes it difficult to identify a unique central fringe. For $M = 5$, the limit is $D = 25/15{,}700 = 1{\cdot}6 \times 10^{-3}$ in. Thus if the ability to identify a zero fringe when using white light is required, the difference in thickness of glass in the beams should be limited to about 1 or 2×10^{-3} in.

For $M = 50$, on the other hand, the limit becomes $0{\cdot}16$ in. Thus if identification of a zero fringe with white light is not required, the necessary limits are very wide.

(*b*) *Refracting prism.*—Suppose in the absence of dispersion the beams are incident approximately normally on a plane screen, where they are inclined to each other at angle α. Introduce into one beam a wedge of small angle, which increases the inclination of the rays at the screen by $\phi(\mu - 1)$. Then the total inclination is $\alpha + \phi(\mu - 1)$.

The fringe spacing for wavelength λ is

$$\frac{\lambda}{\alpha + \phi(\mu - 1)} = b \, .$$

Hence

$$\frac{db}{d\lambda} = \frac{+1}{\{\alpha + \phi(\mu - 1)\}^2} \left\{\alpha - \phi + \phi\left(\mu - \lambda \frac{d\mu}{d\lambda}\right)\right\}$$

$$\frac{db}{d\lambda} = 0 \text{ if } \alpha - \phi + \phi\left(\mu - \lambda \frac{d\mu}{d\lambda}\right) = 0 \, ,$$

or

$$\alpha + \phi(\mu - 1) = \phi\lambda \frac{d\mu}{d\lambda}$$

so that

$$b = \left(\phi \frac{d\mu}{d\lambda}\right)^{-1} .$$

Thus for a given prism there is one fringe spacing and direction for which the fringe spacing has a stationary value with respect to wavelength at the wavelength in question. In practice a large number of fringes may be obtained with white light if the interferometer is adjusted to give the correct spacing and direction*. Fig. 6 shows fringes obtained with white light and a $2\frac{1}{4}$-deg prism, for comparison with Fig. 4 for no dispersion. If the thicknesses of glass in the two beams are equal, there is a zero fringe position at which fringes due to all wavelengths reinforce, and the contrast is then high. Under these conditions the fringe number N is zero for all wavelengths at the zero fringe position $x = 0$, and $\partial^2 N/\partial\lambda \, \partial x = 0$. The refracting plate, which gives less contrasty and less achromatic fringes, has only $\partial N/\partial\lambda = 0$. It is, however, difficult in practice to obtain high and uniform fringe contrast with a prism under these conditions.

* The possibility of obtaining achromatic fringes by such methods is well known (*see*, for example, Preston, *Theory of Light*, section 97). Its application to the Mach-Zehnder interferometer has been noted by Th. Fromme, ' Ein Achromatisches Interferometer ', Actes du 2eme Congres International de Photographie et Cinematographie Ultra-Rapides, 1954,

(*c*) *Effect of additional fringe shifts on ' white-light ' fringes.*—White-light fringes produced by dispersion, by a prism or diffraction grating, result when the fringe number l/λ is independent of λ over an area of the screen, *i.e.*, when $\partial^2 N/\partial\lambda\partial x = 0$. Taking the origin of x where $l = 0$, this means that for the range of x and λ in question, $l = \beta\lambda x$ where β is a constant.

Now introduce an additional path difference l_1 independent of λ. Then $l = l_1 + \beta\lambda x$, and the fringe number $N = \beta x + l_1/\lambda$. For a constant fringe number, $x = (N/\beta) - (l_1/\beta\lambda)$. Thus the position of the fringe is no longer independent of wavelength and the fringes are no longer achromatic.

This means that the use of ' white-light ' fringes is usually of little or no practical advantage, since the optical system on which measurements are to be made is most unlikely to produce a dispersion which would allow the fringes to remain achromatic.

3. *Optics of the Ideal Four-Mirror Interferometer.*—3.1. *The Mach-Zehnder Interferometer.*—The Mach-Zehnder interferometer, arranged as in Fig. 7 and described for example in Refs. 7, 12, has become the standard type for use in aerodynamic research. The optical properties of the interferometer which account for this are as follows:

(*a*) The spacing of the beams, and the distance between the mirrors, may be adjusted to any desired value, subject to the necessity of retaining sufficient rigidity in the frame. The beams are uniform and parallel and pass once only through the working-section and compensating chamber.

(*b*) With no disturbance present, the path difference may be easily adjusted to zero. Thus the number of fringes required is the least possible, and the permissible band width, and hence intensity, a maximum.

(*c*) With no disturbance, the instrument may be adjusted so that rays meeting and interfering on the screen emerge from the source almost coincident, so that a large source may be used, which gives enough light to permit the use of very short exposure times.

(*d*) Little light is absorbed, and two beams emerge, so that nearly half of the incident light, of the waveband transmitted by the monochromator, reaches the screen.

(*e*) The five adjustments are simply related to the direction and spacing of the fringes obtained, with no disturbance, in the source and screen planes, and to the fringe number at a fixed point of the screen.

3.2. *The Ideal Four-Mirror Interferometer.*—The spacing and direction of the fringes, and the fringe contrast, obtained with a real interferometer, depend largely on the positions of the four mirrors, and these are normally used for adjustment. The effect of the mirror positions may be investigated by considering an ideal interferometer whose optical elements are four perfectly plane mirrors of zero thickness, two of which are semi-reflecting, and a collimating lens free from aberration.

Fig. 8 is a diagram of such an interferometer. Two rays leave the source A, which is in the focal plane of the collimating lens, pass round the two paths through the interferometer and intersect at point B. The conditions for interference are that the wavelengths are the same, the rays emerge from the same point A and are therefore parallel after passing the lens, and the rays meet and are similarly polarised at the point B. If the co-ordinates of A and B are respectively x', y', and x, y, z, then for a given point A the fringe number, direction and spacing at B depend on l, $\partial l/\partial x$, $\partial l/\partial y$, $\partial l/\partial z$, while the fringe contrast depends on the source configuration and the variation of l with x' and y'. Since the position of A determines the direction of the rays after passing the lens, and since the path length is the same in either direction, we have to consider the path difference between pairs of rays which start from B, go round the two paths and emerge parallel. The variation with inclination determines the fringe pattern in the source plane, and hence the effect of source size, The variation with position of B for a given direction determines the fringe configuration in the emergent beam for a given source position.

3.3. *Effect of Reflection at a Plane Mirror.*—This is determined by the laws of reflection, namely that the incident ray, the normal and the reflected ray lie in the same plane, and the angles of incidence and reflection are equal. The relevant consequences are as follows:

(*a*) Light coming from a point after reflection appears to proceed from an image point lying on the same normal to the mirror plane at an equal distance on the opposite side of this plane.

(*b*) The position of this image is independent of the direction of the reflected ray but depends on the mirror position.

(*c*) Rotation of the mirror about any axis in its plane rotates the image about the same axis through twice the angle.

(*d*) Rotation of the mirror about any axis normal to its plane has no effect on the image.

(*e*) Traversing the mirror in the direction of the normal traverses the image through twice the distance in the same direction.

3.4. *Path Difference at One Point.*—From the preceding sections it appears that the path difference l_{AB} is the same as that between rays emerging parallel to each other from the images B', B'' of B in mirrors 4, 3 and 2, 1, respectively (Fig. 8). From Fig. 9, if the distance $B'B''$ is ε, the path difference is $\varepsilon \cos \psi$, where ψ is the angle between the rays and the line joining the images.

Now the image in the source plane of points B, B', B'', lies on the line parallel to the rays through the centre of the lens (Fig. 10). Thus the fringes in the source plane (lines of constant $\varepsilon \cos \psi$) are the intersections of this plane with cones, whose apex is the lens centre, whose axis lies parallel to the line joining the images, and whose semi-angles are given by $\varepsilon \cos \psi = N\lambda$.

Usually the source size is small, less than $0{\cdot}1f$, and so we are concerned only with rays making small angles with the lens axis. Take co-ordinates z along this axis, with z increasing in the direction of the light path, x and y perpendicular to the axis, using the axis system and sign conventions shown in Fig. 11*. Then if the differences between the co-ordinates of B' and B'' are ε_x, ε_y, ε_z, the path difference is approximately:

$$\varepsilon_x\omega_y - \varepsilon_y\omega_x + \varepsilon_z - \varepsilon_z\left(\frac{\omega_x^2 + \omega_y^2}{2}\right)$$

where ω_x and ω_y are the angles in the yz and zx planes between the rays and the lens axis. Since ω_x and ω_y are less than $0{\cdot}1$, the last term is less than 1 per cent of ε_z and is usually negligible.

If the co-ordinates of the image of B in the source plane are x', y', then $\omega_y = -x'/f$, $\omega_x = +y'/f$, and the path difference is:

$$l = -\frac{\varepsilon_x}{f}x' - \frac{\varepsilon_y}{f}y' + \varepsilon_z - \frac{\varepsilon_z}{2f^2}(x'^2 + y'^2). \quad .. \quad .. \quad .. \quad (3.1)$$

3.5. *General Expression for Path Difference.*—Suppose the origin of the co-ordinate system x, y, z is the image of point C in the emergent beam, and suppose the co-ordinates of the other image of C are ε_{x0}, ε_{y0}, ε_{z0}. Then since the distance between corresponding points in the two images are the same, and since the angles are small, we can express ε_x, ε_y, ε_z as:

$$\left.\begin{aligned} \varepsilon_x &= \varepsilon_{x0} - y\alpha_z + z\alpha_y \\ \varepsilon_y &= \varepsilon_{y0} - z\alpha_x + x\alpha_z \\ \varepsilon_z &= \varepsilon_{z0} - x\alpha_y + y\alpha_x \end{aligned}\right\}, \quad .. \quad .. \quad .. \quad .. \quad .. \quad (3.2)$$

* The sign conventions and axis system given here differ from those of the original paper[12] (A.R.C. 18,733). The axis system given here is a right-handed system, and the signs of the ω's have been made consistent with those of the α's.

where α_x, α_y, α_z are small rotations about the x, y and z axes. Fig. 11 gives a geometrical diagram of these displacements.

Substituting (3.2) in (3.1), and neglecting the term in $x'^2 + y'^2$, we obtain:

$$l = \varepsilon_{z0} - x\alpha_y + y\alpha_x - \frac{x'}{f}(\varepsilon_{x0} - y\alpha_z + z\alpha_y) - \frac{y'}{f}(\varepsilon_{y0} - z\alpha_x + x\alpha_z) \quad \ldots \quad (3.3)$$

3.6. *Fringes in the Emergent Beam.*—If the source is a point on the lens axis, $x' = y' = 0$, and $l = \varepsilon_{z0} - x\alpha_y + y\alpha_x$. The path difference thus varies linearly with x and y, and the fringes are thus planes, uniformly spaced. The spacing in the x and y directions is λ/α_y and λ/α_x respectively, and the spacing perpendicular to the fringe plane $\lambda/\sqrt{(\alpha_x^2 + \alpha_y^2)}$.

More directly, the fact that the fringes are uniformly spaced planes is clear from the fact that both wave fronts are plane. The relation between spacing and inclination is that given in section 2.3 and demonstrated in Fig. 2.

The fringes appear to be parallel to the z-axis ($\partial l/\partial z = 0$), owing to the neglect of terms in α_x^2 and α_y^2 in equation (3.2). In fact the fringes are inclined to the z-axis at angles $\alpha_x/2$, $\alpha_y/2$ as shown in section 2.3.

If the source is a point off the lens axis, we obtain:

$$l = \varepsilon_{z0} - x\left(\alpha_y + \frac{y'}{f}\alpha_z\right) + y\left(\alpha_x + \frac{x'}{f}\alpha_z\right) + z\left(-\frac{x'}{f}\alpha_y + \frac{y'}{f}\alpha_x\right) - \frac{x'}{f}\varepsilon_{x0} - \frac{y'}{f}\varepsilon_{y0}.$$

The fringes are now planes roughly parallel to the line joining the source to the lens centre. Their spacing is the same as for the source on the axis if $\alpha_z = 0$. For any value of α_z, the spacings in the x and y directions are $\lambda/\{\alpha_y + (y'/f)\alpha_z\}$ and $\lambda/\{\alpha_x + (x'/f)\alpha_z\}$ respectively.

3.7. *Fringes in the Source Plane.*—So far as the effect of change of source position is concerned, only the variations in the path difference over the source plane are important. We thus have to consider $l - \varepsilon_z$, since ε_z is the path difference for a source at the origin $x' = y' = 0$.

Now $l - \varepsilon_z = -(x'/f)\varepsilon_x - (y'/f)\varepsilon_y - (\varepsilon_z/2f^2)(x'^2 + y'^2)$, and the first two terms give a set of straight fringes whose spacing in the x and y directions is $\lambda f/\varepsilon_x$ and $\lambda f/\varepsilon_y$. The last term gives circular fringes of radii r' given by $r'^2 = 2f^2(\lambda N/\varepsilon_z)$. The radius of the first is $r'/f = \sqrt{(2\lambda/\varepsilon_z)}$, which is greater than $0 \cdot 1$ unless $\varepsilon_z > 200\lambda$. In aerodynamic interferometry this value is unlikely to be reached in practice and so the last term is usually negligible.

Neglecting this term, we have

$$l - \varepsilon_z = -\frac{x'}{f}\varepsilon_x - \frac{y'}{f}\varepsilon_y \quad \ldots \quad (3.4)$$

Thus if $\varepsilon_x = \varepsilon_y = 0$, that is, if the two images everywhere coincide, or if they are displaced only along the axis of the lens, there are no fringes in the source plane and the permissible source size is practically unlimited.

Substituting in (3.4) from (3.2) we obtain

$$l - \varepsilon_z = -\frac{x'}{f}(\varepsilon_{x0} - y\alpha_z + z\alpha_y) - \frac{y'}{f}(\varepsilon_{y0} - z\alpha_x + x\alpha_z) \quad \ldots \quad (3.5)$$

(*a*) $\alpha_z = 0$.—If $\alpha_z = 0$, $l - \varepsilon_z = -(x'/f)(\varepsilon_{x0} + z\alpha_y) - (y'/f)(\varepsilon_{y0} - z\alpha_x)$.

This is independent of x and y. Thus if we have a screen normal to the rays, the effect of changing the source position is the same for all points on the screen. Thus with any source configuration the fringe contrast is the same at all points on the screen.

The fringes in the source plane are linear and inclined to the x-axis at an angle β' given by:

$$\tan \beta' = -\frac{(\varepsilon_{x0} + z\alpha_y)}{\varepsilon_{y0} - z\alpha_x} \quad \ldots \quad (3.6)$$

Their spacing is $(f\lambda)/\sqrt{\{(\varepsilon_{x0} + z\alpha_y)^2 + (\varepsilon_{y0} - z\alpha_x)^2\}} = b'$. The permissible source configuration is thus a set of bands of width $b'/4$ to $3b'/4$ (section 2.6 and Appendix I) spaced at distance b' apart and aligned parallel to the fringes.

(*b*) $\alpha_z = 0$, $\varepsilon_{x0} = \varepsilon_{y0} = 0$.—In this case the displacement of the images consists of a rotation about an axis perpendicular to the lens axis. From equation (3.6), $\tan \beta' = +(\alpha_y/\alpha_x)$. From section 3.6, the fringes in the emergent beam are at an angle β given by $\tan \beta = +(\alpha_y/\alpha_x)$. Thus $\beta = \beta'$, and the permissible source consists of bands parallel to the fringes in the emergent beam. The spacing of the fringes in the source plane is $b' = (f/z)\{\lambda/\sqrt{(\alpha_x^2 + \alpha_y^2)}\}$, which is f/z times the spacing of the fringes in the emergent beam.

If the source consists of narrow bands spaced at distance d', the fringes will be clear when $d' = Nb'$ where N is any integer. In terms of the fringe spacing in the emergent beam:

$$d' = Nb' = \frac{Nfb}{z}$$

or

$$z = \frac{Nfb}{d'}.$$

Thus the fringes are in focus at intervals along the z-axis of $(f/d')b$. Fig. 12 shows the result obtained by placing the screen at 45 deg to the z-axis with $f/d = 20$. In Fig. 12a the 45-deg rotation was about an axis parallel to the fringes, while in Fig. 12b the axis was perpendicular to the fringes. Thus in Fig. 12a the number of fringes per ' beat ' is 20, while in Fig. 12b the distance between ' beats ' along the screen is $20\sqrt{2}$ times the fringe spacing.

If the source consists of a single band of width $d' = kb'$, the fringe contrast will depend on k as shown in Appendix I. Taking a reasonable criterion as $k = \frac{1}{2}$, the depth of focus of the fringe is given by:

$$d' = \frac{b'}{2} = \frac{fb}{2z},$$

$$z = \frac{fb}{2d'}.$$

(*c*) $\alpha_z = 0$, $\varepsilon_{x0} = \varepsilon_{y0} = 0$, $z = 0$.—This case is the same as the last but with the screen in the plane $z = 0$. The displacement of the images consists of a rotation about an axis perpendicular to the lens axis and in the same plane as the screen.

With this type of displacement, from (3.5), $l - \varepsilon_z$ is everywhere zero, and so there is no practical limit to the source size. Since α_x and α_y are not necessarily zero, any fringe spacing and direction in the emergent beam is theoretically possible. We shall show below, section 4.2, that with the usual arrangement of the mirrors in the form of a parallelogram it is, however, impossible to obtain $\alpha_z = 0$ with $\alpha_x \neq 0$, so that only one fringe direction is possible with the unlimited source size.

(*d*) $\alpha_z \neq 0$, $\varepsilon_{x0} = \varepsilon_{y0} = 0$, $z = 0$.—This gives $l - \varepsilon_z = (\alpha_z/f)(x'y - y'x)$.

The spacing of the fringes in the source plane is $(\lambda/f)/\{\alpha_z\sqrt{(x^2 + y^2)}\}$ and their direction β is given by $\tan \beta = y/x$. Thus the spacing is inversely proportional to the distance of the point x, y on the screen from the lens axis, and the direction parallel to the line joining this point to the axis. Effects of different source configurations are as follows:

(i) *Circular source of radius r'*.—This gives contrasty fringes at the point x, y, if $2r' \leqslant (k\lambda f)/(\alpha_z r)$ where k is from $\frac{1}{4}$ to $\frac{3}{4}$ (Appendix I) and $r = \sqrt{(x^2 + y^2)}$. Thus the region of contrasty fringes is circular, centred on the z-axis, and of radius $r \leqslant (k\lambda f)/(2\alpha_z r')$.

Fig. 13a shows the result, with $r'/f = 0{\cdot}05$. In this figure, $\alpha_z = -\alpha_x$, and so the fringe spacing $b = \lambda/\alpha_z$. Substituting, we obtain $r \leqslant 10kb$, and so the number of fringes visible should be $20k$. In fact about 20 fringes are visible, confirming that the contrast becomes very low at about $k = 1$.

(ii) *Linear source of width d' and direction β'*.—Fringes will be clear at x, y, if $y/x = \tan \beta'$ and if

$$d' < \frac{k\lambda f}{\alpha_z r'}$$

or

$$r' < \frac{k\lambda f}{\alpha_z d'}$$

Thus clear fringes are obtained along a line in the same direction as the slit source, and the length of the line is inversely proportional to the width of the source. In practice a band of fringes appears, and the width of the band is inversely proportional to the effective length of the source.

Figs. 13b and 13c show the results with $\alpha_z = -\alpha_x$ and with the slit of length $0{\cdot}1f$ and width $0{\cdot}013f$, aligned along and perpendicular to the fringes.

(iii) *Series of circular sources*.—The fringes due to point x, y in the emergent beam are spaced at $b' = (\lambda f)/(\alpha_z r)$. The spacings in the x and y directions are thus $b_x' = (\lambda f)/(\alpha_z x)$ and $b_y' = (\lambda f)/(\alpha_z y)$. If, therefore, the source consists of a series of circles or squares of width d_y' and spacing d_x' along the x-axis, then clear fringes will appear if $d_x' = Nb_x' = (N\lambda f)/(\alpha_z x)$ where N is any integer, $d_y' < kb_y'$, or $d_y' < (k\lambda f)/(\alpha_z y)$. Thus fringes appear at points $y < (k\lambda f)/(\alpha_z d_y')$ along lines parallel to the y-axis at values of x given by $x = (Nf\lambda)/(\alpha_z d_x')$.

3.8. *Fringes in Planes Other than the Focal Plane of the Lens*.—Let the two images of point x, y be at B', B'', Fig. 14, and let the source plane be distant q from the focal plane. Then the interfering rays will appear to come from the image x'', y'' of the source x', y'. This image is in a plane distant f^2/q from the other focal plane of the lens. When z is measured from this focal plane, the distance from B' to the image along the z-axis is $(f^2/q) - z$. Since x'', y'' is the image of x', y', the path difference from B', B'' to x'', y'' is the same as to x', y'. If the angle subtended by $B'B''$ at x'', y'' is small, the path difference is, as in section 3.4,

$$l = \varepsilon_x \omega_y - \varepsilon_y \omega_x + \varepsilon_z - \varepsilon_z \frac{(\omega_x^2 + \omega_y^2)}{2},$$

and the last term is usually negligible.

The angles ω_x and ω_y between the rays and the lens axis are approximately:

$$\omega_y = \frac{x'' - x}{(f^2/q) - z}, \qquad \omega_x = \frac{-(y'' - y)}{(f^2/q) - z}.$$

Since the magnification is $-f/q$,

$$x'' = -\frac{f}{q}x', \qquad y'' = -\frac{f}{q}y'.$$

Substituting,

$$\omega_y = -\frac{(fx' + qx)}{f^2 - qz},$$

$$\omega_x = +\frac{(fy' + qy)}{f^2 - qz}.$$

The derivative with respect to q is:

$$-\frac{\partial l}{\partial q} = \frac{z}{f^2}(x'\varepsilon_x + y'\varepsilon_y) + \frac{x}{f^2}(\varepsilon_{x0} + z\alpha_y) + \frac{y}{f^2}(\varepsilon_{y0} - z\alpha_x) .$$

In terms of the derivatives with respect to x' and y' at $q = 0$,

$$\frac{\partial l}{\partial q} = \frac{\partial l}{\partial x'}\left(\frac{x}{f} + \frac{x'z}{f^2}\right) + \frac{\partial l}{\partial y'}\left(\frac{y}{f} + \frac{y'z}{f^2}\right) .$$

If $x' = y' = 0$, we can express this in polar co-ordinates as:

$$\frac{\partial l}{\partial q} = \frac{y}{b'}\frac{r}{f}\cos(\beta' - \theta) ,$$

where b' is the fringe spacing in the x', y' plane. β' the fringe direction, $r = \sqrt{(x^2 + y^2)}$ and $\theta = \tan^{-1}(y/x)$. Thus the permissible source depth is

$$\frac{k\lambda}{\partial l/\partial q} = kb'\frac{f}{r}\sec(\beta' - \theta) .$$

The ratio of the depth to the permissible width is thus $(f/r)\sec(\beta' - \theta)$, whose minimum value is twice the reciprocal of the lens aperture.

The terms in x' and y' are negligible in practice, since if we use a single source of width $x' = d'$, then we must have $d'(\partial l/\partial x') < k\lambda$, and so the x' term in $\partial l/\partial q$ is less than $k\lambda z/f^2$. Since z/f is of order unity, the change in q for $(\partial l/\partial q)\delta q = k\lambda$ is of the same order as f, and so represents no restriction in practice.

3.9. *Effect of Aberrations of the Collimating Lens.*—Place a point source in the focal plane of a lens without aberrations, and consider the path lengths of the emergent rays at a plane near the lens and normal to its axis. The path length of a ray passing through this plane at x_0, y_0, differs from that of the ray passing through at $x = y = 0$ by $l = (x'/f)x_0 + (y'/f)y_0$. If the lens has aberrations, we may express this path difference as $l = (x'/f)x_0 + (y'/f)y_0 + L(x_0, y_0, x', y', \lambda)$. The inclination to the axis of the ray passing through x_0, y_0 is now:

$$\left.\begin{aligned} \omega_y &= -\frac{\partial l}{\partial x_0} = -\frac{x'}{f} - \frac{\partial L}{\partial x_0} \\ \omega_x &= \frac{\partial l}{\partial y_0} = \frac{y'}{f} + \frac{\partial L}{\partial y_0} \end{aligned}\right\} \quad \ldots\ldots\ldots\ldots\ldots\ldots \quad (3.7)$$

From section 3.4, the change in the path difference is:

$$-\varepsilon_x\frac{\partial L}{\partial x_0} - \varepsilon_y\frac{\partial L}{\partial y_0}$$

where, if we take the origin of z at the surface near the lens at which x_0, y_0, are measured $x_0 = x - z\omega_y$, $y_0 = y + z\omega_x$. The path difference for a given lens depends only on the displacements ε_x and ε_y and becomes zero when these are zero. Thus, with the ideal interferometer, it is always possible to obtain straight fringes of any required direction and spacing, however bad the lens may be.

From equation (3.7) it appears that the aberration is equivalent to a change of source position of $f\partial L/\partial x_0$ and $f\partial L/\partial y$. Thus the effect of aberration is related to that of source size. If the adjustment is such that a movement $\delta x'$ of the source in the x' direction produces a fringe shift of one fringe then the permissible length of the source is $k\delta x'$. If the aberration is $\partial L/\partial x_0$, this produces unit fringe shift when $f\partial L/\partial x_0 = \delta x'$. The effects of aberration will thus be important in practice only if the circle of confusion in the focal plane which arises when a parallel beam is incident on the lens is larger than the size of source which is to be used.

Since the source is normally small and placed on the lens axis, three aberrations, astigmatism, spherical and chromatic aberration, are important in practice.

(*a*) *Astigmatism.*—For astigmatism, $L = (x_0^2/2f^2)(z_s - z_x) + (y_0^2/2f^2)(z_s - z_y)$, where z_s, z_x and z_y are the values of z of the source and of the foci in the zx and zy planes respectively. Hence $\partial L/\partial x_0 = (x_0/f^2)(z_s - z_x)$ and $\partial L/\partial y_0 = (y_0/f^2)(z_s - z_y)$ and so the fringe number due to the aberration is:

$$-\frac{\varepsilon_x x_0}{\lambda f^2}(z_s - z_x) - \frac{\varepsilon_y y_0}{\lambda f^2}(z_s - z_y) .$$

The fringes are thus straight lines whose spacing in either direction is inversely proportional to the distance from the source to the corresponding focal point, and to the image displacement in that direction.

(*b*) *Spherical aberration.*—For spherical aberration, $L = Ar^4$, where r is the radius $\sqrt{(x_0^2 + y_0^2)}$. Hence $\partial L/\partial x_0 = 4Ar^2x_0$ and $\partial L/\partial y_0 = 4Ar^2y_0$. The change in path difference is $-4Ar^2(x_0\varepsilon_x + y_0\varepsilon_y)$, and the circle of confusion in the axial focal plane has radius $4Ar^3f$.

Figs. 15a and 15b show results, with $\varepsilon_x = 0$, $\varepsilon_y = 0{\cdot}027$ in., $\lambda = 5{,}460$ A.U. The spherical aberration was measured by using a parallel incident beam, small apertures at radii 1 in., $1{\cdot}5$ in., 2 in. and $2{\cdot}5$ in., and placing a photographic plate at the axial focus. Fig. 15c shows the result, and measurement of this gives $A = 1{\cdot}10 \times 10^{-4}$ in.$^{-3}$. Hence the fringe shift due to the aberration is approximately $(4Ar^2y\varepsilon_y)/\lambda$, neglecting $x - x_0$ and $y - y_0$, which equals $0{\cdot}552r^2y$. Fig. 16 shows this value, for $x = 0$, plotted against y, and, for comparison, experimental values from Fig. 15b.

(*c*) *Chromatic aberration.*—This gives $L = r^2B(\lambda)$. Hence $\partial L/\partial x_0 = 2x_0B(\lambda)$ and $\partial L/\partial y_0 = 2y_0B(\lambda)$. The change in path difference is $-2B(\lambda)(x_0\varepsilon_x + y_0\varepsilon_y)$. The fringe spacing in the x and y directions is thus:

$$b_x = \frac{\lambda}{\alpha_y + 2B(\lambda)\varepsilon_x}$$

$$b_y = \frac{\lambda}{\alpha_x - 2B(\lambda)\varepsilon_y} .$$

The derivative of b_x with respect to λ is

$$\frac{\partial b_x}{\partial \lambda} = \frac{b_x^2}{\lambda^2}\left\{\alpha_y + 2\varepsilon_x\left(B - \lambda\frac{dB}{d\lambda}\right)\right\},$$

which becomes zero when

$$\alpha_y = -2\varepsilon_x\left(B - \lambda\frac{dB}{d\lambda}\right)$$

or when

$$b_x = \frac{1}{2\varepsilon_y(dB/d\lambda)} .$$

Similarly

$$b_y = \frac{-1}{2\varepsilon_y(dB/d\lambda)} .$$

For a simple thin lens, $1/f$ is proportional to $\mu - 1$, and so $(\mu - 1)f$ is independent of λ. If $L = 0$ when $\mu = \mu_0$, this gives $\partial L/\partial x_0 = x_0[(\mu - \mu_0)/\{(\mu - 1)f\}]$. Hence

$$2(dB/d\lambda) = [1/\{(\mu - 1)f\}](d\mu/d\lambda),$$

and the fringe spacings for achromatic fringes are

$$b_x = \frac{(\mu - 1)f}{\varepsilon_x(d\mu/d\lambda)}$$

$$b_y = \frac{(\mu - 1)f}{\varepsilon_y(d\mu/d\lambda)}.$$

Thus ' white-light ' fringes may be obtained, with any desired spacing and inclination, by using a simple lens with chromatic aberration. For the reasons given in section 2.10 (*c*), however, this is of little advantage in practice.

3.10. *The Four-mirror Instrument as a Wave-Shearing Interferometer.*—Section 3.9 may be regarded as a discussion of the use of the interferometer as a wave-shearing instrument to measure the aberrations of the lens. More generally, if any disturbance is placed in the parallel beam emerging from the lens, and if it increases the optical path by $L(x_0, y_0)$, then the resulting increase in the path difference at the point x, y is $-\varepsilon_x(\partial L/\partial x_0) - \varepsilon_y(\partial L/\partial y_0)$. If the screen is focussed on the disturbance, (x, y) is the image of (x_0, y_0), $z = 0$, and the increase is $-\varepsilon_{x0}(\partial L/\partial x_0) - \varepsilon_{y0}(\partial L/\partial y_0)$. Thus the interferometer measures the change of optical path in a distance equal to the displacement of the images. Fig. 17b shows a photograph of a candle flame taken in this way with $\varepsilon_{y0} = 0$, $\varepsilon_{x0} = 0{\cdot}04$ in. Fig. 17a shows a normal Mach-Zehnder interferogram for comparison.

Owing to the necessity of using displaced images, the permissible source size becomes rather small when the interferometer is used in this way. From section 3.7 (*a*), putting $z = 0$ since the disturbance should be focussed on the screen, the fringe spacing in the source plane is $b' = (f\lambda)/\sqrt{(\varepsilon_{x0}^2 + \varepsilon_{y0}^2)}$. The maximum source width for clear fringes is kb' (Appendix I). Thus for example if $\lambda = 2 \times 10^{-5}$ in., and $\sqrt{(\varepsilon_{x0}^2 + \varepsilon_{y0}^2)} = 0{\cdot}01$ in., and taking $k = \frac{1}{2}$, the maximum source size is given by $b'/f = \frac{1}{2}\{(2 \times 10^{-5})/10^{-2}\} = 1/1000$.

3.11. *Effect of Lenses and Diaphragms in the Emergent Beam.*—(*a*) *Effect of lenses.*—The foregoing discussions, and the figures, show clearly that the fringes are real variations of light intensity at definite positions in space in the emergent beam. Now suppose we place a lens without aberrations in the emergent beam, and consider the fringes at the point x'', y'' which is an image of the point x, y. The optical path from x, y to x'', y'' is independent of the direction of the ray passing through x, y. It is therefore the same for both beams and for all source positions. Thus if all rays passing through x, y also pass through the lens, the variations of intensity at the image position will be the same as at the object position, apart from the magnification factors. The fringe pattern will thus be an exact image of that at the corresponding position in the emergent beam.

Virtual objects.—The point x, y, of which x'', y'' is the image, will often be a virtual object. Fig. 18 shows two arrangements in which the object is real and virtual, and makes clear that this depends only on the relative positions of the screen, lens and interferometer mirrors. If the object is virtual, as it normally will be in practice, the path difference at the image x'', y'' between rays arriving *via* the two paths is the path difference between one ray and the image of the other at the virtual object position. Since the images B', B'' of Figs. 8, 9, 10, and sections 3.4 to 3.8 are now the images of this virtual object, this is the path difference which has been discussed in these sections. Thus the fringes on the screen are the image of those at the point x, y, z; the fringes at x, y, z are real or virtual according as this point is one one side or the other of the mirror 4, but this is immaterial so far as the real fringes on the screen are concerned.

(*b*) *Effect of diaphragms.*—Consider a diaphragm either in front of or at the lens position, and at distance x_D, y_D from the z-axis, at a position distant z_D from the object plane in focus on the

screen. Then, since the rays of the two beams are inclined to the z-axis at angles ω_x, ω_y and $\omega_x + \alpha_x$, $\omega_y + \alpha_y$ respectively, the outer edge of the field of view for the two beams are given by $x - \omega_y z_D = x_D$, and $x - (\omega_y + \alpha_y) z_D = x_D$ respectively, with corresponding equations for the y direction.

First suppose $\omega_x = \omega_y = 0$, that is, a point source. Then the maximum values of x for the two beams differ by $\alpha_y z_D$. Thus the image has an edge strip of width $\alpha_y z_D$ which receives light from one beam only and thus shows no fringes. If the fringe spacing is b_x and the width of the strip Nb_x, then $Nb_x = (\lambda/b_x) z_D$ or $N = (\lambda z_D)/b_x^2$. In practice λ is about 2×10^{-5} in., and z_D usually less than 50 in. This gives $N = 1$ when $b_x = 1/32$ in. Thus the effect is usually negligible.

The effect is qualitatively similar for any diaphragm position except when the diaphragm is near the focus of the source. In this position, if one beam is removed, the result is a schlieren photograph of the disturbance in the other beam. With both beams, the fringes appear only in regions where both schlieren images are bright. Diaphragms in this position should be avoided.

Now suppose ω_y is large compared with α_y. The result is that at the edges of the image, light from both beams arrives from only part of the area of the source. The intensity will be reduced, and the contrast may be increased, depending on the fringe pattern in the source plane.

The effect is again similar for all diaphragm positions, except that for a diaphragm at the position of the image of the source the effective source size is the same everywhere in the field. For the reason given above, however, this is of no use in practice.

Winkler[7], discussing the effect of diaphragms, concludes that a diaphragm at this position does not affect the fringe contrast. His argument assumes, however, that α is large compared with ω. In practice, both are usually of the same order ; the diaphragm will usually increase the contrast over some parts of the field, but this is of no practical advantage.

3.12. *Relation between the Two Emergent Beams—Effect of Reflection Ratio.*—Two beams, (1) and (2), emerge from the interferometer, as shown in Fig. 8. Corresponding to any point B in (1) there is a point B_2 in beam (2) having the same images B', B''. Since there is ideally no absorption, all the light from A which appears to go through B' and B'' actually goes either through B or through B_2. The sum of the intensities at B and B_2 thus equals the intensity in the incident beam.

So the fringe patterns in the two beams are complementary. If there is a light fringe at B there is a dark fringe at the corresponding point B_2. If there is a coloured fringe at B there is a fringe of the complementary colour at B_2.

In beam (1), light *via* each path has been transmitted through one plate and reflected by one. If the interferometer is a parallelogram, so that the angles of incidence are equal, and if the reflection ratios of the two plates are equal, light *via* each path suffers exactly the same operations though in a different order. The intensity *via* each path is the same and the light is similarly polarised. Hence when the waves are exactly out of phase and cancel, the resulting intensity is zero.

In beam (2), on the other hand, light *via* one path is transmitted by both plates while light *via* the other path is reflected by both. Thus unless the reflection ratio of each plate is equal to its transmission ratio, for the two directions of polarization in and normal to the plane of incidence separately, the intensity arriving *via* each path will not be the same. This equality will not normally be achieved, and so the fringe contrast in beam (2) will be poorer than that in beam (1). If the reflection and transmission ratios are not very unequal, however, the contrast may be good enough for the beam to be useful. If plane polarized light is used, full contrast may be obtained if the reflection ratio equals the transmission ratio in the plane of polarization*.

* The discussion of the effect of reflection ratio on contrast given in Ref. 12 is incorrect owing to neglect of the fact that the reflection ratios for the two planes of polarization are unlikely to be equal.

If the reflection ratios of the two plates are unequal, or if the interferometer is not a parallelogram, the intensities in beam (1) due to each path separately, or the extent to which they are polarised, may not be the same, and so the contrast may be reduced even in this beam.

4. *Mirror Adjustments of the Mach-Zehnder Interferometer.*—4.1. *The Plane Four-Mirror Interferometer—Relation between Mirror Adjustments and Image Displacements.*—Consider an interferometer, Fig. 19, adjusted so that rays CD, CE, DF, EF all lie in one plane, the path lengths are equal, i.e., $CD + DF = CE + EF$* and rays resulting from division of a single ray at mirror 1 meet and coincide after leaving mirror 4. Then $l = 0$ and all the image displacements ε_{x0}, ε_{y0}, ε_{z0}, α_x, α_y, α_z are zero.

Now consider the effect of displacements of mirror 1 as follows:

$\frac{\varepsilon_1}{2}$ A translation along the mirror normal, in such direction as to increase the path length of the reflected ray

$\frac{X_1}{2}$ A rotation about an axis in the mirror plane and in plane $CDEF$, anti-clockwise when viewed in the direction of the positive x-axis

$\frac{Y_1}{2}$ A rotation about an axis in the mirror plane and normal to plane $CDEF$, anti-clockwise when viewed in the direction of the positive y-axis.

Then from the laws of reflection, section 3.3, we have

$$\begin{aligned} \alpha_x &= X_1 \cos i_1 \\ \alpha_y &= Y_1 \\ \alpha_z &= -X_1 \sin i_1 . \end{aligned}$$

For $x = y = 0$, $z = z_1$,

$$\begin{aligned} \varepsilon_x &= \varepsilon_1 \sin i_1 \\ \varepsilon_y &= 0 \\ \varepsilon_z &= \varepsilon_1 \cos i_1 . \end{aligned}$$

Substituting in (3.2), we obtain

$$\begin{aligned} \varepsilon_{x0} &= \varepsilon_1 \sin i_1 - z_1 Y_1 \\ \varepsilon_{y0} &= z_1 X_1 \cos i_1 \\ \varepsilon_{z0} &= \varepsilon_1 \cos i_1 \\ \varepsilon_x &= \varepsilon_1 \sin i_1 + y X_1 \sin i_1 + (z - z_1) Y_1 \\ \varepsilon_y &= -(z - z_1) X_1 \cos i_1 - x X_1 \sin i_1 \\ \varepsilon_z &= \varepsilon_1 \cos i_1 - x Y_1 + y X_1 \cos i_1 . \end{aligned}$$

Now to obtain the total image displacements we must add the effects of all the mirrors. Denote the displacements of mirrors 2 to 4 by the corresponding suffixes, and adopt a sign convention such that a mirror rotation or translation is positive if its effect on the image displacements is in the same direction as that of the corresponding positive displacement of mirror 1. The positive directions are shown in Fig. 19. Denoting summation for $k = 1$ to 4 by Σ, we obtain:

$$\left.\begin{aligned} \varepsilon_{z0} &= \Sigma\ \varepsilon_k \cos i_k \\ \varepsilon_{x0} &= \Sigma\ \varepsilon_k \sin i_k - \Sigma\ z_k Y_k \\ \alpha_y &= \Sigma\ Y_k \\ \varepsilon_{y0} &= \Sigma\ z_k X_k \cos i_k \\ \alpha_x &= \Sigma\ X_k \cos i_k \\ \alpha_z &= \Sigma\ -X_k \sin i_k \end{aligned}\right\} \quad \ldots\ \ldots\ \ldots\ \ldots\ \ldots\ \ldots \quad (4.1)$$

* Dr. I. Hall has pointed out that the geometrical condition for this is that the intersections D, E of the rays with mirrors 2 and 3 must lie on an ellipse whose foci are points C and F, where the rays intersect mirrors 1 and 4.

It follows from inspection that of the twelve possible adjustments ε_k, X_k, Y_k, only six are necessary to obtain any desired values of the six displacements.

The last three displacements depend on X_k only. Hence, three of the adjustments X_k are necessary (three of the four mirrors must have fine adjustments about their horizontal* axes) and for α_x and α_z to be independent, two of these must be associated with different values of the incidence i_k. Thus for independence of all the displacements it is necessary and sufficient that the angles of incidence should not all be equal, *i.e.*, that the interferometer is not a parallelogram.

From the first three equations, the other three adjustments may be either one translation ε_k and two rotations Y_k associated with different values of z_k, or one rotation Y_k and two translations ε_k associated with different incidences i_k.

Thus we must either have two mirrors with fine adjustments in rotation about their vertical* axes and one with a fine traverse, or two fine traverses and one vertical axis rotation.

4.2. *The Four-Mirror Parallelogram Interferometer—Mirror Adjustments.*—If the interferometer mirrors are set parallel and arranged in the form of a parallelogram, the incidences i_k all become equal to i. Substituting in (4.1), we obtain,

$$\begin{aligned}
\varepsilon_{z0} &= \cos i \, \Sigma \, \varepsilon_k \\
\varepsilon_{x0} &= \sin i \, \Sigma \, \varepsilon_k - \Sigma \, z_k Y_k \\
\alpha_y &= \Sigma \, Y_k \\
\varepsilon_{y0} &= \cos i \, \Sigma \, z_k X_k \\
\alpha_x &= \cos i \, \Sigma \, X_k \\
\alpha_z &= - \sin i \, \Sigma \, X_k \, .
\end{aligned}$$

It follows that:

(*a*). α_z and α_x are not independent, but are related by $\alpha_z = -\alpha_x \tan i$

(*b*) as a result of (*a*), only five adjustments are necessary to determine the five independent displacements

(*c*) since the equations for ε_{y0} and α_x contain X_k only, two of the adjustments must be rotations about the horizontal axes. These may be of any two of the mirrors, with the restriction that if the parallelogram is a rhombus z_2 and z_3 become equal, so that rotations of these two mirrors may not then be used

(*d*) from the first three equations, the other adjustments must be one translation and two rotations about vertical axes. The translation may be of any of the mirrors, the rotations of any two, with the same restriction as in (*c*) for the horizontal axes.

4.3. *Geometrical Representation of the State of Adjustment.*—Since α_z is proportional to α_x, the image displacements of any point are determined by the image displacements of points on the z-axis. Putting $X_k' = X_k \cos i$, $\varepsilon = \Sigma \, \varepsilon_k$, these are

$$\begin{aligned}
\varepsilon_x &= \varepsilon \sin i + \Sigma (z - z_k) Y_k \\
\varepsilon_y &= \qquad - \Sigma (z - z_k) X_k' \\
\varepsilon_z &= \varepsilon \cos i \, .
\end{aligned}$$

These may be represented as in Fig. 20, which may be regarded as a diagram of the deviations of the axial rays from the paths which they travel when the mirror displacements are zero. Since a deviation of one ray is exactly equivalent in effect to an equal and opposite deviation of the

* ' Horizontal ' and ' vertical ' mean in and perpendicular to plane $CDEF$ respectively.

other ray occurring at the same value of z, the diagram may be drawn as if one ray were undeviated while the other is affected by all four mirrors. In Fig. 21a, showing the yz plane, the ray is first rotated by X_1' at mirror 1, then after distances L_1, L_2 and $L_1 + L_2$ it suffers further rotations X_2', X_3', X_4' at mirrors 2, 3 and 4. Note that if $L_2 < L_1$ the order of the positions 2, 3 would be reversed.

The fringe spacing is $b_y = \lambda/\alpha_x$ and is thus determined by the sum of the angles, $\alpha_x = \Sigma X_k'$, while the focal position at which fringes appear when a vertical slit source is used is at the apparent intersection of the two rays, where $\varepsilon_y = 0$.

Fig. 20b, showing the horizontal xz-plane, is similar except for the initial displacement $\varepsilon \sin i$. The intersection of the rays gives the position at which fringes appear when a horizontal slit is used.

In practice only the five necessary fine adjustments will normally be used; the adjustments in rotation will be on the same two mirrors. Denote the two mirrors by suffixes n, m; and let the distance between them be L. Then the simplified diagrams are as shown in Fig. 21. We obtain:

$$\alpha_x = X_m' + X_n'$$
$$\alpha_y = Y_m + Y_n$$
$$\varepsilon_x = (z - z_n)Y_n + (z - z_n + L)Y_m + \varepsilon \sin i$$
$$\varepsilon_y = (z - z_n)X_n' + (z - z_n + L)X_m' .$$

The focal positions are given by:

$$z - z_n = \frac{-(LY_m + \varepsilon \sin i)}{Y_m + Y_n} \text{ for a horizontal slit}$$

and

$$z - z_n = \frac{-LX_m'}{X_m' + X_n'} \text{ for a vertical slit.}$$

These are the same if:

$$\frac{Y_m + (\varepsilon/L) \sin i}{X_m'} = \frac{\alpha_y}{\alpha_x} = \tan \beta ,$$

where β is the angle of the fringes to the x-axis. If $\varepsilon = 0$, this becomes:

$$\frac{Y_m}{X_m'} = \frac{Y_m + Y_n}{X_m' + X_n'} = \frac{Y_n}{X_n'} = \tan \beta .$$

Thus for clear fringes at the centre of the field, with a large source, and with the zero fringe at the centre of the field, the four rotations must be in inverse proportion to the distance from the mirror to the screen, that is,

$$\frac{X_n'}{X_m'} = -\frac{(z - z_n + L)}{z - z_n} = \frac{Y_n}{Y_m} .$$

The derivative of the focal distance with respect to one of the rotations is the distance between the focal position and the mirror rotated, divided by the image displacement angle α_x or α_y. Thus the mirror which has the most effect on the focal position is the one most distant from it. If the focal position coincides with a mirror, rotation of that mirror affects the fringe spacing without changing the focal position.

4.4. *Significance of the Relation* $a_z = -\alpha_x \tan i$.—If we place a screen normal to the emergent beam, take the origin of z at the screen and make $\varepsilon_{x0} = \varepsilon_{y0} = 0$, then we have

$$\varepsilon_x = -y\alpha_z = +y\alpha_x \tan i$$
$$\varepsilon_y = x\alpha_z = -x\alpha_x \tan i .$$

This was discussed in section 3.7 (d) where it was shown that a circular source of radius r' gives clear fringes in the emergent beam at points less than r from the z-axis, where r is given by

$$r = \frac{k\lambda f}{2\alpha_z r'}$$

$$= \frac{k\lambda f}{2\alpha_x r' \tan i} .$$

Now λ/α_x is the fringe spacing b_y in the y direction. Thus $2r/b_y = (f/r')k \cot i$. Thus we obtain a circular patch of fringes of radius proportional to the fringe spacing in the y direction. The angle α_y, and hence fringe spacing in the x direction, is independent of α_z and so does not affect the result, so long as the vertical fringes are in focus, i.e., $\varepsilon_{x0} = 0$.

Fig. 13 shows the result for $\alpha_y = 0$, $f/r' = 20$, $i = 45$ deg. This gives $2r/b = 20k$, and in fact the patch contains about twenty fringes.

4.5. *Inclined Screens.*—From equation (3.2) and $\alpha_z = -\alpha_x \tan i$, we obtain:

$$\varepsilon_y = \varepsilon_{y0} - \alpha_x(x \tan i + z) .$$

Hence if $\varepsilon_{y0} = 0$, $\varepsilon_y = 0$ when $z = -x \tan i$. Thus by inclining the screen at an angle i so that it lies parallel to the mirrors we can make $\varepsilon_y = 0$, and so obtain clear fringes covering the whole screen by using a vertical slit source. Fig. 22a shows the result, with a slit 2·8 in. long.

The displacement ε_x is

$$\varepsilon_x = +y\alpha_x \tan i - x\alpha_y \tan i, \text{ if } \varepsilon_{x0} = 0 .$$

This is zero if $y/x = \alpha_y/\alpha_x = \tan \beta$. Thus with a large area source, the fringes are clear along a line parallel to the fringes. In polar co-ordinates $\varepsilon_x = r \sin(\theta - \beta)\ \alpha \tan i$, where $\alpha = \sqrt{(\alpha_x^2 + \alpha_y^2)}$ and $\tan \theta = y/x$. Thus if the horizontal width of the source is d_x', clear fringes are obtained for $r \sin(\theta - \beta) \leqslant (\lambda f)/(kd_x'\alpha \tan i)$. The width of the band of clear fringes in terms of the fringe width $b = \lambda/\alpha$ is thus

$$\frac{r \sin(\theta - \beta)}{b} = \frac{f \cot i}{kd_x'} .$$

Fig. 22b shows the result with a circular source of radius $f/20$, and $i = 45$ deg, with horizontal fringes.

5. *Departures from the Ideal—The Optical Elements and the Disturbance under Investigation.*—5.1. *Effect of Glass Plates and Wedges.*—The important practical difference between the ideal interferometer of sections 3 and 4 and the real instrument lies in the fact that the semi-reflecting mirrors are thick glass plates, which may not be exactly parallel or of exactly the same thickness or refractive index. In addition, both beams usually pass through two windows, which may be similarly imperfect.

Thus we have to consider the effect on the permissible source size of differences of thickness, refractive index and wedge angle of such plates. For a parallelogram interferometer there are two important cases, namely plates (tunnel windows or compensating plates) at nearly zero incidence and the mirror plates, which are at the mirror incidence.

5.2. *Glass Plates.*—Consider a plate of refractive index μ, with uniform thickness D and at incidence α (Fig. 23). The increase in path length of the ray due to the plate is

$$\mu AB - AC = D\{\sqrt{(\mu^2 - \sin^2 \alpha)} - \cos \alpha\}$$

$$= DF(\alpha, \mu) .$$

The lateral displacement of the ray, BC, is

$$BC = D\frac{F\sin\alpha}{\sqrt{(\mu^2 - \sin^2\alpha)}}$$
$$= D\frac{\partial F}{\partial\alpha}.$$

Suppose the plate is parallel to the mirrors, so that the axial ray is incident at angle i, and the plane of incidence is the horizontal xz-plane ($CDEF$, Fig. 19), perpendicular to the y-axis. Then from Fig. 24

$$\cos\alpha = \cos\frac{y'}{f}\cos\left(i + \frac{x'}{f}\right). \quad \ldots\ldots\ldots\ldots\ldots\ldots \quad (5.1)$$

Let $\alpha = i + \frac{x'}{f} + \gamma$ where γ is small.

Then $\cos\alpha = \cos\left(i + \frac{x'}{f}\right) - \gamma\sin i$ approximately.

But from (5.1), $\cos\alpha = \cos\left(i + \frac{x'}{f}\right) - \frac{1}{2}\frac{y'^2}{f^2}\cos i$ approximately.

Hence $\gamma = \frac{1}{2}\frac{y'^2}{f^2}\cot i$

$$\alpha = i + \frac{x'}{f} + \frac{1}{2}\frac{y'^2}{f^2}\cot i.$$

The increase in path length is $DF(\alpha, \mu)$. Including second-order terms, the change in this due to x', y' is

$$D\{F(\alpha,\mu) - F(i,\mu)\} = D\left\{\left(\frac{x'}{f} + \frac{1}{2}\frac{y'^2}{f^2}\cot i\right)\frac{\partial F}{\partial i} + \frac{1}{2}\frac{x'^2}{f^2}\frac{\partial^2 F}{\partial i^2}\right\}.$$

The derivatives are

$$\frac{\partial F}{\partial i} = \frac{F\sin i}{\sqrt{(\mu^2 - \sin^2 i)}}$$
$$\frac{\partial^2 F}{\partial i^2} = \frac{\partial F}{\partial i}\cot i + \frac{(\mu^2 - 1)\sin^2 i}{(\mu^2 - \sin^2 i)^{3/2}}.$$

Hence the path length is

$$FD + \frac{x'}{f}\left\{\frac{F\sin i}{\sqrt{(\mu^2 - \sin^2 i)}}\right\}D$$
$$+ \frac{1}{2}\frac{x'^2}{f^2}\left\{\frac{F\cos i}{\sqrt{(\mu^2 - \sin^2 i)}} + \frac{(\mu^2 - 1)\sin^2 i}{(\mu^2 - \sin^2 i)^{3/2}}\right\}D$$
$$+ \frac{1}{2}\frac{y'^2}{f^2}\left\{\frac{F\cos i}{\sqrt{(\mu^2 - \sin^2 i)}}\right\}D.$$

From sections 3.4 and 3.5, the path difference due to the image displacements in the absence of the plate is

$$l = \varepsilon_{z0} - x\alpha_y + y\alpha_x$$
$$- \frac{x'}{f}(\varepsilon_{x0} - y\alpha_z + z\alpha_y)$$
$$- \frac{y'}{f}(\varepsilon_{y0} - z\alpha_x + x\alpha_z)$$
$$- \frac{1}{2}\left(\frac{x'^2}{f^2} + \frac{y'^2}{f^2}\right)(\varepsilon_{z0} - x\alpha_y + y\alpha_x).$$

To show the effect of the plate we may put $\alpha_x = \alpha_y = \alpha_z = 0$. Fringes due to wavelength λ will reinforce if $\varepsilon_{z0} = -D\{F - \lambda(\partial F/\partial\lambda)\}$. Hence the total path difference due to x' and y' is

$$
\begin{aligned}
&-\frac{x'}{f}\left\{\varepsilon_{x0} - \frac{DF\sin i}{\sqrt{(\mu^2 - \sin^2 i)}}\right\} \\
&-\frac{y'}{f}\,\varepsilon_{y0} \\
&+\tfrac{1}{2}\left(\frac{x'^2}{f^2} + \frac{y'^2}{f^2}\right)\left\{F - \lambda\frac{\partial F}{\partial\lambda} + \frac{F\cos i}{\sqrt{(\mu^2 - \sin^2 i)}}\right\} D \\
&+\tfrac{1}{2}\frac{x'^2}{f^2}\frac{(\mu^2 - 1)\sin^2 i}{(\mu^2 - \sin^2 i)^{3/2}} D\,.
\end{aligned}
$$

The linear terms vanish if we make ε_{y0} zero and ε_{x0} equal to $(DF\sin i)/\sqrt{(\mu^2 - \sin^2 i)}$, which is the lateral displacement BC, Fig. 23. This in fact follows directly from section 2.6, since the inclination of the rays at the source is $1/f$ times the actual displacement.

The fringes in the source plane are then ellipses, whose semi-major and semi-minor axes are given by

$$
\begin{aligned}
\frac{y'^2}{f^2} &= \frac{2N\lambda}{AD} \\
\frac{x'^2}{f^2} &= \frac{2N\lambda}{(A + B)D}\,,
\end{aligned}
$$

where

$$
\begin{aligned}
A &= F - \lambda\frac{\partial F}{\partial\lambda} + \frac{F\cos i}{\sqrt{(\mu^2 - \sin^2 i)}} \\
B &= \frac{(\mu^2 - 1)\sin^2 i}{(\mu^2 - \sin^2 i)^{3/2}}\,.
\end{aligned}
$$

Section 5.7 below shows that a reasonable spacing for the first fringe ($N = 1$) is $b_1'/f = 0{\cdot}0172$. The corresponding restriction on D is therefore given by

$$
D = \frac{2\lambda}{(A + B)}\left(\frac{f}{b_1'}\right)^2.
$$

With $\mu = 1{\cdot}5$, $\lambda = 4{,}500$ A.U., $d\mu/d\lambda = -2{\cdot}3 \times 10^{-5}$, $i = 45$ deg, the constants are $A = 1{\cdot}06$, $B = 0{\cdot}27$, and these values give $D = 0{\cdot}095$ in.

Thus the restriction is not severe. In practice a closer limit on difference of thickness is desirable in order to avoid excessive dispersion, as section 2.10 (*a*) shows.

5.3. *Effect of Difference of Incidence of the Plates.*—If the incidence is not the same at the two plates, the factors A, B, will differ, and there will be an elliptical fringe pattern in the source plane whose path difference is

$$
\begin{aligned}
&+\tfrac{1}{2}\left(\frac{x'^2}{f^2} + \frac{y'^2}{f^2}\right) D\frac{\partial A}{\partial i}\,(i_4 - i_1) \\
&+\tfrac{1}{2}\frac{x'^2}{f^2} D\frac{\partial B}{\partial i}\,(i_4 - i_1)\,.
\end{aligned}
$$

With the same constants as before, the derivatives are approximately

$$
\begin{aligned}
\frac{\partial A}{\partial i} &= 0{\cdot}0051 \text{ per deg,} \\
\frac{\partial B}{\partial i} &= 0{\cdot}0135 \text{ per deg.}
\end{aligned}
$$

With the value of b_i'/f obtained in section 5.17, the restriction on the incidence difference, for $D = 1$ in., is

$$i_4 - i_1 = \frac{2\lambda}{0{\cdot}0186} \times \left(\frac{1}{0{\cdot}0172}\right)^2$$
$$= 6{\cdot}4 \text{ deg.}$$

This restriction is thus of little practical significance since for other reasons the interferometer is usually adjusted to the parallelogram arrangement with an accuracy better than one degree.

The fringes in the source plane due to difference of thickness and of incidence may to some extent be arranged to compensate one another. They will not compensate exactly since $\{1/(A + B)\}\{(\partial A/\partial i) + (\partial B/\partial i)\}$ will not equal $(1/A)\ (\partial A/\partial i)$. This compensation would not normally be used since it would involve a departure from the parallelogram arrangement, and a special adjustment technique designed to reduce second-order terms in the source-plane fringe pattern.

5.4 *Effect of Difference of Refractive Index of the Plates.*—As with difference of incidence, this will produce a difference between the value of A and B for the two plates. The corresponding path difference is

$$+ \tfrac{1}{2}\left(\frac{x'^2}{f^2} + \frac{y'^2}{f^2}\right) D \frac{\partial A}{\partial \mu}(\mu_4 - \mu_1)$$
$$+ \tfrac{1}{2}\frac{x'^2}{f^2} D \frac{\partial B}{\partial \mu}(\mu_4 - \mu_1) .$$

With the same constants as before, and assuming that $d\mu/d\lambda$ is the same for both plates, the derivatives are approximately

$$\frac{\partial A}{\partial \mu} = 1{\cdot}43$$
$$\frac{\partial B}{\partial \mu} = -\,0{\cdot}04 .$$

For $D = 1$ in., and $b_1'/f = 0{\cdot}0172$ (section 5.17), the restriction is:

$$\mu_4 - \mu_1 = \frac{2\lambda}{1{\cdot}39 \times (0{\cdot}0172)^2}$$
$$= 0{\cdot}086 .$$

A much more severe restriction in practice would again be that necessary to avoid excessive dispersion (*see* section 2.10 (*a*)).

Similar remarks to those of the previous section apply to the possibility of compensation between fringes in the source plane due to difference of incidence and of refractive index.

5.5. *Plates at Zero Incidence.*—At zero incidence, A and B become:

$$A = \frac{\mu^2 - 1}{\mu} - \lambda \frac{d\mu}{d\lambda}$$
$$B = 0 .$$

The derivatives with incidence, $\partial A/\partial i$ and $\partial B/\partial i$, are both zero, and, again on the assumption that $d\mu/d\lambda$ is the same for both plates, the derivative with refractive index is

$$\frac{\partial A}{\partial \mu} = \frac{\mu^2 + 1}{\mu^2} .$$

With the usual constants the values are

$$A = 0{\cdot}94\,, \qquad \frac{\partial A}{\partial \mu} = 1{\cdot}44\,.$$

Thus there is now no restriction, so far as the linear or second-order terms are concerned, on the difference between the angles of incidence at the plates.

The restriction on difference in thickness between the plates is slightly less severe than for the 45-deg incidence. For $b_2'/f = 0{\cdot}0172$ (section 5.17), the thickness difference is $0{\cdot}13$ in.

The restriction on difference of refractive index is slightly more severe than at 45-deg incidence. For $b_1'/f = 0{\cdot}0172$, the difference is $0{\cdot}083$.

5.6. *Effects of Wedge Angles of Glass Plates—Effect of Second-order Terms in* ε.—Since the wedges may produce considerable deflections which are compensated by rotating the mirrors, it is best to include second-order terms in the equations for ε_x, ε_y, ε_z. These become:

$$\varepsilon_x = \varepsilon_{x0} - y\alpha_z + z\alpha_y - \frac{x}{2}(\alpha_y^2 + \alpha_z^2) + y\alpha_x\alpha_y$$

$$\varepsilon_y = \varepsilon_{y0} - z\alpha_x + x\alpha_z - \frac{y}{2}(\alpha_z^2 + \alpha_x^2) + z\alpha_y\alpha_z$$

$$\varepsilon_z = \varepsilon_{z0} - x\alpha_y + y\alpha_x - \frac{z}{2}(\alpha_x^2 + \alpha_y^2) + x\alpha_z\alpha_x\,.$$

The extra term in the path difference l is

$$-\frac{z}{2}(\alpha_x^2 + \alpha_y^2) + x\alpha_z\alpha_x\,,$$

since the product terms in

$$\frac{x'}{f}\alpha^2\,, \frac{y'}{f}\alpha^2$$

are negligible.

5.7. *Path Difference Introduced by a Wedge.*—Fig. 25 shows the path of a ray incident at the same point on a screen before and after introducing a wedge. The path difference between the rays at the line AB is $DF(\alpha, \mu)$, where D is the thickness of the wedge at the actual point of incidence of the ray. The path difference at point C is therefore $DF(\alpha, \mu) + L(\theta^2/2)$, where θ is the deviation produced by the wedge.

Since θ is the rate of change of path length perpendicular to the incident ray, the deviation is $F(\alpha, \mu)$ multiplied by the rate of change of wedge thickness in the direction normal to the incident ray and to the apex of the wedge.

5.8. *Wedge with its Apex Parallel to the y-axis.*—Fig. 26 shows the geometry. The wedge thickness at the point of incidence of the ray from point x', y' of the source is $\phi x_0 \sec i$, and x_0 is given by

$$x_0\left\{1 + \left(\theta - \frac{x'}{f}\right)\tan i\right\} = x - \left(\theta - \frac{x'}{f}\right)z$$

or, including second-order terms

$$x_0 = x - (z + x\tan i)\left\{\left(\theta - \frac{x'}{f}\right) - \left(\theta - \frac{x'}{f}\right)^2 \tan i\right\}.$$

The deviation θ is:

$$\theta = \frac{\partial}{\partial x}(DF) = F\frac{\partial D}{\partial x} = F\phi \sec i \text{ approximately.}$$

Hence, retaining second-order terms in x'/f,

$$x_0 = x - (z + x\tan i)\left(-\frac{x'}{f} - \frac{x'^2}{f^2}\tan i + F\phi\sec i\right).$$

Terms in θ^2 and $\theta(x'/f)$ may be neglected since in practice θ will not exceed 1/50, and their inclusion merely alters very slightly the derivatives with x'/f and x'^2/f^2 in the final expression for the path variation. Unless the source aperture is unusually large the terms in x'^2/f^2 are also negligible, as is shown below. They are, however, retained at this stage so as to show the relative magnitude of quadratic and linear terms, and because in one case, section 5.9 below, the linear term is zero. Hence, using the expression for the path length in a plate given in section 5.2, the path increase due to the wedge is

$$\phi\sec i\left\{x - (z + x\tan i)\left(-\frac{x'}{f} - \frac{x'^2}{f^2}\tan i + F\phi\sec i\right)\right\}$$
$$\times\left\{F + \frac{x'}{f}\frac{F\sin i}{\sqrt{(\mu^2 - \sin^2 i)}} + \tfrac{1}{2}\left(\frac{x'^2}{f^2} + \frac{y'^2}{f^2}\right)\frac{F\cos i}{\sqrt{(\mu^2 - \sin^2 i)}} + \tfrac{1}{2}\frac{x'^2}{f^2}\frac{(\mu^2 - 1)\sin^2 i}{(\mu^2 - \sin^2 i)^{3/2}}\right\}$$
$$+ (z + x\tan i)\frac{(F^2\phi^2\sec^2 i)}{2},$$

while the rotation of the mirrors to compensate the deviation $F\phi\sec i$ subtracts terms

$$F\phi\sec i\left\{x + \frac{x'}{f}z - \frac{(x'^2 + y'^2)}{2f^2}x - \frac{z}{2}F\phi\sec i\right\}$$

Hence the sum is as follows:

$$+\frac{x'}{f}xF\phi\sec i\left\{\frac{\sin i}{\sqrt{(\mu^2 - \sin^2 i)}} + \tan i\right\}$$
$$+\frac{x'^2}{f^2}\phi\sec i\left[+F(z + x\tan i)\left\{\frac{\sin i}{\sqrt{(\mu^2 - \sin^2 i)}} + \tan i\right\}\right.$$
$$\left.+\frac{x}{2}\left\{F + \frac{F\cos i}{\sqrt{(\mu^2 - \sin^2 i)}} + \frac{(\mu^2 - 1)\sin^2 i}{(\mu^2 - \sin^2 i)^{3/2}}\right\}\right]$$
$$+\frac{y'^2}{f^2}\phi\sec i\frac{x}{2}\left\{F + \frac{F\cos i}{\sqrt{(\mu^2 - \sin^2 i)}}\right\}.$$

(*a*) *The linear term.*—Consider first the linear term. This is:

$$\frac{x'}{f}xF\phi\frac{\sin i}{\cos^2 i\sqrt{(\mu^2 - \sin^2 i)}}\{\sqrt{(\mu^2 - \sin^2 i)} + \cos i\} = \frac{x'}{f}x\phi\frac{(\mu^2 - 1)\sin i}{\sqrt{(\mu^2 - \sin^2 i)}\cos^2 i}.$$

This cannot now be compensated since it is not constant over the field but is proportional to x. For $i = 45$ deg, $\mu = 1{\cdot}5$, its value is $1{\cdot}34(x'x/f)\phi$.

The restriction is more easily expressed in terms of the variation in thickness of the plate. The change of thickness from the centre to the edge is $\delta = x\phi\sec i$, and in terms of this the path difference is:

$$\frac{x'}{f}\delta\frac{(\mu^2 - 1)\tan i}{\sqrt{(\mu^2 - \sin^2 i)}} = 0{\cdot}95\frac{x'}{f}\delta \text{ for } i = 45 \text{ deg}, \mu = 1{\cdot}5.$$

For $b_1'/f = 0{\cdot}148$ (section 5.17), the restriction on δ is

$$\delta = \frac{\lambda}{0{\cdot}95 \times 0{\cdot}148} = 7{\cdot}1\lambda = 1{\cdot}3 \times 10^{-4} \text{ in.}$$

Thus the total variation in thickness of the plate should not exceed 14·2 wavelengths or $2{\cdot}6 \times 10^{-4}$ in.

(*b*) *The quadratic term.*—The quadratic term is:

$$\frac{x'^2}{f^2}\phi \sec i \left\{\frac{(\mu^2-1)\tan i}{\sqrt{(\mu^2-\sin^2 i)}}(z + x\tan i) + \frac{x}{2}\frac{\mu^2(\mu^2-1)}{(\mu^2-\sin^2 i)^{3/2}}\right\}$$
$$+\frac{y'^2}{f^2}\phi \sec i \frac{x}{2}\frac{(\mu^2-1)}{\sqrt{(\mu^2-\sin^2 i)}}$$

For $i = 45$ deg, $\mu = 1{\cdot}5$, this becomes

$$\frac{x'^2}{f^2}\phi \sec i\,(0{\cdot}95z + 1{\cdot}56x)$$
$$+\frac{y'^2}{f^2}\phi \sec i \times 0{\cdot}47x\,.$$

In terms of the thickness variation δ, the term is

$$\frac{x'^2}{f^2}\delta\left(\frac{0{\cdot}95z}{x} + 1{\cdot}56\right) + \frac{y'^2}{f^2}\delta \times 0{\cdot}47\,.$$

Hence for $b_1'/f = 0{\cdot}0172$ (section 5.17), the permissible value of δ is given by

$$\delta\left(\frac{0{\cdot}95z}{x} + 1{\cdot}56\right) = \frac{2\lambda}{(0{\cdot}0172)^2} = 0{\cdot}12 \text{ in.}$$

Thus the restriction arising from this term would be comparable with that from the linear term only if z/x were of the order of 1,000. In practice it is unlikely to exceed about 20.

5.9. *Wedge Angles of Windows and Compensating Plates.*—At zero incidence the linear term, (*a*) above, vanishes, and the quadratic term becomes

$$\left(\frac{x'^2}{f^2} + \frac{y'^2}{f^2}\right)\frac{x\phi}{2}\frac{(\mu^2-1)}{\mu} = \frac{(\mu^2-1)}{2\mu}\delta\frac{r'^2}{f^2}.$$

Hence for $b_1'/f = 0{\cdot}0172$ (section 5.17) the permissible value of δ is given by

$$\delta = \frac{2\mu}{\mu^2-1}\frac{2\lambda}{(0{\cdot}0172)^2}.$$

For $\mu = 1{\cdot}5$, $\lambda = 4{,}500$ A.U., $\delta = 0{\cdot}29$ in. and so there is practically no restriction on the permissible wedge angles of plates at zero incidence, if the apex of the wedge is parallel to the y-axis.

5.10. *Wedge with its Apex Normal to the y-Axis and Parallel to the Mirror Plane.*—Fig. 27 shows the geometry. The wedge thickness at the point of incidence of the ray from point x', y' is ϕy_0, and y_0 is given by

$$y_0 = y + \left(\frac{y'}{f} - \theta\right)(z + x\tan i)\left(1 + \frac{x'}{f}\tan i\right),$$

where the deviation $\theta = F\phi$. Hence, using the expression for the path length in a plate given in section 5.2, the path increase due to the wedge is

$$\phi\left\{y + \left(\frac{y'}{f} - F\phi\right)(z + x\tan i)\left(1 + \frac{x'}{f}\tan i\right)\right\}$$
$$\times\left\{F + \frac{x'}{f}\frac{F\sin i}{\sqrt{(\mu^2-\sin^2 i)}} + \tfrac{1}{2}\left(\frac{x'^2}{f^2} + \frac{y'^2}{f^2}\right)\frac{F\cos i}{\sqrt{(\mu^2-\sin^2 i)}} + \tfrac{1}{2}\frac{x'^2}{f^2}\frac{(\mu^2-1)\sin^2 i}{(\mu^2-\sin^2 i)^{3/2}}\right\}$$
$$+\frac{z}{2}F^2\phi^2\,.$$

The rotation of the mirrors to compensate the deviation $F\phi$ subtracts terms

$$yF\phi\left\{1-\frac{(x'^2+y'^2)}{2f^2}\right\}-\frac{x'}{f}yF\phi\tan i+\frac{y'}{f}F\phi(z-x\tan i)$$
$$-\frac{z}{2}F^2\phi^2-xF^2\phi^2\tan i\,.$$

The sum is therefore:

$$+\frac{x'y}{f}F\phi\left\{\tan i+\frac{\sin i}{\sqrt{(\mu^2-\sin^2 i)}}\right\}$$
$$+\frac{x'y'}{f^2}z\phi F\left\{\frac{\sin i}{\sqrt{(\mu^2-\sin^2 i)}}+\tan i\right\}+\frac{x'y'}{f^2}x\phi F\tan^2 i$$
$$+\tfrac{1}{2}\frac{x'^2}{f^2}\phi y\left\{F+\frac{F\cos i}{\sqrt{(\mu^2-\sin^2 i)}}+\frac{(\mu^2-1)\sin^2 i}{(\mu^2-\sin^2 i)^{3/2}}\right\}$$
$$+\tfrac{1}{2}\frac{y'^2}{f^2}\phi y\left\{F+\frac{F\cos i}{\sqrt{(\mu^2-\sin^2 i)}}\right\}.$$

(*a*) *The linear term.*—This is:

$$+\frac{x'y}{f}\frac{F\phi\tan i}{\sqrt{(\mu^2-sin^2 i)}}\{\sqrt{(\mu^2-\sin^2 i)}+\cos i\}=+\frac{x'y}{f}\frac{\phi(\mu^2-1)\tan i}{\sqrt{(\mu^2-\sin^2 i)}}\,.$$

This is similar to the linear term for the wedge with its apex parallel to the y-axis, with y replacing x and ϕ replacing $\phi\sec i$. In terms of the variation in thickness of the plate $\delta=y\phi$, the path difference is the same, namely

$$\frac{x'}{f}\frac{\delta(\mu^2-1)\tan i}{\sqrt{(\mu^2-\sin^2 i)}}\,.$$

The necessary restriction on δ is the same and, since the two wedge directions both produce vertical fringes (*i.e.*, both terms are proportional to x'), the restriction is in fact on the total variation in thickness of the plate, in whatever direction this may be. This variation should not exceed 14·2 wave-lengths or $2{\cdot}6\times10^{-4}$ in.

(*b*) *The quadratic term.*—The only quadratic term of importance is the term in $x'y'$, namely:

$$+\frac{x'y'}{f^2}z\phi\frac{(\mu^2-1)\tan i}{\sqrt{(\mu^2-\sin^2 i)}}+\frac{x'y'}{f^2}x\phi F\tan^2 i\,.$$

For $i=45$ deg, $\mu=1{\cdot}5$, this is:

$$\frac{x'y'}{f^2}\phi(0{\cdot}95z+0{\cdot}61x)\,.$$

If the source is circular and of radius r', the maximum path variation is

$$\frac{r'^2}{2f^2}\phi(0{\cdot}95z+0{\cdot}61x)\,.$$

In terms of the thickness variation $\delta=\phi y$ this is

$$\frac{r'^2}{2f^2}\phi\left(0{\cdot}95\frac{z}{y}+0{\cdot}61\frac{x}{y}\right).$$

With $b_1'/f=0{\cdot}0172$ (section 5.17), $\lambda=4{,}500$ A.U., the restriction on δ is given by

$$\delta\left(0{\cdot}95\frac{z}{y}+0{\cdot}61\frac{x}{y}\right)=\frac{2\lambda}{(0{\cdot}0172)^2}=0{\cdot}12\text{ in.}$$

Thus the term becomes comparable with the linear term only when z/y is of the order of 1,000. In practice z/y is unlikely to exceed about 20, and so this term is negligible.

5.11. *Wedge with its Apex Parallel to the x-Axis.*—This is the case of a window or compensating plate at zero incidence, with the apex of its wedge parallel to the x-axis. The result may not be deduced directly from section 5.10 above by letting $i = 0$, since in this section the wedge was assumed parallel to the mirrors. The incidence becomes zero only in the expression for the path increase due to the wedge itself, and not in the compensating terms due to the mirror rotations.

The path increase due to the wedge becomes:

$$\phi\left\{y + \left(\frac{y'}{f} - (\mu - 1)\phi\right)z\right\}\left\{\mu - 1 + \tfrac{1}{2}\left(\frac{x'^2}{f^2} + \frac{y'^2}{f^2}\right)\frac{\mu - 1}{\mu}\right\} + \frac{z}{2}(\mu - 1)^2\phi^2 .$$

The compensating terms become

$$y(\mu - 1)\phi\left\{1 - \frac{(x'^2 + y'^2)}{2f^2}\right\} - \frac{x'}{f}y(\mu - 1)\phi \tan i + \frac{y'}{f}(\mu - 1)\phi(z + x \tan i)$$
$$- \frac{z}{2}(\mu - 1)^2\phi^2 - x(\mu - 1)^2\phi^2 \tan i .$$

Neglecting the term independent of x' and y', the sum is:

$$+ \frac{x'}{f}y\phi(\mu - 1) \tan i$$
$$- \frac{y'}{f}x\phi(\mu - 1) \tan i$$
$$+ \tfrac{1}{2}\left(\frac{x'^2}{f^2} + \frac{y'^2}{f^2}\right)y\phi\,\frac{(\mu^2 - 1)}{\mu} .$$

The linear terms give a source plane fringe distribution like that obtained by making $\alpha_z \neq 0$, section 3.7 (d). The necessary restriction on ϕ arises from the term in x', which may combine with the effect of wedge angles of the semi-reflecting plates. In terms of the thickness variation $\delta = y\phi$, this term is

$$\frac{x'}{f}\phi(\mu - 1) \tan i .$$

For $\mu = 1{\cdot}5$, $i = 45$ deg, and $b_1'/f = 0{\cdot}148$ (section 5.16), the restriction on δ is

$$\delta = \frac{2\lambda}{0{\cdot}148}$$
$$= 13{\cdot}5 \text{ wavelengths or } 2{\cdot}4 \times 10^{-4} \text{ in.}$$

The total variation in thickness across the window in this direction must therefore not exceed $27{\cdot}0$ wavelengths or $4{\cdot}8 \times 10^{-4}$ in. It should be noted that in this case the source-plane path variation is entirely due to the rotations of the mirrors required to compensate the deviation produced by the wedge. If we have a second wedge of equal and opposite angle, distant Z from the first, the sum of the terms due to the two wedges is

$$\phi Z\left\{\frac{y'}{f} - (\mu - 1)\phi\right\}\left\{\mu - 1 + \tfrac{1}{2}\left(\frac{x'^2}{f^2} + \frac{y'^2}{f^2}\right)\frac{\mu - 1}{\mu}\right\} + \frac{Z}{2}(\mu - 1)^2\phi^2$$

and the linear term $(y/f)Z\phi(\mu - 1)$ is compensated by making $\varepsilon_{y0} = -Z\phi(\mu - 1)$.

If one of the compensating plates is arranged to rotate, and if its wedge angle is sufficiently large, it may always be arranged so as to compensate the deviations produced by the other plates and windows in the α_x direction. If this is done, the restrictions on the wedge angles will depend on the quadratic terms only, and will be, at worst, of the same order as that given in section 5.9 for a wedge with its apex parallel to the y-axis.

5.12. *Effects of the Disturbance under Investigation.*—The preceding sections show that clear fringes may be obtained even with very imperfect adjustment and imperfect optical elements, if the source aperture and band width are very small. But if these are small, the intensity of light transmitted is very small, and so a long exposure is required to obtain a photograph. The photograph will then not show clear fringes unless the conditions are very steady. If the interferometer is used for aerodynamic density measurements with a wind tunnel or shock tube the conditions will not be very steady, and to obtain clear fringes the exposure time must be short, often of the order of one microsecond. So to get enough light we must increase the source aperture and band width as far as possible.

Sections 5.2 to 5.11 show that the necessary restrictions on wedge angles, differences of incidence, thickness and refractive index are not particularly severe, and it is not difficult to obtain mirrors and plates which will meet these limits even for very large source apertures. We must therefore study the effects of increasing source aperture and band width on the interferogram in the presence of the disturbance under investigation. This will give a criterion for a suitable source aperture. We may then use this value, with the results of the previous sections, to determine reasonable limits for the imperfections of the optical elements, and to determine the accuracy of adjustment necessary.

5.13. *Two-Dimensional Disturbance.*—Consider a two-dimensional object such as a two-dimensional model in a wind tunnel (Fig. 28). The rays which arrive at point A on the screen are those which appear to come from the image point B, assumed to be approximately in the centre of the tunnel. Owing to the refractive index gradient in the tunnel, the rays actually take curved paths such as DE, FG. The path change due to the tunnel is $\int \mu dz$ along the actual path, but this is usually interpreted as being equal to $\mu_B L$, where μ_B is the refractive index at the image point B. The difference will depend on the path of the rays, which depends on the exact density distribution, but the order of magnitude may be expressed in terms of the deviation of the ray h, and the fringe spacing.

If the total angular deviation of the rays in passing through the tunnel is α, the fringe spacing is $b = \lambda/\alpha$, and the maximum linear deviation h is of the order of $\alpha L/2$. Thus the deviation becomes equal to the fringe spacing if $\frac{1}{2}\alpha L = \lambda/\alpha$ or $\alpha = \sqrt{(2\lambda/L)}$. If the deviation is smaller than this its effect on the accuracy should be of comparatively little importance, while if it is larger it will be difficult to relate the fringe to a definite position in the field. Thus there is an upper limit to the refractive index gradient which can be measured, and this is given approximately by $\alpha = \sqrt{(2\lambda/L)}$.

If the source has radius r' and if the screen is focussed on the centre-line of the tunnel, the cone of light entering the tunnel which arrives at any one point on the screen will have a base of width $r'L/f$. The effect of this on the variation of path length between rays in the cone again depends on the exact refractive index distribution. If, however, the base width is less than the fringe spacing, this variation should be small, whereas it may become large if the base width is considerably larger than the fringe spacing. Thus for a fringe spacing $b = \lambda/\alpha$, the source size should have little effect on the contrast if $r'L/f$ does not exceed λ/α.

Now the maximum value of α is given above as $\alpha = \sqrt{(2\lambda/L)}$, and hence the permissible source radius is given by

$$\frac{r'L}{f} = \lambda\sqrt{\frac{L}{2\lambda}}$$

$$\frac{r'}{f} = \sqrt{\frac{\lambda}{2L}}.$$

Although there is no definite restriction, the usual range of tunnel widths suitable for interferometry is from about 1 to 20 inches. Thus for $\lambda = 4{,}500$ A.U., the range of source aperture is from $2r'/f = 1{\cdot}3 \times 10^{-3}$ to $6{\cdot}0 \times 10^{-3}$.

5.14. *Effect of Focussing.*—Suppose the screen is not focussed on the centre of the disturbance but at some plane distant Z from it. The distance, in a plane parallel to the screen, between the mean height at which the ray passes through the tunnel and the focal position becomes $\alpha(Z + L/4)$. The fringe position is thus altered by an amount proportional to the refractive index gradient, and there is thus an apparent distortion, as in a shadowgraph of the disturbance taken with the screen at the same position.

If there are rapid variations in the refractive index gradient, this may result in light from two different points in the object arriving at the same point on the screen, with loss of fringe definition and contrast. In addition, even with a constant refractive index gradient there will be a linear term in the source plane path variation, equal to $(y'/f)\alpha z$, where y' is the source co-ordinate in the direction of the deviation α. This will result in loss of fringe contrast even in parts of the field where the shadowgraph effect is negligible.

Thus, for good fringe contrast the disturbance must be focussed on the screen and, if the refractive index variations are sufficiently rapid, a suitable method of focussing is to adjust the lens or screen positions so as to minimise the intensity variations when the compensating beam is cut off.

5.15. *Effect of an Out-of-Focus Disturbance.*—It is sometimes necessary or convenient to place the compensating chamber in an out-of-focus part of the beam. In particular, with a wind tunnel, both beams may pass through the tunnel, and if so the compensating section is out of focus by a distance equal to the distance between mirrors 1 and 2 along the light path. The flow in this section may not be uniform, although there should be no sudden refractive index changes such as those in shock waves or boundary layers in the working-section.

Suppose the maximum refractive-index gradient in the compensating section is such as to give a fringe spacing b_2. It will not usually be practicable to compensate this by mirror rotations, since it is usually necessary to take a photograph in the same condition with no flow through the tunnel. Thus if the source dimension along the gradient is d', the fringe contrast will be reduced if $d'Z/f > kb_2$ and so the criterion for the maximum refractive index gradient is $b = (Z/k)(d'/f)$. For $d'/f = 6{\cdot}0 \times 10^{-3}$ and $k = \frac{1}{4}$ this gives $b/Z = 0{\cdot}024$. The restriction is thus fairly severe, since if Z is 10 in. the minimum fringe spacing is $0{\cdot}24$ in.

5.16. *Effect of Ray Deflections on the Path through the Window and Semi-reflecting Plate.*—Consider a ray passing at nearly normal incidence through a parallel glass plate, Fig. 29. If the ray is slightly deflected at A, the emergent ray appears to come from B, and the distance AB is $D(\partial^2 F/\partial i^2)$, which at zero incidence equals $\{(\mu - 1)/\mu\}D$. Thus if the point B is focussed on the screen in the absence of the plate, then when the plate is present there is no path difference due to incidence variation for rays slightly deflected at A.

So, for example, if the interferometer is used with a wind tunnel whose centre-line is at A, and which has thick glass windows, the camera must be focussed on the centre-line with the window in position. In the absence of the window, point B, and not A, should be in focus.

Now consider a ray passing through a plate, for example, the semi-reflecting plate 4, which is not at nearly normal incidence. Rays deflected at point A in the plane of incidence again appear to come from point B, and the distance $A'B$ along the light path is again $D(\partial^2 F/\partial i^2)$. Rays deflected in the plane normal to the plane of incidence, on the other hand, appear to come from point C, where $A'C = D(\partial F/\partial i)\cot i$. This may be deduced from the observation that a small deflection normal to the plane of incidence is equivalent to a rotation about the normal, AC.

Thus, with the glass plate present, it is impossible to focus the object exactly on the screen for both planes of deviation at once. The distance between the two focal planes is $D\{(\partial^2 F/\partial i^2) - (\partial F/\partial i)\cot i\}$, which equals $D[\{(\mu^2 - 1)\sin^2 i\}/(\mu^2 - \sin^2 i)^{3/2}]$ (section 5.2). For $i = 45$ deg and $\mu = 1{\cdot}5$, this is $0{\cdot}27D$. So if the camera is focussed midway between the two planes, each will be out out of focus by a distance $0{\cdot}135D$.

The effect of this out-of-focus distance is similar to that discussed in section 5.15 for the compensating chamber. If the source dimension is d' and the fringe spacing due to the deviation is b then the contrast will be reduced if $d'Z/f > kb$, where z is the out-of-focus distance. For $k = \frac{1}{4}$, $Z = 0{\cdot}135D$, $D = 1$ in. and $d'/f = 6{\cdot}0 \times 10^{-3}$, this gives $b < 4 \times 6{\cdot}0 \times 10^{-3} \times 0{\cdot}135$ in. or $b < 3{\cdot}2 \times 10^{-3}$ in.

This fringe spacing is approximately equal to the limiting value which would be obtained from the considerations of section 5.13, and is rather smaller than the minimum which is normally useful in practical wind-tunnel work. If, however, this aberration does cause difficulty it may be eliminated by two alternative methods. Howes and Buchele[13] use the interferometer with the working-section between mirrors 3 and 4, so that the light deflected in the tunnel is reflected at plate 4, and this aberration does not arise. The resulting arrangement would not always be convenient, and another possibility is to use the normal arrangement and place in the emergent beam an extra glass plate of the same thickness as the semi-reflecting plate 4 and at the same incidence, but with its plane of incidence normal to that of the mirrors.

5.17. *Specifications for Interferometer Optical Elements.*—Loss of fringe contrast arises from three causes, namely:

(1) Stray light, particularly from reflections from the windows and the back surfaces of the plates

(2) Inequality of intensity of the light *via* the two paths, which may arise from different reflection ratio or incidence of the plates, or different absorption in the two beams

(3) Effects depending on the size and spectral range of the source.

The amount of stray light may be reduced by using suitable diaphragms and by coating the surfaces to reduce reflection. Inequality of intensity may be practically eliminated by using the same semi-reflecting coating for the two plates, arranging the instrument as a parallelogram and using the same thickness and quality of glass for the windows in the two beams.

Appendices I and II show how the fringe contrast depends on the source size in relation to the source-plane fringe pattern, and on the source band width and number of fringes required.

The source-plane path variation depends on three factors:

(*a*) The state of adjustment

(*b*) The disturbance under investigation

(*c*) The imperfections of the optical elements.

With a well-designed interferometer the adjustment should be easy to use and should not limit the contrast. The disturbance under investigation sets a limit to the source size which may be used if the definition is to be the best possible. It is therefore reasonable to design the optical elements so that, when this size of source is used, their imperfections will give rise to only a small loss of fringe contrast.

For a simple interferometer with two windows in each beam, sections 5.1 to 5.11 show that, if the surfaces of the elements are flat and if they have uniform refractive index, the relevant imperfections are as follows:

(*a*) Those giving rise to linear terms in the source plane path variation, namely:

(i) Wedge angles of the two semi-reflecting plates, with the wedge apices in any direction

(ii) Wedge angles of the four windows, with the wedge apices horizontal.

(*b*) Those giving rise to quadratic terms in the source-plane path variation, namely:

(i) Difference in thickness
(ii) Difference in incidence
(iii) Difference in refractive index
} of the two semi-reflecting plates.

(iv) Difference in thickness
(v) Difference in refractive index
} between the pairs of windows in the two beams.

(A) *The linear terms—Wedge angles.*—These give rise to by far the most severe restrictions, and it therefore seems reasonable to allow them to have an appreciable, though not large, effect on the contrast. Suppose we take the larger of the two source sizes given in section 5.13, namely $2r'/f = 6{\cdot}0 \times 10^{-3}$, and with this source let the wedge angles give a ratio of minimum to maximum intensity of 0·05. From Appendix I, the corresponding ratio d'/b' is 0·243, and hence $b'/f = (6{\cdot}0 \times 10^{-3})/0{\cdot}243 = 0{\cdot}0247$.

For the vertical fringe direction (path variation proportional to x'), sections 5.6 to 5.11 show that there are six terms, namely the four windows and two plates, and so if each gives the same fringe spacing b_1', $b_1'/f = 6 \times 0{\cdot}0247 = 0{\cdot}148$.

This value is used above in sections 5.8 to 5.11. The resulting restriction is that the variation in thickness across each semi-reflecting plate must not exceed 14·2 wavelengths or $2{\cdot}6 \times 10^{-4}$ in. (at $\lambda = 4{,}500$ A.U.). For the windows the corresponding figures are 27·0 wavelengths or $4{\cdot}8 \times 10^{-4}$ in.

If one of the windows is adjustable, as suggested in section 5.11, only the wedge angles of the plates need be considered, and so the restrictions become three times as great, namely 42·6 wavelengths or $7{\cdot}8 \times 10^{-4}$ in.

(B) *The quadratic terms—Differences in thickness, incidence and refractive index.*—The quadratic terms are very small, and so it seems reasonable to keep their effects very small. Suppose we allow a ratio of minimum to maximum intensity, from this source, of 0·02. From Appendix I, the corresponding ratio d'/b' is 0·78, and hence $b'/f = (6{\cdot}0 \times 10^{-3})/0{\cdot}78 = 7{\cdot}7 \times 10^{-3}$.

As shown above there are five terms to consider. If each produces a source-plane path variation of $\lambda(x'^2/b_1'^2)$, the total is $\lambda(x'^2/b'^2) = 5\lambda(x'^2/b_1'^2)$. Hence $b_1' = \sqrt{(5)}b'$, and $b_1'/f = 0{\cdot}0172$.

This value is used above in sections 5.2 to 5.5, and the resulting restrictions are as follows:

(i) The thicknesses of the semi-reflecting plates should not differ by more than 0·09 in.

(ii) The angles of incidence of the plates should not differ by more than 6 deg

(iii) The refractive indices of the plates should not differ by more than 0·09

(iv) The sum of the thicknesses of the windows in one beam should not differ from that in the other by more than 0·13 in.

(v) The refractive indices of the windows in the two beams should not differ by more than 0·08.

The criteria obtained have been calculated using the following particular values:

Incidence of plates	45 deg
Refractive index of plates and windows	1·5
Thickness of plates and windows	1·0 in.
Source size	$d'/f = 6{\cdot}0 \times 10^{-3}$
Wavelength	4,500 A.U.

They should therefore be taken only as examples suggesting suitable methods of calculation and showing the order of magnitude of the results. In particular, the limitations on wedge angles become less critical as the angle of incidence is decreased; at an incidence of 30 deg they are 1·86 times as great as those given for 45 deg. In addition, a closer limit on the difference in optical thickness of the glass in the two beams is usually set by the necessity of avoiding excessive dispersion, *see* section 2.10 (*a*).

(C) *Limits on flatness and refractive index variation.*—A limit on flatness of a fraction of a wavelength (from 1/10 to $\frac{1}{4}$) is usually specified, in order to obtain reasonably straight fringes. This may sometimes be an advantage but is often not strictly necessary. The limitation arising from loss of fringe contrast results from the fact that variations in thickness or refractive index, or deviations from flatness of the reflecting surfaces, constitute uncompensated and out-of-focus wedge angles. The type of limitation necessary is thus that considered in section 5.15.

Since the effects of lack of flatness, variations in thickness and refractive index of all the optical elements may combine, the effect of each should be kept very small, and a reasonable value of k is perhaps $0{\cdot}02$. With a source size of $6{\cdot}0 \times 10^{-3}f$, this gives, for the permissible fringe spacing, $b/Z = (6{\cdot}0 \times 10^{-3})/0{\cdot}02 = 0{\cdot}3$.

Thus if the out-of-focus distance Z is 10 in., the fringe spacing is 3 in., and the permissible variation from flatness, or from uniform optical thickness, is 1/3 of a wavelength per inch.

This is of the same order as, though rather less strict than, the criteria usually applied. The dependence on Z shows that the limits become more severe as the distances between the mirrors increase.

6. *Methods of Adjustment for the Mach-Zehnder Interferometer.*—6.1. *Methods of Adjustment.*—The objects of the adjustments to the interferometer are:

(*a*) to produce a desired spacing of the beams, to align them with respect to the model or windows, and to obtain the maximum possible field size

(*b*) to produce fringes on the screen with the desired spacing and direction

(*c*) to bring the desired fringe number to the centre of the field of view. Usually this will be the zero fringe, or, if there is dispersion, the fringe having most contrast for the wavelength to be used

(*d*) to make the fringe contrast as great as possible for these conditions of fringe spacing and source size.

Adjustments (*b*), (*c*) and (*d*) are related to the image displacements as follows:

(*b*) is equivalent to obtaining desired values of α_x and α_y

(*c*) is equivalent to obtaining the desired value of ε_{z0}, which will usually be zero if there is no dispersion

(*c*) is equivalent to obtaining desired values of ε_{x0} and ε_{y0}. These will be the values which make the source-plane path variation as small as possible*.

Many possible methods of adjustment have been described. Of these there are a few which require little or no apparatus additional to that normally used on the interferometer, which are simple and easily adapted to any interferometer arrangement, and only these methods will be described here.

Usually there are at least two separate stages in the adjustment, since the methods suitable for the final adjustments do not work if the image displacements are too large. In practice, the time taken depends largely on choosing methods of adjustment whose ranges overlap considerably. That is, the initial adjustment should reduce the image displacements to values well below the maximum values which the final adjustment methods will accept. Since the accuracy required of the initial adjustments thus depends on the methods to be used for final adjustment, it is convenient to consider the latter stages first.

6.2. *Fine Adjustments by Interference Optics.*—(*a*) *To obtain the desired fringe number* (ε_{z0}).—This involves traversing a mirror to reduce the path difference to zero, or, if there is dispersion, to the value giving most contrast. The traverse motion affects both ε_{z0} and ε_{x0} (section 4.2). Since the object is to set ε_{z0} to the value at which the contrast is maximum with respect to ε_{z0} with ε_{x0} kept constant, it follows that either ε_{x0} must be kept nearly constant, or its effect on fringe contrast must be made negligible. The former may in theory be done by rotating the mirrors to alter $\Sigma z_k Y_k$ (section 4.2). In practice, this usually means that three adjustments

* In the ideal interferometer of sections 2 and 3, the linear terms of the source-plane path variation at the centre of the field vanish when ε_x and ε_y are zero. When glass plates are present they vanish when the actual displacements, the sum of ε_x or ε_y and the displacements due to the glass, are zero. The adjustments reduce the actual displacements to zero, as is required. For brevity, however, the methods will be described as if for an ideal interferometer, and the displacements referred to as ε_x and ε_y. Similarly the adjustments reduce the actual angles between corresponding rays in the emergent beam, but for brevity these will be referred to as α_x, α_y.

must be altered continuously or in successive small steps, and this is difficult unless the displacements are very small. Also it is desirable to obtain the correct value of ε_{z0} before doing the final adjustments to ε_{x0} and ε_{y0}. This can only be done by using a very small source.

Thus the care necessary in reducing ε_{x0} and ε_{y0} before traversing, and the length of the path difference which can be accepted at this stage, depend on how small a source it is practicable to use. Trial shows that with a 28-in. focal-length lens, high-pressure mercury lamp, condenser lens and square aperture, sufficient illumination is obtained on a white card screen with an aperture about 0·02 in. square. If a lens of aperture $f/8$ is placed in the emergent beam and if the eye is placed near its focus, the aperture required is about 0·0015 in. square. The corresponding source apertures are $d'/f = 1/1{,}400$ and 1/18,000 respectively.

There will be an appreciable loss of contrast for values of k greater than about $\frac{1}{2}$ (Fig. 32a). The limits to ε_{x0} and ε_{y0} are therefore about 700 wavelengths or 0·015 in. using a screen or about 9,000 wavelengths or 0·19 in. using the eye at the focus of a lens. Since with a 45-deg interferometer a change of ε_{z0} gives an equal change of ε_{x0}, the path difference which can be accepted is also approximately 0·015 in. and 0·19 in. for the two arrangements.

It is very easy by mechanical measurement or geometric optics to reduce all the displacements well below the larger limit, but comparatively difficult, particularly if dispersion is present, to reduce ε_{z0} below the lower limit by these methods. Thus the most practical first step after the initial adjustments is to reduce α_x and α_y (*see* below), place a lens in the emergent beam, reduce the source size to give a source aperture of the order of 1/18,000, place the eye near the focus of the lens and traverse the mirror until the fringe of highest contrast comes into view.

If a rapid traverse motion is available it is not necessary to know which way to traverse, since the possible range of 0·1 or 0·2 in. can be scanned in a very short time. One means of knowing the correct direction by interference optics is to use a source which gives just enough fringes to cover the error in ε_{z0}, so that the correct direction is that in which the fringe contrast increases. The method becomes difficult to use if the increase of contrast is slow, however, and a rapid traverse motion is a considerable advantage.

(*b*) *To reduce the displacements* ε_{x0}, ε_{y0}—*Source size and fringe contrast method.*—If we take the origin of z at the screen or the plane on which the eye is focussed, the source-plane fringe spacing is $\lambda f/\varepsilon_{x0}$ and $\lambda f/\varepsilon_{y0}$. Hence the contrast of the observed fringes will fall to zero if the source size is increased until it equals these values, i.e., $d_x' = \lambda f/\varepsilon_{x0}$ or $d_y' = \lambda f/\varepsilon_{y0}$ (Appendix I, Fig. 32a). Thus unless the displacements are zero, contrast falls as source size is increased up to these values. If we set the source size to a value, say, $d' = \frac{1}{2}(\lambda f/\varepsilon)$, at which the contrast is varying rapidly, and then rotate a mirror so as to change ε, we can see whether the direction of the rotation is correct by its effect on the contrast.

From sections 4.2 and 4.3 it appears that rotation of either mirror has the same effect on the fringe spacing, whereas the effect on the displacement is proportional to the distance of the mirror from the focal plane.

Hence the technique is as follows:

(i) Increase the source size in one direction only (the direction parallel to the displacement which is to be reduced) until the fringe contrast becomes poor, but not so far that the fringes become invisible.

(ii) Rotate the mirror furthest from the focal plane about the axis perpendicular to the displacement and to the slit-shaped source, in such a direction as to increase the fringe contrast.

(iii) Rotate the mirror nearest the focal plane about an axis parallel to that of (ii) so as to increase the fringe spacing, which will usually have been reduced by process (ii).

(iv) Repeat (ii) and (iii) in succession once or twice.

(v) Increase the source size in the other direction and repeat processes (ii), (iii), (iv), this time rotating the mirrors about their other axes.

Thus, to reduce ε_{x0}, the horizontal width of the source must be increased and the mirrors rotated about their vertical axes. Then to reduce ε_{y0} the vertical height of the source is increased and the mirrors rotated about horizontal axes.

After this stage the displacements will usually be small enough to allow a source size sufficient to illuminate a screen. The successive rotations may then continue, with progressive increase of source size until a reasonable fringe contrast is obtained even with a source consisting of an illuminated ground glass with an aperture of about $f/20$ or $f/10$.

(*c*) *Source-plane fringe method.*—An alternative method when the displacements are fairly small is to observe the source-plane fringes directly and rotate the mirrors so as to increase their spacing. They may be observed by placing a ground glass screen in front of the collimating lens and looking into the emergent beam, using a pinhole in front of the eye if necessary. The contrast of the source-plane fringes depends on the ratio of the diameter of the pupil or pinhole to the spacing of the fringes in the emergent beam.

The sequence of mirror rotations necessary to increase the spacing of fringes in the source plane and in the emergent beam is of course the same as that described in the previous section for the source-size and fringe-contrast method.

This method is probably the one which is most suitable and most precise for the final stage of the adjustment, when the source-plane fringe spacing exceeds say $\frac{1}{4}$ in. It is not difficult to find ways of observing both sets of fringes at once, for example a ground glass screen in front of the collimating lens covering half the aperture, with another in the emergent beam covering the other half.

6.3. *Intermediate Adjustments by Geometric Optics.*—The methods described above may be used to reduce the displacements from values of say 0·1 to 0·2 in., which may be obtained easily by the initial adjustment method given later. So far as the displacements ε_x and ε_y are concerned, however, there are methods of intermediate range and accuracy which can make the adjustment more rapid.

(*a*) *The near and far cross-hair method.*—Several slightly varying versions of this method have been described[5,14]. The most convenient in practice seems to be to use the source itself, virtually at infinity, as one ' cross-hair ' and to have a real pair of cross-hairs in front of the collimating lens, or as near as possible to mirror 1 (Fig. 30a).

If the eye is placed in the emergent beam before adjustment, two images of the source and two images of the cross-hairs will appear. The apparent separations of the images are the values of the image displacements ε_x and ε_y for the co-ordinates of the source and cross-hairs respectively. Since the source is at infinity, its images are separated by angles α_x and α_y. If we take the origin of z at the cross-hair position, the cross-hair images, on the z-axis, are separated by ε_{x0} and ε_{y0}. Hence to reduce α_x and α_y to zero we must make the source images coincide, while to reduce ε_{x0} and ε_{y0} to zero we make the cross-hair images coincide.

The sequence of mirror rotations necessary is the same as that described for the source-size and fringe-contrast method. The mirror nearest the cross-hairs is used to reduce α_x and α_y by making the source images coincide, then the mirror further from the cross-hairs is used to reduce ε_{x0} and ε_{y0} by making the cross-hair images coincide.

Since for accuracy in reducing α_x and α_y the source must be small, the cross-wires should be illuminated by a lamp placed beside and in front of the collimating lens and shining across its beam.

Alternatively a lens may be placed in the emergent beam, and the real images of the source and cross-hairs on screens may be used. Another method is to use the shadows of the cross-hairs cast on a screen in the emergent beam, with no lens. In this case, to reduce the separation of the shadows, the mirror furthest from the screen, not that furthest from the cross-hairs themselves,

must be rotated. An advantage of the methods using screens is that as soon as sufficiently clear fringes appear the method may be combined with and continued by the source-size fringe-contrast method.

(*b*) *Price's method*[10].—This method has roughly the same scope and accuracy as the preceding one. A point source is placed near mirror 4 (Fig. 30b) so that light from it is transmitted to mirror 3 and reflected to mirror 2. A plane mirror is placed just beyond mirror 1 in either of the two positions shown. Then if the eye is placed near mirror 4 so as to receive light transmitted from mirror 2, four images of the source appear, since there are four possible light-paths, namely,

$$4-3-1-1-3-4$$
$$4-3-1-1-2-4$$
$$4-2-1-1-2-4$$
$$4-2-1-1-3-4$$

By sequences of mirror rotations similar to those described for the other methods, it is possible to bring the four images into coincidence, and this is the condition in which the displacements are zero.

The method in practice appears rather less satisfactory than the near and far cross-hair method, owing to the difficulty of distinguishing between four exactly similar images when these are close together, and also the fact that it is necessary to set up a source and mirror in positions where these are not normally used.

When the displacements are sufficiently small, if the point source is replaced by an illuminated ground glass screen, two sets of fringes appear. One set appears to be in focus in the plane of the source, the other nearer to the eye. These are affected by the mirror rotations in ways analogous to the source-plane and emergent-beam fringes in the normal arrangement. The interferometer may thus be adjusted accurately by increasing the spacing of the two sets of fringes.

6.4. *Methods for Initial Adjustment.*—From the previous sections it appears that, so far as the problem of reducing the image displacements is concerned, the only requirement for the initial adjustment is that it must reduce ε_{z0} below an upper limit of about 0·1 to 0·2 in. In fact, however, there are other requirements which depend to some extent on the particular design and application of the instrument. It is usually desirable to adjust the interferometer so that the light paths form a parallelogram and so that the field size is as large as possible, and it may be necessary to adjust the beam spacing to a particular value. If, in addition, the methods used give values of the displacements considerably lower than those strictly necessary, this will save time in the later stages of adjustment.

The initial adjustments may be done entirely by mechanical measurement, by methods which will depend on the design. Methods for obtaining maximum field size will also vary, and are fairly obvious. A convenient method is to direct the incident light beam so that light from mirror 1 exactly fills mirror 3. Then rotate 1 until the light reflected by it exactly fills 2. Then adjust the interferometer to a parallelogram arrangement with zero image displacements (section 6.4 (*a*) below), without rotating mirror 1 or traversing any except 4. Lastly, traverse mirror 4 in its own plane so that the beams *via* 2 and 3 fill it exactly.

If there are suitable slides for the mirrors in directions parallel to the beams 1–2 and 3–4, the beam spacing may be easily changed without disturbing the adjustment to maximum field size.

(*a*) *To obtain a parallelogram arrangement.*—One less fine adjustment is required if the interferometer is a parallelogram (section 4.2). If it were not, the semi-reflecting plates would need to be of different thickness (section 3.3) and a compensating plate would be required. Where both beams pass through a wind tunnel both should be normal to the tunnel windows. Also if the

interferometer is accurately adjusted to a parallelogram arrangement, and if there is no dispersion, the path difference is thereby reduced to zero. This is the most difficult adjustment to make by any other method, so if the mirrors can be made accurately parallel the adjustment time is shortened considerably.

The simplest method* for a small interferometer, where this is practicable, is to place a plane mirror (an unsilvered glass plate gives sufficient reflection) across the two beams 1–3 and 2–4 (position 1, Fig. 31). Two return images of the source appear, close to the source itself, by the light paths *A*–*B*–*C* and *A*–1–2–*D*–2–1–*E*. If the mirrors 1 and 2, and hence beams 1–3 and 2–4, are made parallel, the two images coincide.

Similarly if the mirror is placed across beams 1–2 and 3–4 (position 2, Fig. 31), these beams may be made parallel by making the two return images coincide. This is done by rotating mirror 3, since mirror 1 must be left parallel to 2.

Mirror 4 is then made parallel to the others by placing the eye in the emergent beam and rotating the mirror until the two images of the source coincide. At this stage, and within the accuracy of the method, α_x, α_y and ε_{y0} are zero, ε_{x0} and ε_{z0} are not zero but are proportional to one another since the Y_k are zero (section 4.2). Thus the last step is to traverse mirror 4 until the images of the near cross-hairs (section 6.3 (*a*)) coincide.

If the auxiliary mirror or glass plate is sufficiently flat, this method has an accuracy comparable with that of the intermediate-stage adjustments of section 6.3. In this case, unless there is a large difference in the thicknesses of glass in the two beams, a source large enough to illuminate a screen should be used and the adjustment continued by rapid traversing to find the fringe with highest contrast, and then by improving the contrast by the source-size and fringe-contrast method.

If a sufficiently large optically flat plate is not available, a normal piece of plate glass will give a less accurate result, and the more complete adjustment methods given above may be necessary.

For a large interferometer, or if the lay-out makes it impossible to place a single piece of glass across the beams, two small mirrors fixed parallel to one another and at the appropriate spacing on a metal beam may be used.

7. *Conclusions.*—The paper shows that it is possible to give a complete theory of the Mach-Zehnder interferometer, showing the effects on fringe contrast of the mirror positions, source configuration and optical imperfections. The following is a summary of the detailed conclusions:

The discussion of the source spectrum shows, by comparing rectangular and Gaussian distributions, that the number of clear fringes obtained with the usual type of distribution should be between half and one times the ratio of the mean wavelength to the half-width. It is possible by means of a small-angle prism to obtain fringes whose spacing is independent of wavelength and so use white light, but this is of no practical value.

Discussion of the effects of source size is based on the observation that this depends on the fringe pattern produced in the source plane by placing a source at the point in the emergent beam. This makes the effects easy to visualize and also suggests a useful method for final adjustment.

The fringe distribution in the source plane depends only on the separation of the two images of the point of the screen. With the ideal instrument the images of the co-ordinate system in the emergent beam may be treated as rigid bodies. The effects of all possible displacements of one relative to the other have been discussed.

Study of the effects of mirror movements shows that all the image displacements may be altered independently unless the interferometer is a parallelogram. Arranging the interferometer as a parallelogram thus reduces the number of adjustments from six to five, at the expense of a

* This is a slight modification of a method developed by K. J. Habell.

slight loss of contrast at the edges of the field with a large source and ' horizontal ' fringes parallel to the plane of the parallelogram. The parallelogram has other practical advantages including ease of adjustment.

The section on the relation between the two emergent beams shows that the reflection ratio of the semi-reflecting mirrors has a critical effect on the fringe contrast in the beam which is not normally used. This beam may be used if the reflection ratio is sufficiently near 50 per cent in both planes of polarisation.

The sections on the effects of imperfect optical elements show that the allowable tolerances are very wide, except for those on wedge angles and on surface flatness and refractive index variation. Fairly close limits on differences of thickness may be desirable, to avoid excessive dispersion.

Aberrations of the collimating lens have a negligible effect on the fringes if the interferometer is properly adjusted.

With methods of adjustment now available a well-designed instrument may be set up in a short time even under difficult conditions such as occur with different glass thicknesses in the two beams. The final adjustment methods are accurate enough to ensure that no loss of fringe contrast need arise from imperfect adjustment.

Acknowledgement.—Acknowledgement is due to H. K. Zienkiewicz of the Mechanics of Fluids Laboratory, University of Manchester, for very helpful criticism and corrections.

NOTATION

(A) *English symbols in alphabetical order*

a		Amplitude of wave arriving *via* each path separately
A	$= F - \lambda \frac{\partial F}{\partial \lambda} + F \frac{\cos i}{\sqrt{(\mu^2 - \sin^2 i)}}$	(section 5.2)
B	$= \frac{(\mu^2 - 1) \sin^2 i}{(\mu^2 - \sin^2 i)^{3/2}}$	(section 5.2)
b		Fringe spacing normal to the fringes
b_x		Fringe spacing in the direction of the x-axis
b_y		Fringe spacing in the direction of the y-axis
		} in the emergent beam
b'		Fringe spacing normal to the fringes
b_x'		Fringe spacing in the direction of the x-axis
b_y'		Fringe spacing in the direction of the y-axis
		} in the source plane
D		Thickness, or difference in thickness, of glass plates or windows
d'		Source width, or distance between elements of the source
d_x', d_y'		Width or spacing of elements of the source in the x and y directions, respectively
$F(i, \mu)$	$= \sqrt{(\mu^2 - \sin^2 i)} - \cos i$	
f		Focal length of the collimating lens
h		Linear displacement of a ray passing through a wind tunnel

i		(i) Intensity arriving *via* each path separately due to unit volume or unit area of the source
		(ii) Angle of incidence of the axial ray at the mirrors of a parallelogram interferometer
i_1 to i_4		Angles of incidence of the axial ray at the mirrors
I_0		Total intensity from the whole source *via* each path separately
I		Total intensity due to the whole source and both paths
k	$=$	d'/b'
Suffix $_k$		Refers to any of 1 to 4: Σ denotes summation over $k = 1$ to $k = 4$
L		(i) Change in optical path due to lens aberration or to the disturbance to be measured in a wave-shearing interferometer (sections 3.9, 3.10)
		(ii) Distance between two mirrors (section 4.3)
		(iii) Distance from a wedge (section 5.7)
		(iv) Wind tunnel width (section 5.13)
L_1		Distance between mirrors 1 and 2 or 3 and 4
L_2		Distance between mirrors 1 and 3 or 2 and 4
l		Path difference ($l = N\lambda$)
$_{m,n}$		Suffixes to X, Y, z referring to the two adjustable mirrors
N		Fringe number
N_0		Fringe number at $x' = y' = 0$ (Appendix I)
q		Distance along the lens axis, between the source plane and the focal plane of the lens
r	$=$	$\sqrt{(x^2 + y^2)}$
r'	$=$	$\sqrt{(x'^2 + y'^2)}$
$\frac{X_1}{2}$ to $\frac{X_4}{2}$		Rotations of the mirrors about ' horizontal ' axes ,*i.e.*, axes in the mirror plane and in plane $CDEF$ (Fig. 20)
$\frac{Y_1}{2}$ to $\frac{Y_4}{2}$		Rotations of the mirrors about ' vertical ' axes, *i.e.*, axes in the mirror plane and normal to plane $CDEF$ (Fig. 20)
X_k'	$=$	$X_k \cos i$
x, y, z		Co-ordinates of a point in the real or virtual emergent beam
x', y'		Co-ordinates of a point in the region of the source
x'', y''		Co-ordinates x and y of the image of a source point x', y' produced by the lens
x_0, y_0		(i) Co-ordinates x and y of the intersection of a ray with a reference plane near the lens (section 3.9)

x_0, y_0, z_0	(ii) Co-ordinates x, y, and z of the intersection of a ray with a wedge (section 5.6)
x_D, y_D, z_D	Co-ordinates x, y and z of a point on the edge of a diaphragm
Z	(i) Distance between two wedges (section 5.11)
	(ii) Out-of-focus distance of a compensating chamber (section 5.15)
z_1 to z_4	z co-ordinates of the intersection of the axial ray with the mirrors

(B) *Greek symbols in alphabetical order*

α	(i) Angle between interfering rays from the two paths
	(ii) Angle of incidence of any ray at a mirror
$\alpha_x, \alpha_y, \alpha_z$	Angles between the two images of the co-ordinate system in the emergent beam, about the x, y and z axes of one image
β	Inclination to the x-axis of fringes in the emergent beam
β'	Inclination to the x'-axis of fringes in the source plane, or of a slit source
δ	Variation in thickness of a plate from centre to edge, due to wedge angle
ε	(i) Distance between the two images of a point in the emergent beam (section 3.4)
	(ii) $\Sigma\varepsilon_k$, the sum of the mirror translations (section 4.3)
$\varepsilon_x, \varepsilon_y, \varepsilon_z$	Differences between the co-ordinates of the two images of any point in the emergent beam
$\varepsilon_{x0}, \varepsilon_{y0}, \varepsilon_{z0}$	Differences between the co-ordinates of the two images of the origin of co-ordinates in the emergent beam
$\frac{\varepsilon_1}{2}$ to $\frac{\varepsilon_4}{2}$	Translations of mirrors 1 to 4 along the normals
θ	(i) $\tan^{-1}(y/x)$ (sections 3, 4)
	(ii) Deviation produced by a wedge (section 5)
λ	Wavelength
λ_1	Spectral band width of the source
μ	Refractive index
ξ, η, ζ	Co-ordinates relative to the light rays (section 2.3)
ϕ	Prism angle or wedge angle of glass plates or windows
ψ	Angle between the rays and the line joining the images
ω_x, ω_y	Angles, about the x and y axes, respectively, between rays and the lens axes

REFERENCES

No.	Author	Title, etc.
1	G. Hansen	Uber ein Interferometer nach Zehnder-Mach. *Z. tech. Phys.* Nr. 9. 1931.
2	H. Schardin	Theorie und Anwendung des Mach- Zehnderschen Interferenzrefraktometers. *Z. Instrum.* Bd. 53. 1933.
		Theory and applications of the Mach-Zehnder interferometer. R.A.E. Trans. 79. 1946.
3	Th. Zobel	Development and construction of an interferometer for optical measurements of density fields. N.A.C.A. Tech. Memo. 1184. 1947.
4	E. Lamla	Concerning the light path in a Mach-Zehnder interferometer. R.A.E. Trans. 80. Aero. Trans. 6. A.R.C. 9654. January, 1946.
5	Hottenroth	On some experiences in the use of the Mach-Zehnder interferometer. (F.B. 1924. December, 1943.) MAP—V45—67T. G.D.C. 10/1417T. A.R.C. 11,332. February, 1946.
6	W. Kinder	Theorie des Mach-Zehnder Interferometers und Beschreibung eines Gerätes mit Einspiegeleinstellung. *Optik.* Band 1. Heft 6. 1946.
7	E. H. Winkler	Analytical studies of the Mach-Zehnder interferometer. Naval Ordnance Laboratory Report NOLR 1077. 1947.
8	F. D. Bennett	Optimum source size for the Mach-Zehnder interferometer. *J. App. Phys.* Vol. 22, No. 2. February, 1951.
9	F. D. Bennett	Effect of size and spectral purity of source on fringe pattern of the Mach-Zehnder interferometer. *J. App. Phys.* Vol. 22, No. 6. June, 1951.
10	E. W. Price	Initial adjustment of the Mach-Zehnder interferometer. *Rev. Sci. Inst.* Vol. 23, No. 4. 1952.
11	H. Hannes	Zur Grundstellung des Mach-Zehnder Interferometers. *Optik,* Band 12, Heft 1. 1955.
12	L. H. Tanner	The optics of the Mach-Zehnder interferometer. A.R.C. 18,733.
13	W. L. Howes and D. R. Buchele ..	Practical considerations in specific applications of gas-flow interferometry. N.A.C.A. Tech. Note 3507. July, 1955.
14	P. B. Gooderum, G. P. Wood and M. J. Brevoort.	Investigation with an interferometer of the turbulent mixing of a free supersonic jet. N.A.C.A. Report 963. 1950.
15	Gilbert	Mém. couronnés de l'Acad. de Bruxelles. tom. XXXI. p. 1. 1863. (Preston, *Theory of Light,* p. 223.)

APPENDIX I

Relation between Fringe Contrast, Size of Source and Fringe Spacing in the Source Plane

(*a*) *Linear terms.*—Suppose the fringes in the source plane corresponding to a point B in the emergent beam are approximately linear, with spacing b'. Take axes x' perpendicular and y' parallel to the fringes, and let the fringe number at the origin be N_0. Then the fringe number at x', y' is $N_0 + x'/b'$. If, with one beam removed, unit area of source at x', y' contributes intensity i at B, then with both beams it will contribute intensity $4i \cos^2 (N_0 + x'/b')$. Thus the total intensity is

$$I = \int 4i \cos^2 \pi \left(N_0 + \frac{x'}{b'} \right) dx' \, dy' .$$

Now the fringe contrast at B is the ratio of the maximum and minimum values of this integral with respect to N_0. If the source is symmetrical about $x = 0$, the minimum and maximum values are at $N_0 = \frac{1}{2}$ and $N_0 = 0$ and the ratio is

$$\frac{\int i \sin^2 \pi \frac{x'}{b'} dx' dy'}{\int i \cos^2 \pi \frac{x'}{b'} dx' dy'} .$$

If the source is rectangular and uniform, of width d', this becomes

$$\frac{\int_{-d'/2}^{d'/2} 1 - \cos 2\pi \frac{x'}{b'} dx'}{\int_{-d'/2}^{d'/2} 1 + \cos 2\pi \frac{x'}{b'} dx'}$$

$$= \frac{\pi k - \sin \pi k}{\pi k + \sin \pi k} \text{ where } k = \frac{d'}{b'} .$$

The ratio of minimum to maximum intensity, shown in Fig. 32a, thus increases from zero when the source is small to unity when the source width equals the fringe spacing. The fringes in the emergent beam then vanish, but reappear with low contrast and a shift of half the spacing as the source size is further increased. The fringes vanish at integral values of k, and are very faint for all values of k greater than unity.

By using photographic materials of high contrast, and a suitable exposure, it is possible to get a good print with a light intensity contrast of 2, and a usable print with a contrast of 1·5. Thus from Fig. 32a it appears that even under ideal conditions, the contrast will be insufficient if k exceeds about 0·8. In practice the contrast will be reduced by scattered light, by light reflected at lens surfaces and at the back surfaces of the plates, and by lack of monochromatism of the light and filter combination. It may be desirable to reduce the exposure below that giving the best contrast, so as to reduce the source duration. Thus even with a point source the contrast may be little more then enough to produce a good print, and so any further reduction due to increase of source size must be quite small. So far as imperfections of the optical elements are concerned, section 5 shows that wedge angles of the windows and plates, which produce linear terms in the source-plane path variation, are by far the most serious. The criterion used in sections 5.6 to 5.11 is that the combined effect of these imperfections should be such as to produce a ratio of minimum to maximum intensity of not more than 0·05, corresponding to $k = 0·243$.

(*b*) *Quadratic terms.*—Suppose the source-plane path variation is proportional to x'^2, that is, the fringes are still linear and parallel to the y' axis but the path variation with x' is parabolic. The path difference may be expressed as $l = \lambda\{N_0 + (x'^2/b'^2)\}$, where b' is the value of x' at which the path differs by one wavelength from its value at $x' = 0$. The fringe number is thus $N_0 + x'^2/b'^2$.

For a uniform rectangular source of width d', and intensity i per unit width *via* each beam separately, the resulting intensity is:

$$I = 4i \int_{-d'/2}^{d'/2} \cos^2 \pi \left(N_0 + \frac{x'^2}{b'^2}\right) dx' .$$

The derivative of this with respect to N_0 is

$$\frac{dI}{dN_0} = -4i\pi \left[\sin 2\pi N_0 \int_{-d'/2}^{d'/2} \cos 2\pi \frac{x'^2}{b'^2} dx' + \cos 2\pi N_0 \int_{-d'/2}^{d'/2} \sin 2\pi \frac{x'^2}{b'^2} dx'\right]$$

$$= -4i\pi b' \left[A\left(\frac{d'}{b'}\right) \sin 2\pi N_0 + B\left(\frac{d'}{b'}\right) \cos 2\pi N_0\right]$$

where

$$A\left(\frac{d'}{b'}\right) = \int_0^{d'/b'} \cos\frac{\pi}{2}v^2\,dv\,, \qquad B\left(\frac{d'}{b'}\right) = \int_0^{d'/b'} \sin\frac{\pi}{2}v^2\,dv\,.$$

Hence the intensity has a stationary value when $\tan 2\pi N_0 = -B/A$. The intensity is

$$I = 4i\left[\frac{d'}{2} + \frac{b'}{2}A\cos 2\pi N_0 - \frac{b'}{2}B\sin 2\pi N_0\right].$$

If $\tan 2\pi N_0 = -B/A$, this becomes

$$I = \frac{b'}{2}\left[\frac{d'}{b'} \pm \sqrt{(A^2 + B^2)}\right].$$

The ratio of minimum to maximum intensity is thus:

$$\frac{(d'/b') - \sqrt{(A^2 + B^2)}}{(d'/b') + \sqrt{(A^2 + B^2)}}.$$

A and B are Fresnel's integrals and are tabulated in Ref. 15. Fig. 32b shows the ratio plotted against d'/b'. The ratio rises much more slowly than for the linear path variation, does not pass through unity but tends to unity as d'/b' tends to infinity.

Various imperfections of the optical elements, namely differences in thickness, incidence and refractive index between the windows and plates in the two beams, give rise to quadratic terms in the source-plane path variation. Since these in any case do not involve severe restrictions on the imperfections, they may be kept very small. The criterion used in sections 5.2 to 5.5 is that the combined effect of these imperfections should result in a ratio of minimum to maximum intensity of not more than 0·02. This corresponds to $d'/b' = 0{\cdot}78$.

APPENDIX II

Relation between Fringe Contrast and the Spectral Band Width of the Source, with no Dispersion

Consider a point at which the path difference is l, which, since there is no dispersion, is independent of the wavelength λ. If the intensity per unit wavelength arriving *via* each path separately is $i(\lambda)$, the total intensity is

$$4\int_0^\infty i\cos^2\frac{\pi l}{\lambda}\,d\lambda\,.$$

Suppose that i differs from zero only over a narrow range of wavelengths near $\lambda = \lambda_0$. Then we may put $\lambda = \lambda_0 + \varepsilon$, and neglect $\varepsilon^2/\lambda_0^2$ and higher powers.

The intensity becomes:

$$I = 4\int_{-\infty}^{\infty} i\cos^2\frac{\pi l}{\lambda_0}\left(1 - \frac{\varepsilon}{\lambda_0}\right)d\varepsilon$$

$$= 2\int_{-\infty}^{\infty} i\left[1 + \cos 2\frac{\pi l}{\lambda_0}\left(1 - \frac{\varepsilon}{\lambda_0}\right)\right]d\varepsilon\,.$$

If the intensity distribution is symmetrical about λ_0, *i.e.*, if $i(\varepsilon) = i(-\varepsilon)$, this becomes

$$I = 2\int_{-\infty}^{\infty} i\, d\varepsilon + 2\cos 2\frac{\pi l}{\lambda_0}\int_{-\infty}^{\infty} i\cos 2\pi\frac{l\varepsilon}{\lambda_0^2}\, d\varepsilon .$$

(*a*) *Rectangular intensity distribution.*—First consider an intensity-wavelength distribution having constant intensity i over the range $\lambda = \lambda_0 \pm \frac{1}{2}\lambda_1$, *i.e.*, a rectangular distribution of width λ_1. The intensity is

$$I = 2i\lambda_1 + 2i\lambda_1\cos 2\frac{\pi l}{\lambda_0}\left[\frac{\lambda_0^2}{\pi l\lambda_1}\sin\frac{\pi l\lambda_1}{\lambda_0^2}\right].$$

The ratio of minimum to maximum intensity with respect to l is, putting $l\lambda_1/\lambda_0^2 = k$,

$$\frac{1 - (\sin \pi k/\pi k)}{1 + (\sin \pi k/\pi k)} = \frac{\pi k - \sin \pi k}{\pi k + \sin \pi k}.$$

This is the same relation as that of Appendix I for the variation of contrast with source size for a linear source-plane path variation. The contrast falls to zero when $k = 1$, and the fringe number is then $l/\lambda_0 = \lambda_0/\lambda_1$. Thus the number of fringes visible each side of the zero fringe is a fraction, less than unity, of the ratio λ_0/λ_1. For photography the minimum contrast which will give a good print is about 2. There will be a loss of contrast due to other causes however, and so the acceptable ratio of minimum to maximum intensity due to the spectral width is probably not more than about $\frac{1}{4}$. This gives $k = 0{\cdot}53$ and a total number of clear fringes of $1{\cdot}06\ \lambda_0/\lambda_1$.

(*b*) *Gaussian intensity distribution*[9].—The intensity-wavelength distribution of a spectral line or interference filter is better represented by a Gaussian curve[9]. If the distribution is $i = I_0 \exp -(\varepsilon/\varepsilon_0)^2$, the intensity becomes:

$$\begin{aligned}\frac{I}{I_0} &= 2\int_{-\infty}^{\infty} \exp -(\varepsilon/\varepsilon_0)^2\, d\varepsilon + 2\cos 2\pi\frac{l}{\lambda_0}\int_{-\infty}^{\infty} \exp -(\varepsilon/\varepsilon_0)^2 \cos 2\pi\frac{l\varepsilon}{\lambda_0^2}\, d\varepsilon \\ &= 2\sqrt{(\pi)}\,\varepsilon_0 + 2\sqrt{(\pi)}\,\varepsilon_0\cos 2\pi\frac{l}{\lambda_0}\exp -(\pi l\varepsilon_0/\lambda_0^2)^2 .\end{aligned}$$

The ratio of minimum to maximum intensity is thus, putting $l\varepsilon_0/\lambda_0^2 = k_1$,

$$\frac{1 - \exp -\pi^2 k_1^2}{1 + \exp -\pi^2 k_1^2} = \tanh\frac{\pi^2 k_1^2}{2}.$$

For small values of k_1 this is approximately $\frac{1}{2}(\pi^2 k_1^2)$, while the corresponding ratio for the rectangular distribution is $\frac{1}{12}(\pi^2 k^2)$. The two are thus equal if $k = \sqrt{(6)}k_1$ and $\lambda_1 = \sqrt{(6)}\,\varepsilon_0$.

The half-width λ_1' of the exponential distribution is given by

$$\begin{aligned}\exp -(\lambda_1'/2\varepsilon_0)^2 &= \tfrac{1}{2} \\ \lambda_1' &= 2\varepsilon_0\sqrt{(\log 2)} \\ &= 1{\cdot}665\,\varepsilon_0 .\end{aligned}$$

Thus the two distributions give the same loss of contrast, when the contrast is high, if $\lambda_1 = 1{\cdot}47\lambda_1'$.

Fig. 33 shows, for comparison, graphs of minimum to maximum intensity ratio for the Gaussian distribution and for the rectangular distribution of width $1{\cdot}47$ times the half-width of the Gaussian curve. For the Gaussian distribution the intensity ratio reaches $\frac{1}{4}$ when $N(\lambda_1'/\lambda_0) = 0{\cdot}379$. Thus, using this criterion, this distribution gives a total number of clear fringes of $0{\cdot}76(\lambda_0/\lambda_1')$.

APPENDIX III

The Twyman-Green Interferometer

Fig. 33 shows that, so far as the optics of the ideal interferometers are concerned, the Twyman-Green arrangement may be considered a special case of the Mach-Zehnder in which the two semi-reflecting plates coalesce and in which the incidence at the plane mirrors becomes zero.

Using the notation of section 4, we have, for the Twyman-Green arrangement:

$$\begin{aligned} i_3 &= i_2 = 0\,, \\ i_4 &= -\,i_1\,, \\ X_4 &= X_1\,, \\ Y_4 &= Y_1\,, \\ \varepsilon_4 &= \varepsilon_1\,, \\ z_3 &= z_2 = z_1 + L \\ z_4 &= z_1 + 2L\,. \end{aligned}$$

Hence equations (4.1) become:

$$\begin{aligned} \varepsilon_{z0} &= \varepsilon_2 + \varepsilon_3 + 2\varepsilon_1 \cos i_1\,, \\ \varepsilon_{x0} &= -\,\Sigma z_k Y_k = -\,(z_1 + L)(2Y_1 + Y_2 + Y_3) \\ \alpha_y &= 2Y_1 + Y_2 + Y_3 \\ \varepsilon_{y0} &= (z_1 + L)(2X_1 \cos i_1 + X_2 + X_3) \\ \alpha_x &= 2X_1 \cos i_1 + X_2 + X_3 \\ \alpha_z &= 0\,. \end{aligned}$$

Rearranging these, and expressing ε_{x0} and ε_{y0} in terms of α_x and α_y, we obtain:

$$\begin{aligned} \alpha_x &= 2X_1 \cos i_1 + X_2 + X_3 \\ \alpha_y &= 2Y_1 \qquad\quad + Y_2 + Y_3 \\ \alpha_z &= 0 \\ \varepsilon_{x0} &= -\,\alpha_y(z_1 + L) \\ \varepsilon_{y0} &= \alpha_x(z_1 + L) \\ \varepsilon_{z0} &= 2\varepsilon_1 \cos i_1 + \varepsilon_2 + \varepsilon_3\,. \end{aligned}$$

It follows that only three of the displacements can be adjusted independently, and only three of the nine possible adjustments are necessary. These three must be one translation, one vertical axis rotation and one horizontal axis rotation. Any of the three mirrors may be used for each of these necessary adjustments.

Substituting the above equations in equations (3.2) we obtain,

$$\varepsilon_x = \varepsilon_{x0} + z\alpha_y = \alpha_y\{z - (z_1 + L)\}\,,$$

and

$$\varepsilon_y = \varepsilon_{y0} - z\alpha_x = -\,\alpha_x\{z - (z_1 + L)\}\,.$$

Thus at $z = z_1 + L(= z_2 = z_3)$, ε_x and ε_y are zero. The source-plane fringe distribution is therefore that discussed in section 3.7 (*b*), with the origin of z at mirror 2. If the plane of mirrors 2 and 3 is focussed on the screen the permissible source size (for the ideal interferometer) is practically unlimited.

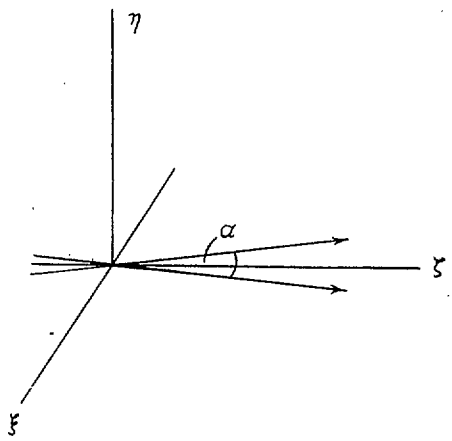

FIG. 1. Co-ordinate system and interfering rays.

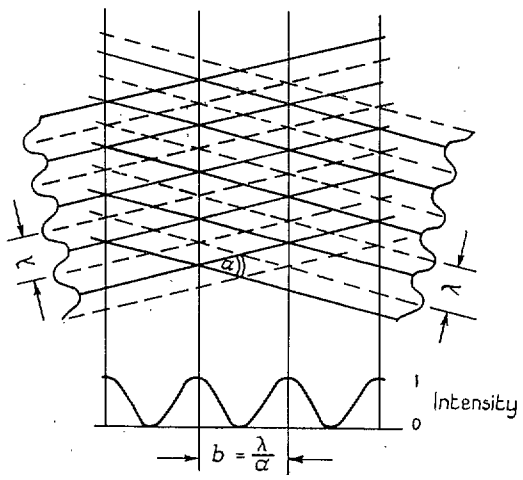

FIG. 2. Relation between fringe spacing and inclination of wave fronts.

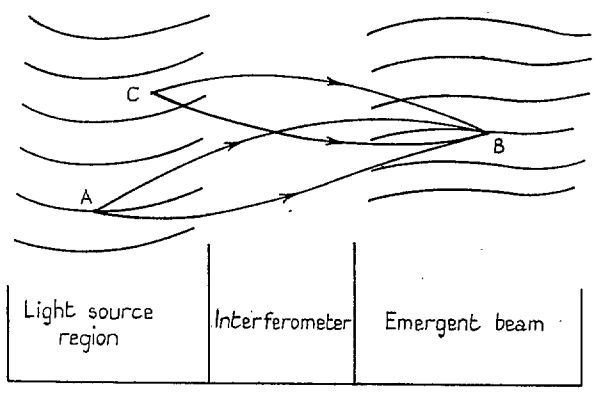

FIG. 3. Reciprocal relation between source and screen.

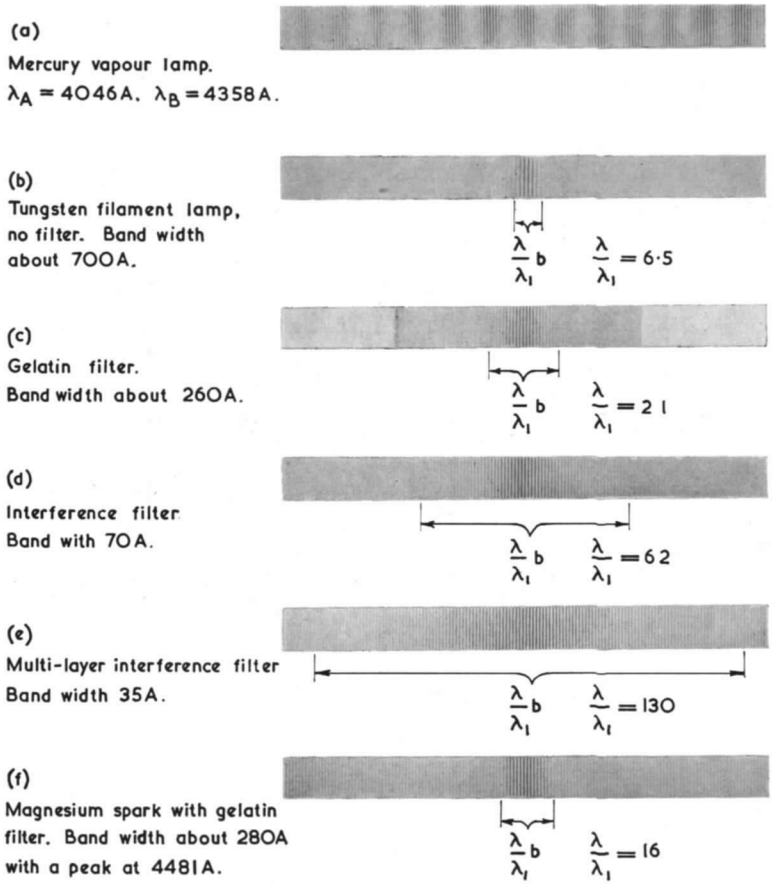

FIGS. 4a to 4f. Effect of the spectral distribution of the source, with no dispersion.

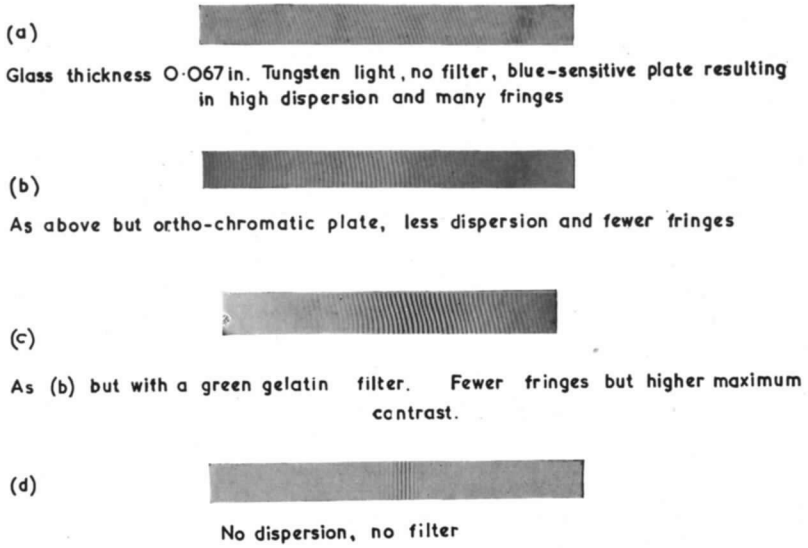

FIGS. 5a to 5c. Effect of a refracting plate.

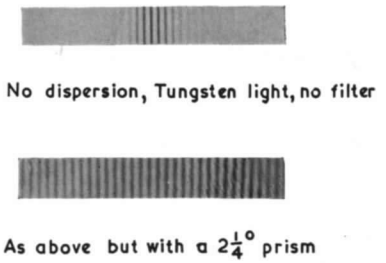

FIGS. 6a and 6b. Effect of a refracting prism.

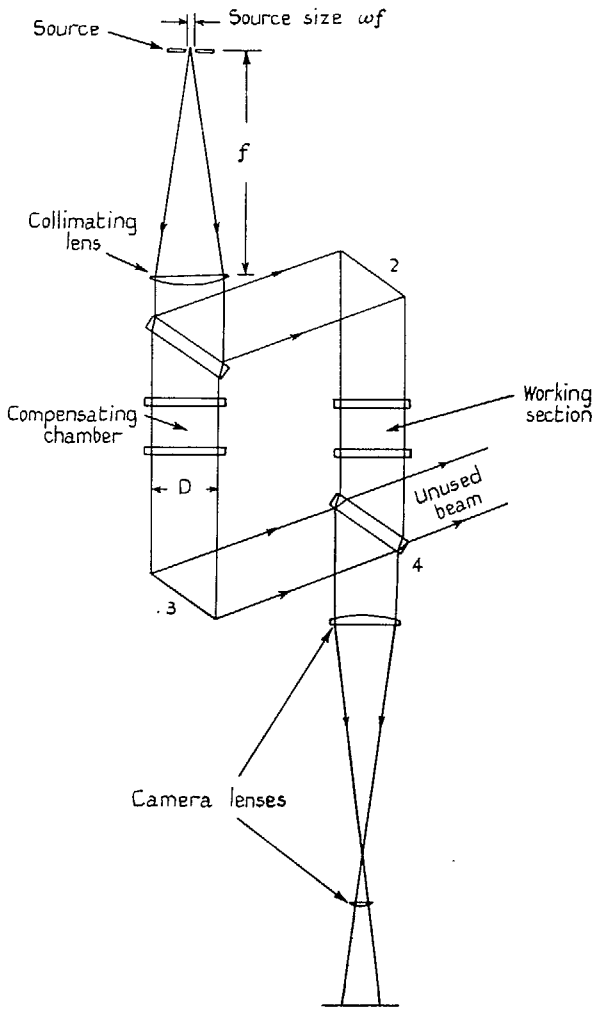

FIG 7. General arrangement of the interferometer.

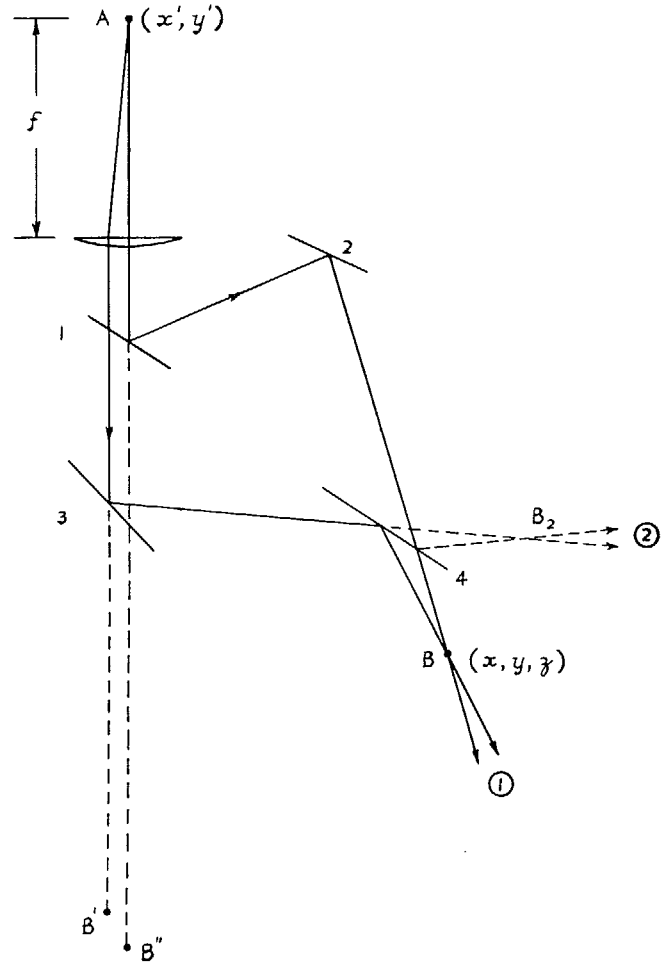

FIG 8. The ideal 4-mirror interferometer. Note that the rays 1–2–4, 1–3–4 need not necessarily lie even approximately in one plane.

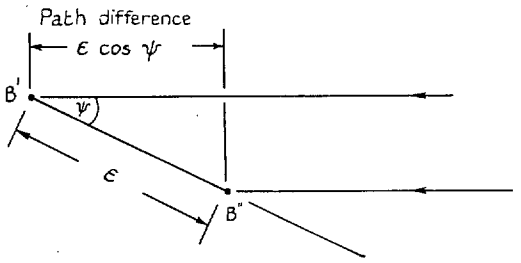

FIG. 9. Path difference in terms of image positions.

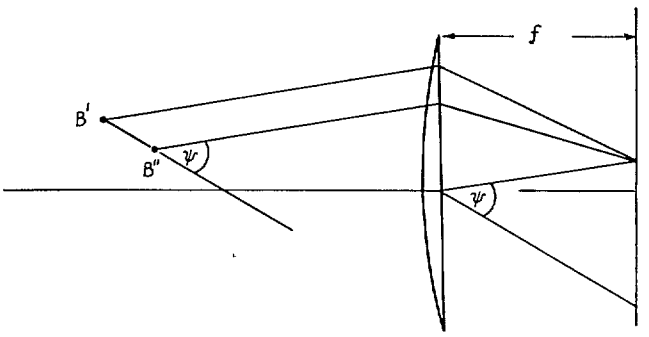

FIG. 10. Conic-section fringes in the source plane.

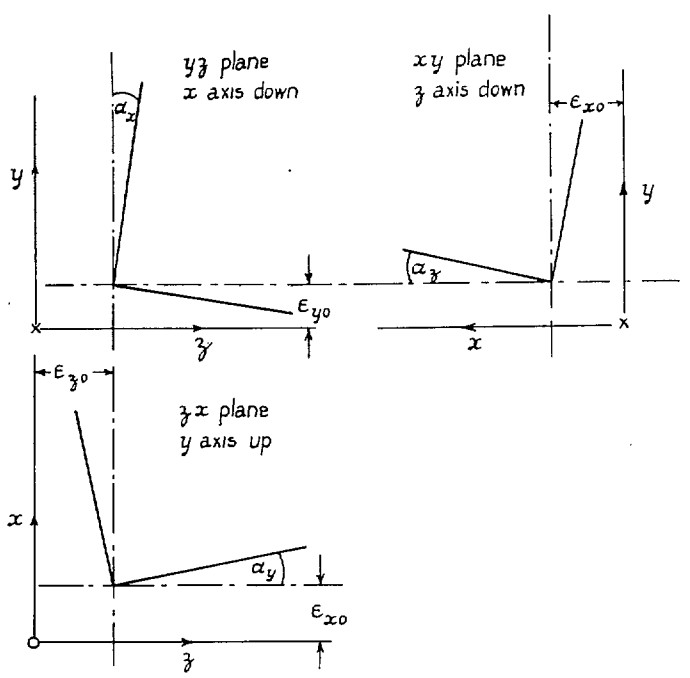

FIG. 11. Displacement of images of points in the emergent beam.

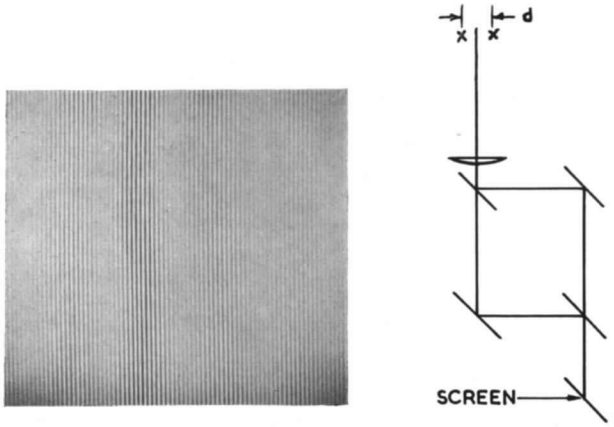

(a) SCREEN ROTATED 45° ABOUT THE VERTICAL AXIS

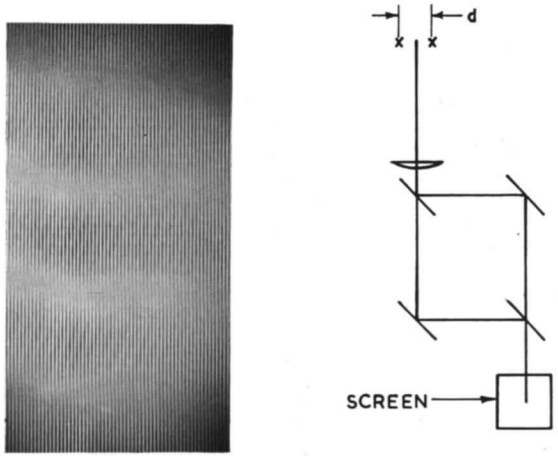

(b) SCREEN ROTATED 45° ABOUT THE HORIZONTAL AXIS

$a_z = 0, \quad \epsilon_{xo} = \epsilon_{yo} = 0, \quad \frac{f}{d} = 20$

FIGS. 12a and 12b. Fringes produced by a source consisting of two vertical slits, with screens inclined at 45 deg.

(a)

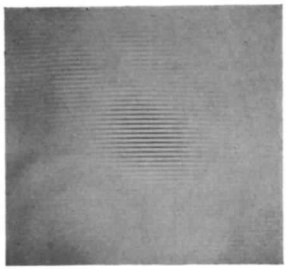

CIRCULAR SOURCE, DIAMETER 0·1 f

(b)

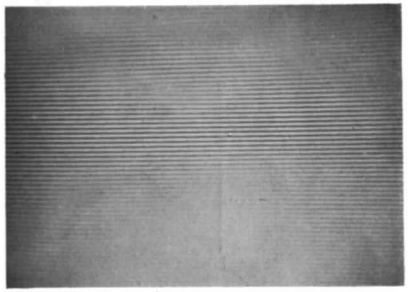

HORIZONTAL SLIT SOURCE

(c)

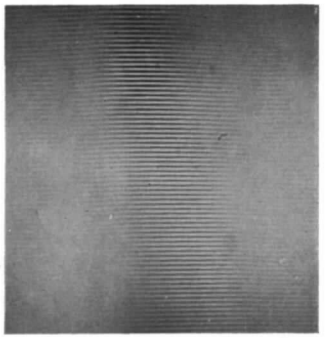

VERTICAL SLIT SOURCE

$\epsilon_{xo} = \epsilon_{yo} = 0, \quad a_x = -a_z = 4 \cdot 95 \times 10^{-4}$

FIGS. 13a to 13c. Effects of the image rotation α_z about the z-axis.

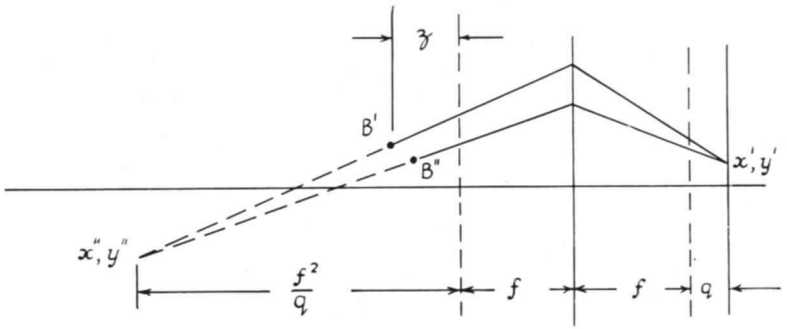

FIG. 14. Source not in the focal plane.

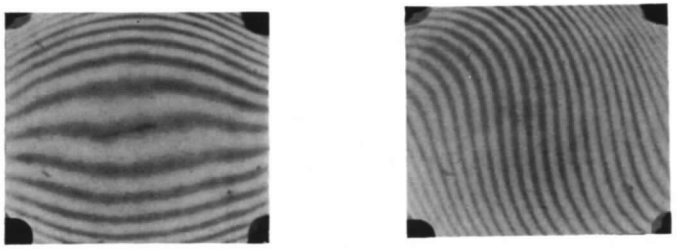

(a) $a_x = 3{\cdot}5 \times 10^{-5}$, $a_y = 0$ (b) $a_x = 0$, $a_y = 1{\cdot}05 \times 10^{-4}$

IMAGE, AT THE AXIAL FOCUS, OF RAYS PASSING THROUGH THE LENS AT DISTANCES OF 1·0, 1·5, 2·0 AND 2·5 IN. FROM THE AXIS

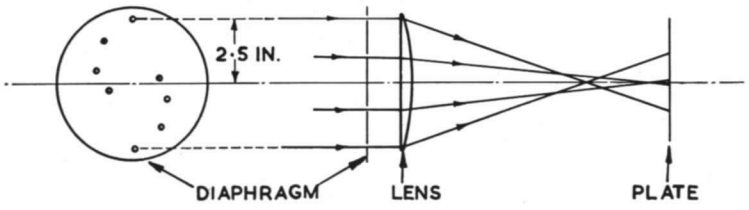

EFFECT OF SPHERICAL ABERRATION OF THE COLLIMATING LENS

FIG. 15.

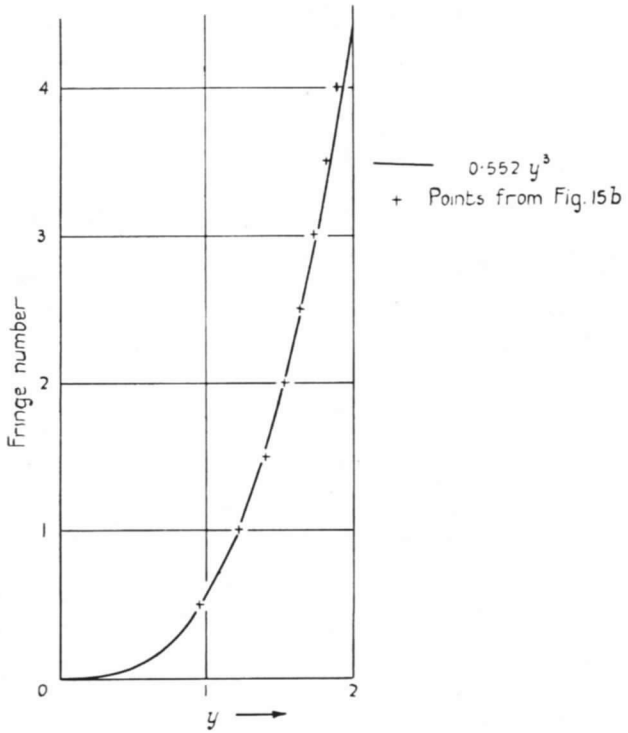

FIG. 16. Graph of fringe shift against y for a lens with spherical aberration.

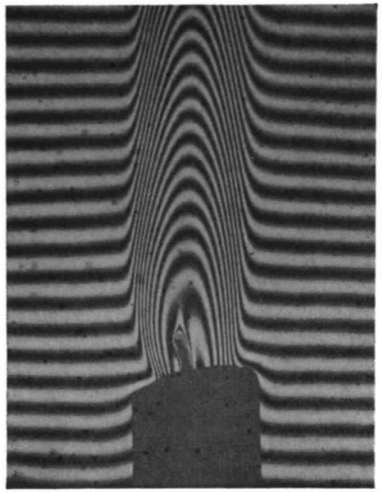

(a) NORMAL MACH–ZEHNDER INTERFEROGRAM

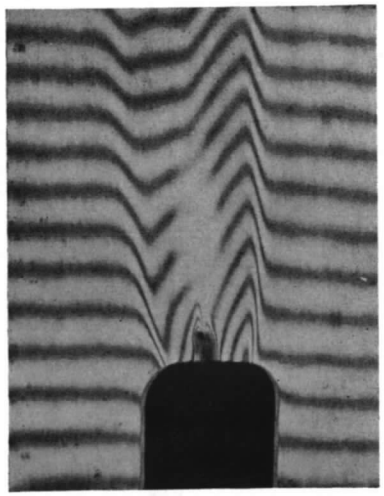

(b) WAVE-SHEARING INTERFEROGRAM (NOTE THE GREATER RELATIVE BRIGHTNESS OF THE FLAME ITSELF IN (b) OWING TO THE SMALL SOURCE SIZE)

FIGS. 17a and 17b. Normal and wave-shearing interferograms of a candle flame.

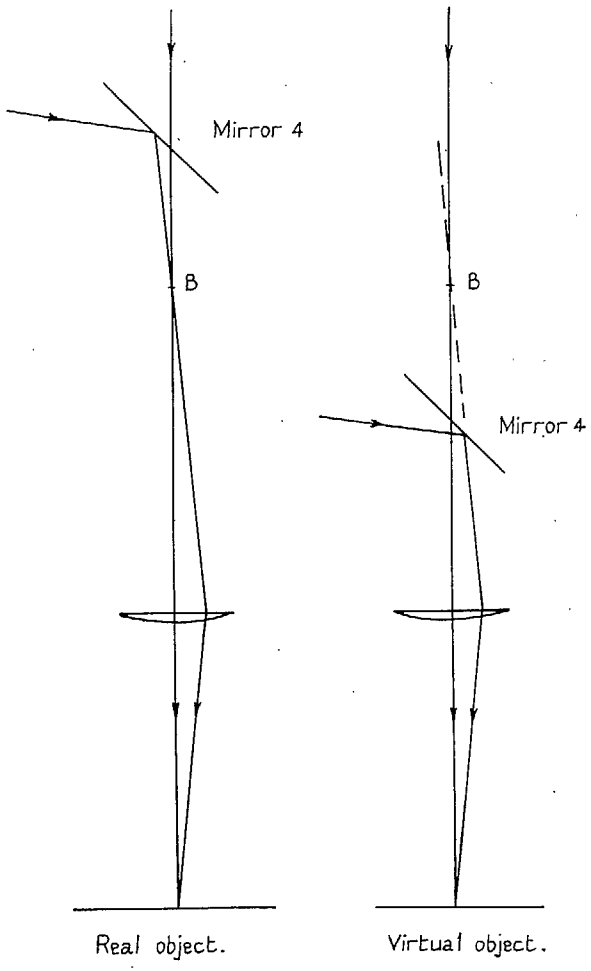

FIG. 18. Arrangements of interferometer and camera producing real images of real and virtual object fringe patterns.

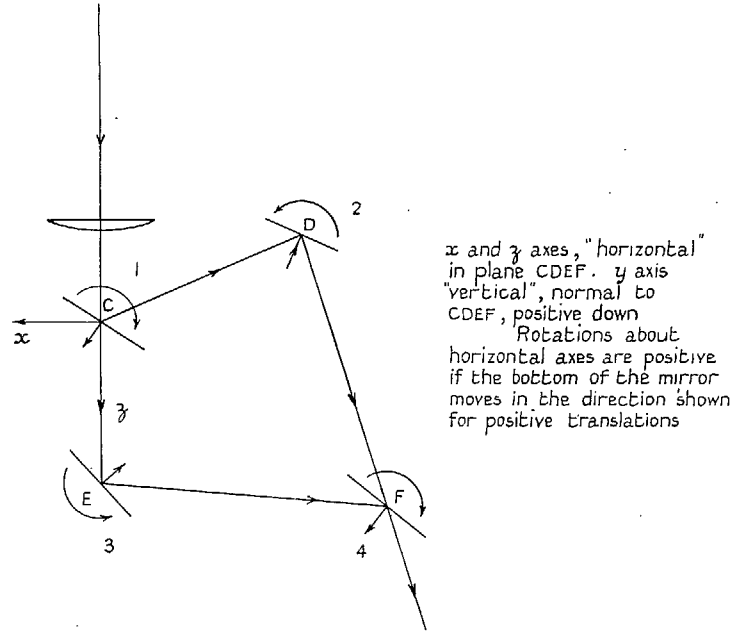

FIG. 19. Plane 4-mirror interferometer with zero image displacements, showing sign convention for mirror displacements.

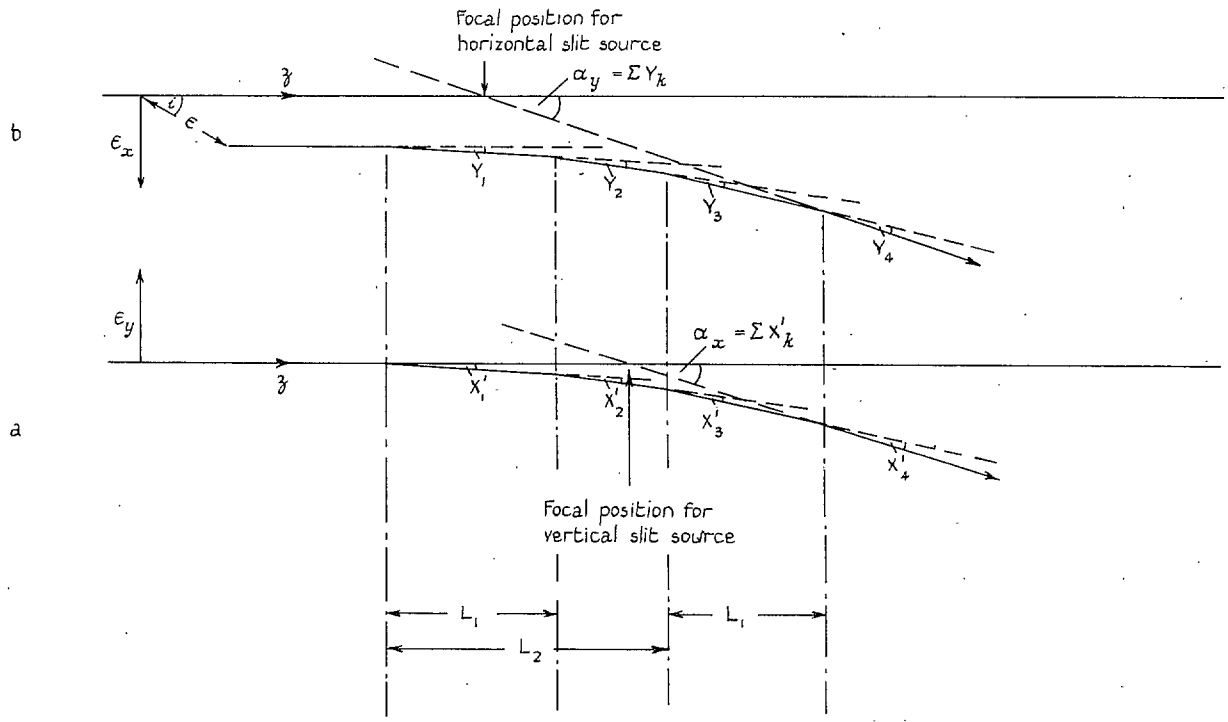

FIG. 20. Geometrical representation of the effects of mirror displacements with a parallelogram interferometer.

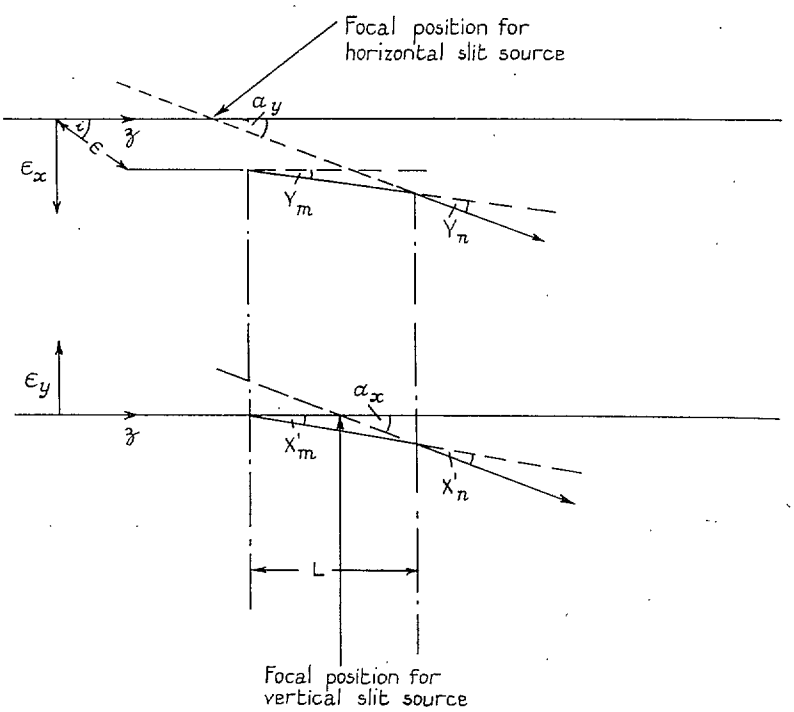

FIG. 21. Effects of five mirror displacements, with a parallelogram interferometer.

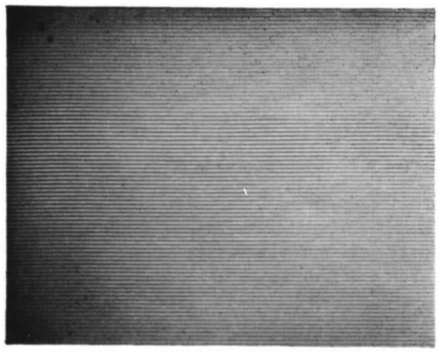

VERTICAL SLIT SOURCE

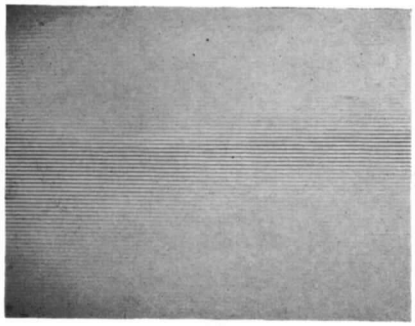

CIRCULAR SOURCE, DIAMETER 0·1 f

$\alpha_z = -\alpha_x = 5{\cdot}75 \times 10^{-4}$

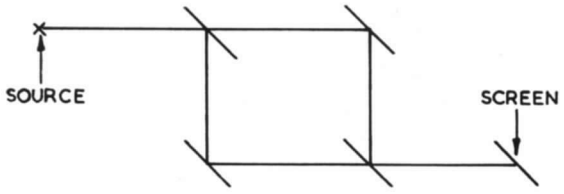

FIG. 22. Effects of the image rotation α_z about the z-axis, with the screen inclined and parallel to the mirrors.

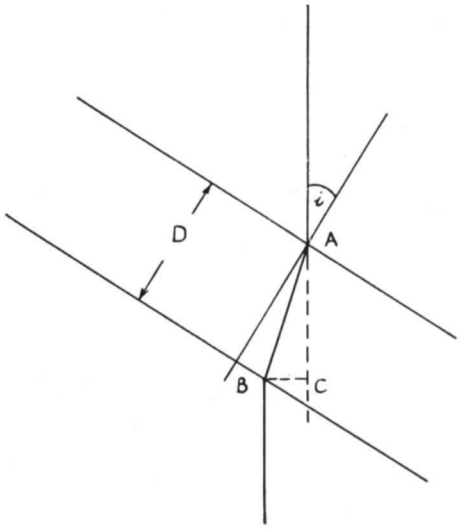

FIG. 23. Optical path in a parallel plate.

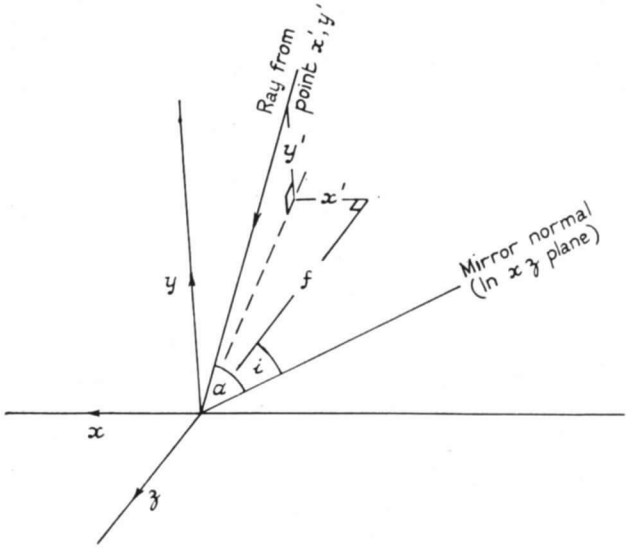

FIG. 24. Effect of source co-ordinates on angle of incidence.

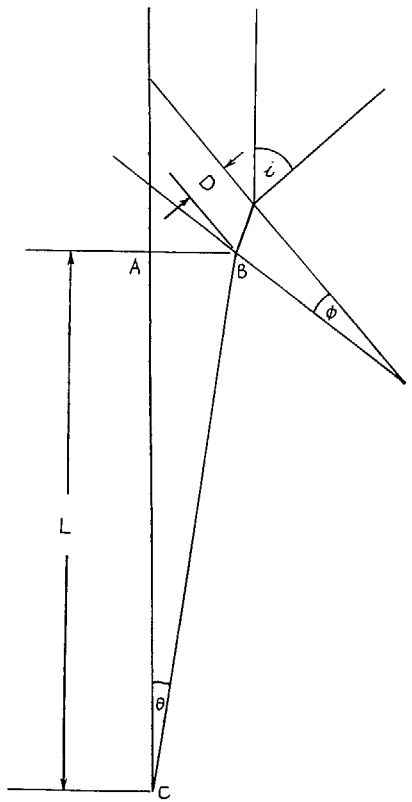

FIG. 25. Optical path through a wedge.

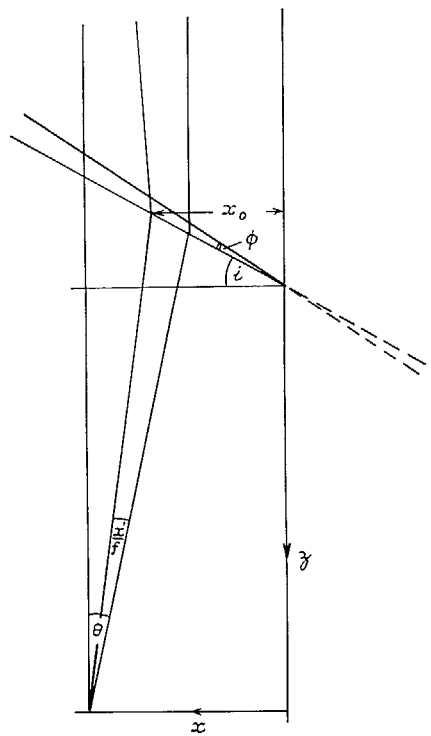

FIG. 26. Wedge with apex parallel to the y-axis.

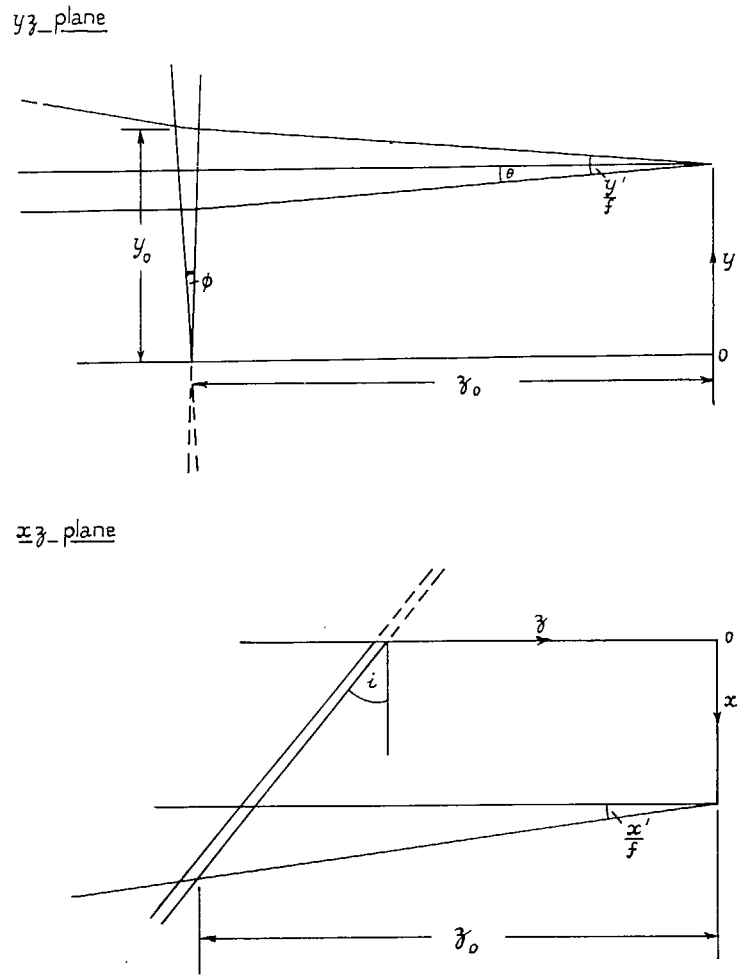

$$y_o = y + \left(\frac{y'}{f} - \theta\right) z_o$$

$$z_o = (z + x \tan i)\left(1 + \frac{x'}{f} \tan i\right)$$

FIG. 27. Wedge with its apex perpendicular to the y-axis.

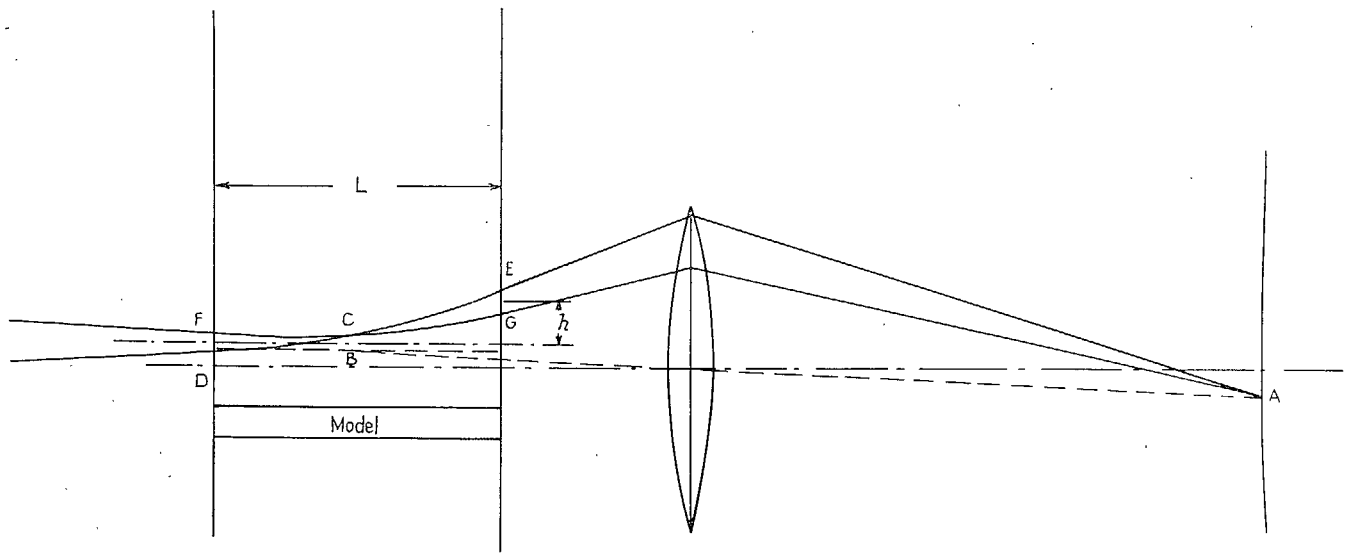

FIG. 28. Displacement of rays passing through a wind tunnel.

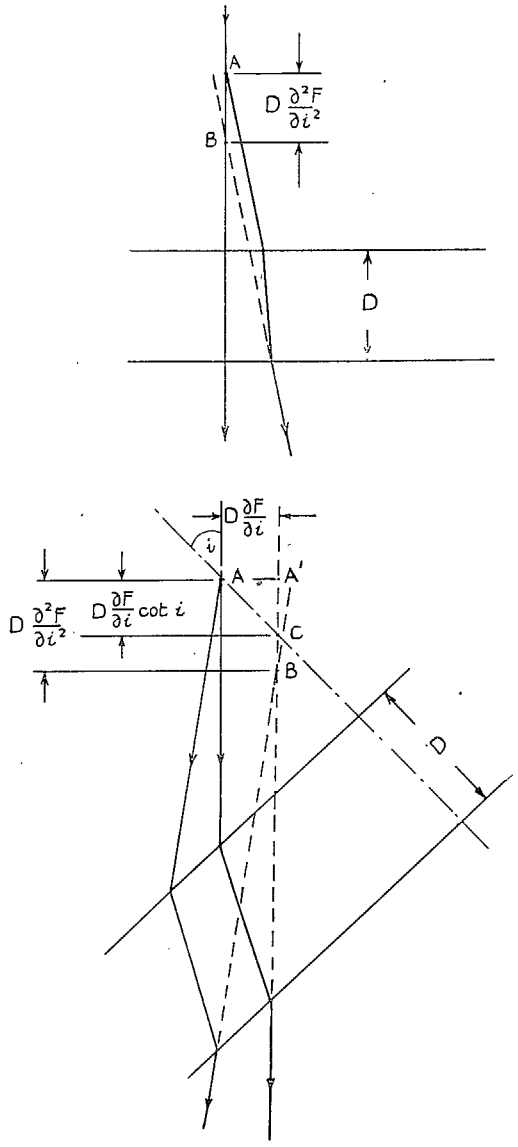

FIG. 29. Effect of ray deflections on the path through the plates.

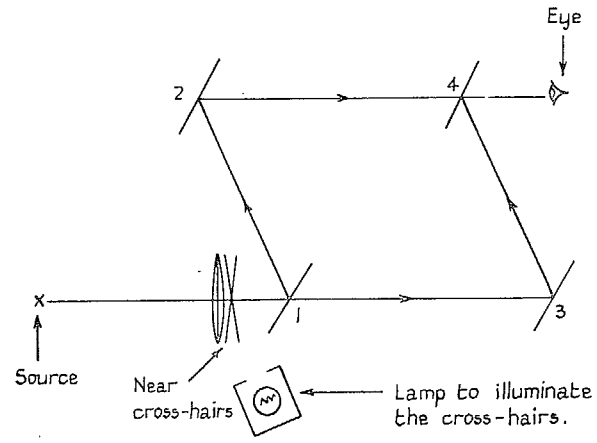

(a) Near and far cross-hair method.

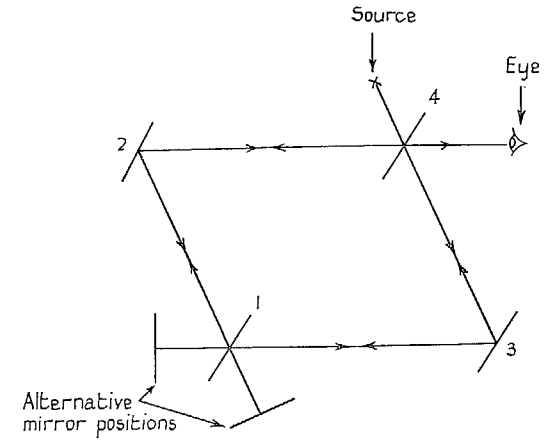

(b) Price's method

FIGS. 30a and 30b. Intermediate methods of adjustment using geometric optics.

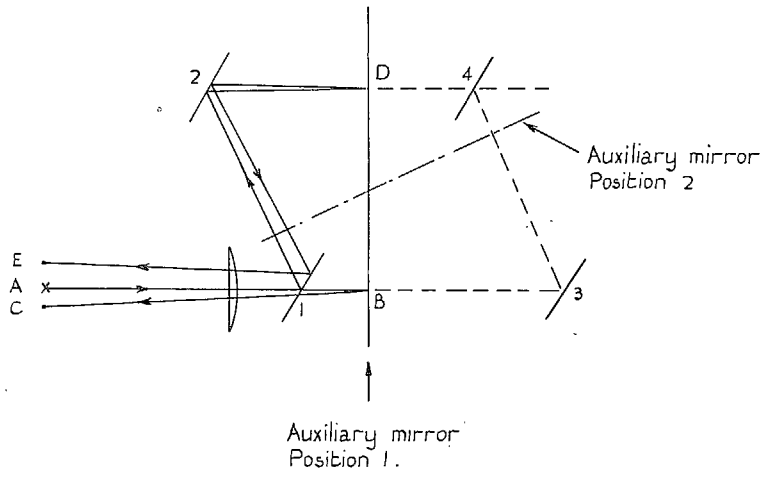

FIG. 31. Method for making the mirrors parallel.

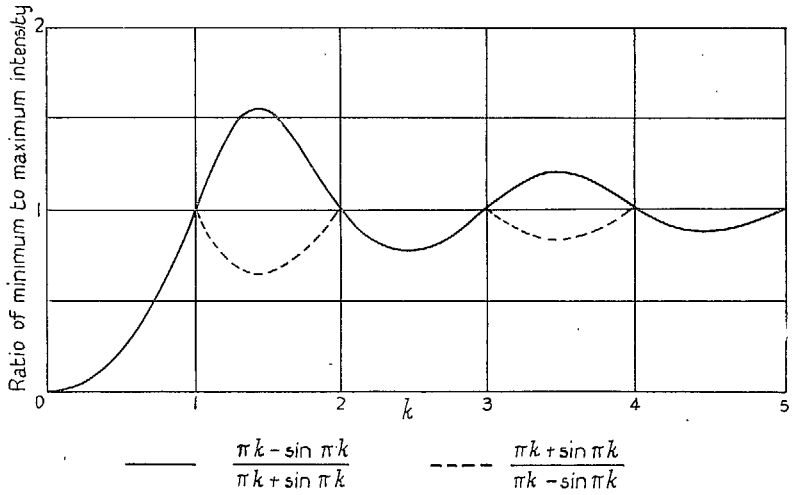

(a) Linear path variation

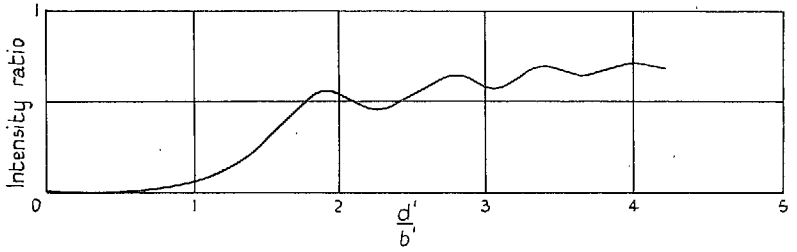

(b) Quadratic path variation

FIGS. 32a and 32b.

(71639) Wt. 52/8943 K 7 12/58 Hw.

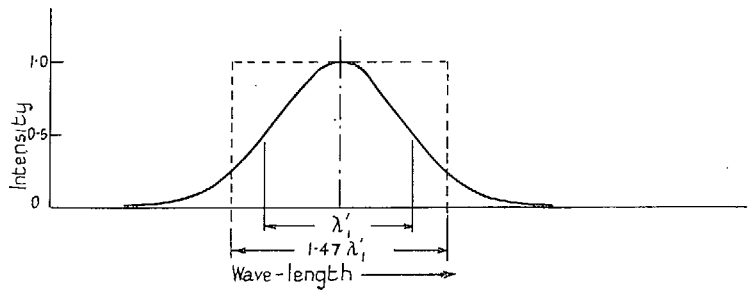

Gaussian and rectangular spectral distributions giving the same contrast for fringes near the zero fringe

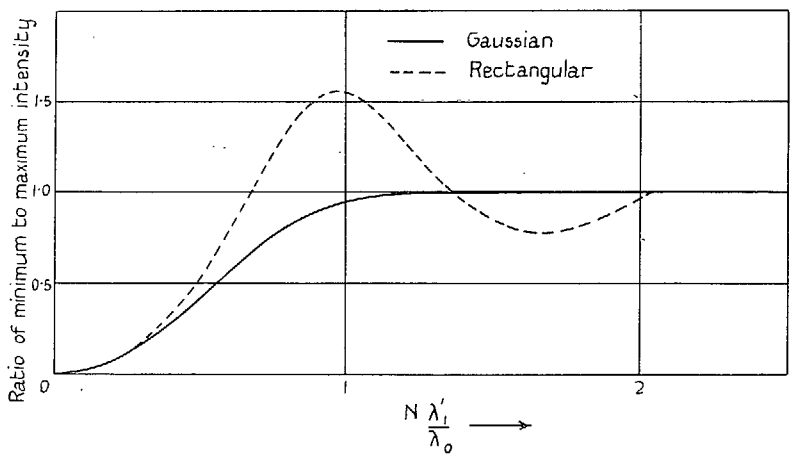

Variation of contrast with fringe number for Gaussian and rectangular spectral distributions

FIG. 33.

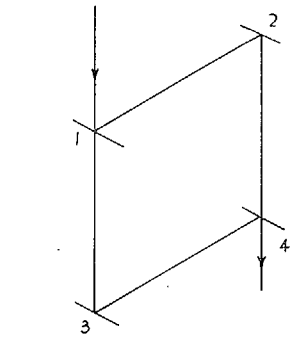

Normal Mach-Zehnder arrangement (parallelogram)

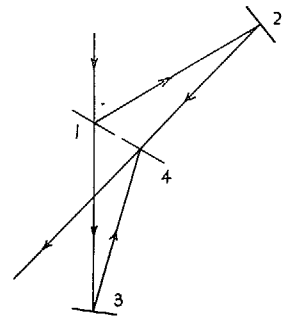

Mach-Zehnder with i_2 and i_3 small and i_4 negative

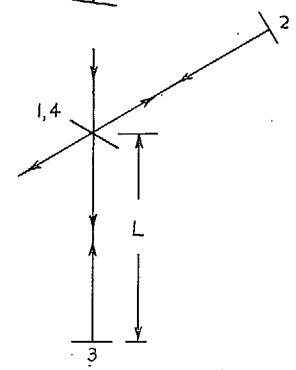

Twyman-Green, for which $i_2 = i_3 = 0$ and $i_4 = -i_1$

FIG. 34. The relation between the Mach-Zehnder and Twyman-Green interferometers.

PRINTED IN GREAT BRITAIN

Publications of the Aeronautical Research Council

ANNUAL TECHNICAL REPORTS OF THE AERONAUTICAL RESEARCH COUNCIL (BOUND VOLUMES)

1939 Vol. I. Aerodynamics General, Performance, Airscrews, Engines. 50*s.* (52*s.*).
Vol. II. Stability and Control, Flutter and Vibration, Instruments, Structures, Seaplanes, etc. 63*s.* (65*s.*)

1940 Aero and Hydrodynamics, Aerofoils, Airscrews, Engines, Flutter, Icing, Stability and Control, Structures, and a miscellaneous section. 50*s.* (52*s.*)

1941 Aero and Hydrodynamics, Aerofoils, Airscrews, Engines, Flutter, Stability and Control, Structures. 63*s.* (65*s.*)

1942 Vol. I. Aero and Hydrodynamics, Aerofoils, Airscrews, Engines. 75*s.* (77*s.*)
Vol. II. Noise, Parachutes, Stability and Control, Structures, Vibration, Wind Tunnels. 47*s.* 6*d.* (49*s.* 6*d.*)

1943 Vol. I. Aerodynamics, Aerofoils, Airscrews. 80*s.* (82*s.*)
Vol. II. Engines, Flutter, Materials, Parachutes, Performance, Stability and Control, Structures. 90*s.* (92*s.* 9*d.*)

1944 Vol. I. Aero and Hydrodynamics, Aerofoils, Aircraft, Airscrews, Controls. 84*s.* (86*s.* 6*d.*)
Vol. II. Flutter and Vibration, Materials, Miscellaneous, Navigation, Parachutes, Performance, Plates and Panels, Stability, Structures, Test Equipment, Wind Tunnels. 84*s.* (86*s.* 6*d.*)

1945 Vol. I. Aero and Hydrodynamics, Aerofoils. 130*s.* (132*s.* 9*d.*)
Vol. II. Aircraft, Airscrews, Controls. 130*s.* (132*s.* 9*d.*)
Vol. III. Flutter and Vibration, Instruments, Miscellaneous, Parachutes, Plates and Panels, Propulsion. 130*s.* (132*s.* 6*d.*)
Vol. IV. Stability, Structures, Wind Tunnels, Wind Tunnel Technique. 130*s.* (132*s.* 6*d.*)

Annual Reports of the Aeronautical Research Council—
1937 2*s.* (2*s.* 2*d.*) 1938 1*s.* 6*d.* (1*s.* 8*d.*) 1939–48 3*s.* (3*s.* 5*d.*)

Index to all Reports and Memoranda published in the Annual Technical Reports, and separately—
April, 1950 - - - - R. & M. 2600 2*s.* 6*d.* (2*s.* 10*d.*)

Author Index to all Reports and Memoranda of the Aeronautical Research Council—
1909—January, 1954 R. & M. No. 2570 15*s.* (15*s.* 8*d.*)

Indexes to the Technical Reports of the Aeronautical Research Council—

December 1, 1936—June 30, 1939	R. & M. No. 1850	1*s.* 3*d.* (1*s.* 5*d.*)
July 1, 1939—June 30, 1945	R. & M. No. 1950	1*s.* (1*s.* 2*d.*)
July 1, 1945—June 30, 1946	R. & M. No. 2050	1*s.* (1*s.* 2*d.*)
July 1, 1946—December 31, 1946	R. & M. No. 2150	1*s.* 3*d.* (1*s.* 5*d.*)
January 1, 1947—June 30, 1947	R. & M. No. 2250	1*s.* 3*d.* (1*s.* 5*d.*)

Published Reports and Memoranda of the Aeronautical Research Council—

Between Nos. 2251–2349	R. & M. No. 2350	1*s.* 9*d.* (1*s.* 11*d.*)
Between Nos. 2351–2449	R. & M. No. 2450	2*s.* (2*s.* 2*d.*)
Between Nos. 2451–2549	R. & M. No. 2550	2*s.* 6*d.* (2*s.* 10*d.*)
Between Nos. 2551–2649	R. & M. No. 2650	2*s.* 6*d.* (2*s.* 10*d.*)
Between Nos. 2651–2749	R. & M. No. 2750	2*s.* 6*d.* (2*s.* 10*d.*)

Prices in brackets include postage

HER MAJESTY'S STATIONERY OFFICE

York House, Kingsway, London W.C.2; 423 Oxford Street, London W.1; 13a Castle Street, Edinburgh 2; 39 King Street, Manchester 2; 2 Edmund Street, Birmingham 3; 109 St. Mary Street, Cardiff; Tower Lane, Bristol 1; 80 Chichester Street, Belfast, *or through any bookseller.*

S.O. Code No. 23-3069